DEVELOPMENT OF IN VITRO SYSTEMS TO STUDY ENDOCRINE DISRUPTORS

A Dissertation

Presented to the Faculty of the Graduate School

of Cornell University

In Partial Fulfillment of the Requirements for the Degree of

Doctor of Philosophy

by

Hui Xu

May 2009

DEVELOPMENT OF IN VITRO SYSTEMS TO STUDY ENDOCRINE DISRUPTORS

Hui Xu, Ph. D.

Cornell University 2009

Environmental estrogenic endocrine disruptors (EDs) are a health concern as the general population is exposed to a variety of EDs at low doses. Rapid screening and in depth understanding of how the body responds to EDs and their mixtures are crucial for toxicological evaluation and health protection. In this work, in vitro systems, including stable cells lines with estrogen induced green fluorescence protein (GFP) expression and micro cell culture analog (microCCA) devices, were developed to study EDs.

A dual cell-line GFP expression system was constructed to study EDs with activities as estrogen receptor agonists or antagonists. The two stable cell lines, Ishikawa-GFP (uterine origin) and MCF7-GFP (breast origin), displayed increased intracellular GFP intensity with estrogens. This system also responded in a tissue specific manner to selective estrogen receptor modulators, raloxifene and tamoxifen. Our results also suggested no low dose synergistic effects between the tested estrogenic compounds.

Physiologically realistic microCCA devices were developed to help predict in vivo responses to EDs. The silicon microCCA device contained a co-culture of three cell lines: MCF7-GFP, Ishikawa-GFP and HepG2/C3A (liver origin). Recirculation of medium mimicked the time dependent changes in drug concentrations and the

microfluidic shear conditions inside a body. An in-line bubble trap was incorporated into the system to overcome air bubble related device failure. Interactions between hydrophobic surfaces and the fluid were investigated. Significant surface adsorption of estrogen to polypropylene based tubing (BPT) was observed. Contaminants leaching out of the BPT tubing were also found to be estrogen receptor agonist. A pneumatic micropump with a pumping rate ~3 ul per min was build with PTFE tubing replacing BPT tubing. Detection of estrogens was demonstrated on a microCCA device integrated with the micropump.

Further, a photopolymerizable hydrogel based method was developed for direct patterning of multiple types of cells into their individual cell culture chambers in a PDMS microCCA. The use of this device as a biosensor was demonstrated by monitoring PEG encapsulated cells in microCCA exposed to a model toxicant, Triton X-100. The results indicate the potential use of PDMS microCCA devices to study EDs.

BIOGRAPHICAL SKETCH

Hui Xu was born to Xiulan Bai and Qinghua Xu on a bright sunny winter day. Her home town, Pingyi in the Shandong Province, China, was full of lovely friends and wonderful memories. She went to Tsinghua University in Beijing at seventeen years old and earned her bachelor's degree in Applied Physics. Three years later she received her Master of Science degree studying the development of mouse embryos with multiphoton microscopy. This combination of engineering, physics and biology led her into the world of Biomedical Engineering. She also first met Xiaodong Chen, her future husband, when she served as the vice president of the Student Technology Innovation Center.

In 2003, Hui attended the Biomedical Engineering program at Cornell University with Dr. Michael L. Shuler as her advisor. She worked on the "Body-on-a-Chip" project and enjoyed her time working in the clean room. In the summer of 2008 she gave birth to a lovely baby girl named Yilan (Sophia). Hui and her family are moving to Northern California, where she will be sure to miss the white snow and gorgeous waterfalls in Ithaca.

To My Parents, Xiulan Bai & Qinghua Xu

致我的父母，白秀兰和徐清华

To Xiaodong, Zhen and Yilan

致晓东，真真和沂岚

For Their Unconditional Love

感谢他们无尽的关爱

ACKNOWLEDGMENTS

First I would like to acknowledge my thesis advisor, Dr. Michael Shuler. His knowledge, foresight and enthusiasm have guided me through my Ph.D. study. Working with him has improved me as an independent thinker and scientific researcher. I am grateful to my committee member Dr. W. Lee Kraus for his kind instructions on molecular biology experiments and his generosity for allowing me full access to his laboratory. I also thank Dr. Harold Craighead for all the helpful advice in my study of biophysics.

This project is finished with the support from many people. I am grateful to the whole Shuler research group for their support and friendship. I thank Paula Miller for cell culture and facility trainings and for always being there to help. Within the microCCA team, Dan Tatosian, Gretchen McAuliffe, Mandy Esch and Jay Jung Hwan Song have been the best co-workers one may ask for. I also have very much enjoyed all the nice talks with BJ Kim, Tricia Echtenkamp, Jordan Altas, Jinpian Diao and many others working on the second floor, Olin Hall. Wangyu Tong and Wei Li, two visiting scientists in out lab, gave me many valuable advices on my project. Jun Wu has been the best collaborator and Dr. C.C Chu has given me many useful suggestions on photopolymerizable polymers. I thank Gary Isaacs, Edwin Cheung and Tong Zhang from Dr. Kraus's lab for their assistance with plasmid construction and cell infection. Special thanks to Shivaun Archer for allowing me to use the BME lab; Glenn Swan for fabricating the chip housings; Dr. Leonard W. Lion and Dr. David Putnam for helpful discussions and technical inputs. I thank Dr. Volker Vogt for his kind gifts of pQCXIP-GFP plasmid and 293T cell line. I also acknowledge Dr. Myles Brown at the Dana-Farber Cancer Institute (Boston, MA) for supplying Ishikawa cell line; and Dr.

Ana Soto and Dr. Carlos Sonnenschein at Tufts University of Medicine (Boston, MA) for providing MCF7-BOS cells.

Financial support for this work was provided in part by the Cornell NanoBiotechnology Center (NBTC), an STC Program of the National Science Foundation (ECS-9876771); A New York State Office of Science, Technology and a Academic Research (NYSTAR) Distinguished Professorship Award (M. L. Shuler); National Science Foundation (BES0342985); and NIH/NIDDK (DK058110) to W. L. Kraus.

Lastly I wish to thank my family especially my parents. I want to thank my parents for giving me a free spirit, for their unconditional love, for all of the sacrifices they have made for me, and for everything. I thank my husband for his support, his encouragement, for his smile and for making me smile. I appreciate my sister for the memorable childhood and for all the beautiful time we have spent together. Last I thank my daughter for making me a mother and for bringing new meaning to my life.

TABLE OF CONTENTS

LIST OF FIGURES

Chapter 1

Chapter 2

Chapter 3

Chapter 4

Chapter 5

LIST OF TABLES

LIST OF ABBREVIATIONS

3D	Three Dimensional
ADMET	Absorption, Distribution, Metabolism, Elimination and Toxicity
BPT	Polypropylene Based Tubing
DI	Deionized
Dox	Doxorubicin
E2	17 Beta - Estradiol
EDs	Endocrine Disruptors
EGFP	Enhanced Green Fluorescence Protein
FBS	Fetal Bovine Serum
GFP	Green Fluorescence Protein
microCCA	Microscale cell culture analog
MXC	Methoxychlor
PBPK	Physiologically-Based Pharmacokinetics
PDMS	Polydimethylsiloxane
PEG	Poly(ethylene glycol)
PF	Pluronic® F-68
SERM	Selective estrogen receptor modulators
VRP	Verapamil

CHAPTER 1*

BACKGROUND AND INTRODUCTION

1.1 In vitro cell co-culture systems

In vitro cell culture has been an essential method in the study of the toxicology of drugs and environmental chemicals for many years. However, traditional toxicity testing usually involves only one single type of cell dosed with one compound or a mixture of compounds. Results from such a test may be an incomplete prediction of in vivo response due to the absence of cell-cell and organ-organ interactions. The organs in the body have complex multicellular structures. The interactions between cells are critical for normal organ development and functions. Although organs are physically separated, they are interconnected by the blood circulation and communicate through secretion, absorption and metabolism of chemicals, including endocrine signals, into and from the blood stream. The existence of a second type of cell may alter the cell responses and functions. For example, co-culture of primary hepatocytes with non-liver-derived endothelial or fibroblasts modulated the liver cell phenotype and specific functions [1]. Co-culture is a more physiologically realistic in vitro model for a living organism. In addition, as toxicological effects may be obvious in one kind of cell but not in another, identical tests are repeated with different cell types with only one type of cell each time. Such experiments are labor-intensive and time-consuming. Co-culture, however, enables simultaneous monitoring on multi types of cells.

---

[1] Portions of this chapter have been published previously. Copyright 2007 from "Novel Cell Culture Systems: Nano and Microtechnology for Toxicology" by Michael L. Shuler and Hui Xu, In: Ekins S, editor. Computational Toxicology: Risk Assessment for Pharmaceutical and Environmental Chemicals. New York: John Wiley & Sons. p 693-724, 2007.

Cell co-culture can be realized in various ways. The following is a brief overview of these co-culture techniques used in biomedical applications.

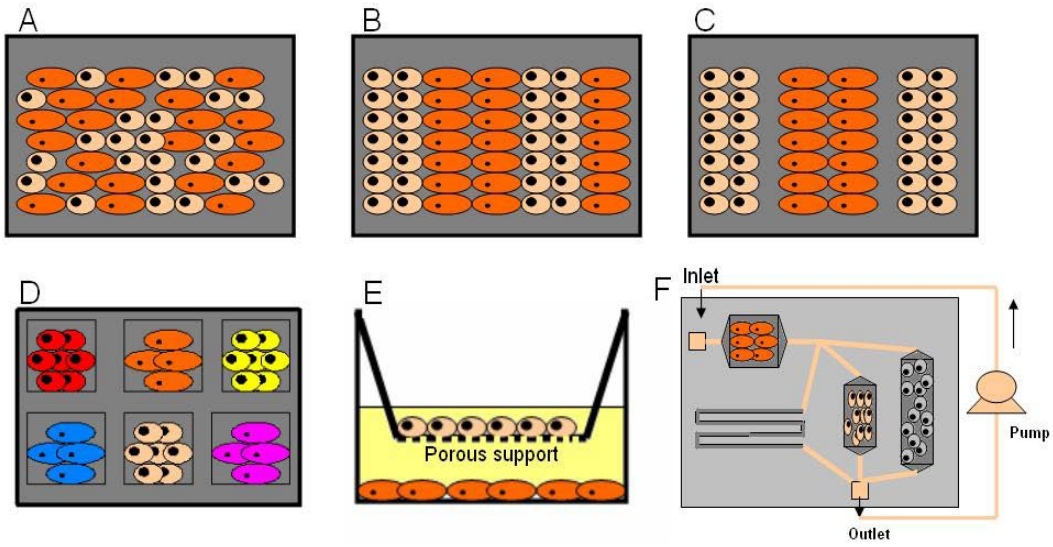

Figure 1.1 Illustration of multiple-type cell co-culture systems: (A) Random mixed; (B) Contact patterning with fuzzy boundaries; Co-culture without cell contact on (C) a flat surface or (D) in chambers; (E) the trans-well system and (F) the micro cell culture analog (microCCA) device.

1.1.1 Randomly distributed cell co-culture

Co-culture can be obtained by mixing multiple types of cells before cell seeding or by seeding one type of cell on top of another [2, 3], which results in random cell contact and distribution (Figure 1.1A). Change of cell seeding density or the ratio of cell population influences the strength of cell-cell interactions. In a mixed co-culture of Caco-2 cells and colorectal cancer HT29-5M21 cells, seeding ratios influenced the paracellular permeability of the cell monolayer [3]. In another study, adult rat hepatocytes maintained on top of a mesenchymal progenitor cell line C3H/10T1/2

cells [4] or rat 3T3 fibroblast cells [5] maintained better viability and higher ethoxyresorufin O-dealkylase (EROD) activity and albumin secretion functions [5].

Randomly distributed cell co-culture is simple in operation, but precise control of cell-cell contact and interactions is difficult. In addition, in many cases it might be difficult to differentiate cell type A apart from type B.

1.1.2 Co-culture with fuzzy boundaries

Nano and microfabrication techniques allow organized patterning of two or more types of cells in contact with defined boundaries, which may become less distinct after cell spreading and growth (Figure 1.1B). Bhatia et al. patterned on glass several stripes of liver and fibroblast cells next to each other using photolithography [6]. Primary rat liver cells were patterned based on surface modification with aminosilanes linked to biomolecules, and 3T3-J2 fibroblasts were attached to the remaining unmodified area through non-specific, serum mediated attachment. Using the same approach, hepatocytes were patterned into round isolated islands while fibroblasts filled the spaces between liver cells [2]. The influence of direct contact on cell functions can be studied by correlating cell function with the distance to the point of direct contact. Induction of hepatic functions in hepatocytes was observed to increase in the vicinity of fibroblasts and maximal induction of liver-specific functions was correlated with maximal initial heterotypic interaction [2]. It was suggested that heterotypic cell contact is necessary for induction of these functions [7]. This technique also enables control over the strength of cell-cell interaction without changing the numbers of each type of cells. But one limit of this method is that with time motile and mitotic cells will eventually intermix and the relative cell numbers can change [6].

1.1.3 Co-culture without cell contact

If the subject of interest is soluble chemical signals in the culture medium, a no-contact cell co-culture system is preferred to eliminate the potential influence through direct contact. By increasing the distance between patterned cell stripes (Figure 1. 1C), Bhatia et al. was able to keep the cells well separated to study how the space between co-culture cells affects their interactions [1]. Cells can also be separated by being confined to certain regions by physical barriers such as deep chambers or straight walls. Li et al. developed an integrated discrete multi-organ cell culture system (IdMOC) [8], which is a cell culture plate with relatively large wells subdivided into small subcompartments (Figure 1.1D). The IdMOC plates were modified from six-well tissue culture plates with seven inner wells of a diameter of 8 mm, a height of 0.8 mm and a capacity of 100 ul. Cells from multiple organs were cultured separately in small wells within one big well. For toxicity testing, drug-containing medium was added to flood all inner wells, thus all cells were exposed to the same medium and communications between cells was allowed. But the cells do not physically contact each other.

The transwell (Figure 1.1E) or other membrane-based methods also enable isolated cell co-cultures. Membrane filters, with a pore size from 0.1 um to 12 um are used as cell growth substrates. Generally one type of cell is seeded onto the membrane with a second type of cells cultured on the bottom of the well.

1.1.4 The cell culture analog

Although the cell culture systems described above enable the observation of some cell-cell and “organ-organ” interactions, the gap between in vitro and in vivo testing is still wide. In those systems, the fluid to cell volume ratio and the relative size of each

‘organ’ are far from their physiological values. In addition, all of these cell culture systems are static while cells in the body experience a more dynamic environment, with blood circulation replenishing nutrition, carrying away waste, transporting chemical signals generated in one cell to other cells, and exerting necessary mechanical forces for cell growth and differentiation.

The cell culture analog (CCA) system is one approach that attempts to bridge this gap. The design of the CCA is guided by physiologically based pharmacokinetic (PBPK) modeling. A PBPK is a mathematical model for predicting the overall plasma and tissue kinetic behaviors based on available data on physicochemical properties and specific absorption, distribution, metabolism, and elimination (ADME) processes [9]. In its design, the fluid fraction feeding each cell culture chamber is the same as the blood fraction received by the corresponding organ in vivo. Plus, the fluid residence time in each chamber equals its in vivo value. The liquid to cell ratio in each cell culture unit is managed to be as close as possible to its physiological value (about 0.5). Shear stress introduced by the flow is calculated and is kept at the physiological level for that type of tissue. A CCA device can be considered as a simplified and minimized human/animal body, in which mammalian cell cultures are used to represent key functions of specific organs, with cell culture medium being used as a blood surrogate.

The CCA was first developed and applied to study the toxicology of naphthalene in rats [10]. A microCCA is a miniature version of the macroscopic CCA. It achieves more physiologically realistic liquid-to-cell ratios in tissue compartments than the macro CCA. A typical microCCA chip is fabricated using the standard photolithography method [11] in a silicon chip 2.5 cm x 2.5 cm in size, with small chambers replacing big flasks for cell culture (Figure 1.1F). The microCCA allows in

situ monitoring of the physiological status of cells and chemical bioaccumulation. The first version of microCCA devices were designed based on the same PBPK model used for the macro CCA, and succeeded in predicting the toxicity of naphthalene on lung cells [11, 12] and to study the multi drug resistance [13].

In chapter four, a microCCA was designed and fabricated for studying environmental estrogenic endocrine disruptors and antiestrogens. Three types of human carcinoma cell culture of the liver, mammary tissue and the endometrial tissue were co-cultured on a one inch square silicon chip. This device allowed simultaneous monitoring of estrogenic responses from all cell lines. Tissue specific effects of selective estrogen receptor modulators (SERMs) were also observed.

1.2 Micro and nano fabrication technique for micro cell culture devices

The integration of modern nano and microfabrication technologies with cell culture has contributed to the development of new devices for toxicological studies and drug evaluations [14, 15]. Minimization of cell culture devices lowers the device cost, decreases chemical usage and waste production, allows massively parallel tests, and most importantly, provides opportunities for researchers to control, monitor and analyze cell responses with few cells, or even at the single-cell or subcellular level [16]. Nano and micro techniques enable manipulations, with nano and micrometer control, on the biochemical composition and topology of the substrate, the medium composition, and the cellular microenvironment [17], which results in an improved mimic of the extracellular microenvironment a cell experiences in vivo, and brings in vitro cell responses closer to in vivo cell responses. Miniature cell-based biosensors have been quickly developed for the functional characterization and detection of a

wide range of biologically active compounds, including drugs, pathogens, toxicants and odorants [14].

Nano and microfabrication technologies have been widely used in biological studies which combine microfluidics and cell handling for microreactors, cell culture, cell stimulation, cell sorting, cell lysis, sample separation, purification, and biochemical analysis [14]. These techniques are capable of fabricating miniature devices for cell culture with specific, pre-designed patterns, and for biochemical analysis with incorporated optical and electrical components. The following is a brief overview of some of the fabrication techniques, including photolithography, electro-beam lithography, soft lithography, hot embossing and laser micromachining (Figure 1.2) with a discussion on their strengths and weaknesses.

1.2.1 Photolithography

Borrowed from the semiconductor industry, photolithography has been well accepted for patterning cells and fabricating micro featured bio-microfluidic devices on silicon and glass substrates [18, 19]. The resolution of photolithography is limited by the optical diffraction, with a minimum feature size around 50 nm [18]. The first step is to generate photo-masks with the desired patterns by direct laser or ultraviolat (UV) light “pattern writing” onto the thin photo-resist layer on a chrome (Cr) coated glass or quartz plate (Figure 1.2). To transfer this pattern onto a silicon or glass substrate, the substrate is spin-coated with photoresist and exposed to ultraviolet light through the mask, which selectively allows light through. The exposed photoresist will be either solubilized (positive-tone photoresist) or crosslinked (negative-tone photoresist), followed by exposure to a developer solution which removes solubilized or un-crosslinked photoresist, and results in a photoresist pattern. This pattern can be used

for direct biomolecular (such as cell adhesion molecules for cell attachment) deposition [1], or for selective dry or wet etching into the substrates to form chambers for cell placement and fluid handling [12]. The remaining photoresist can then be dissolved in acetone or resist remover or etched off by plasma stripping.

The application of photolithography, however, is limited by its requirement for expensive facilities, high processing cost and limited resolution.

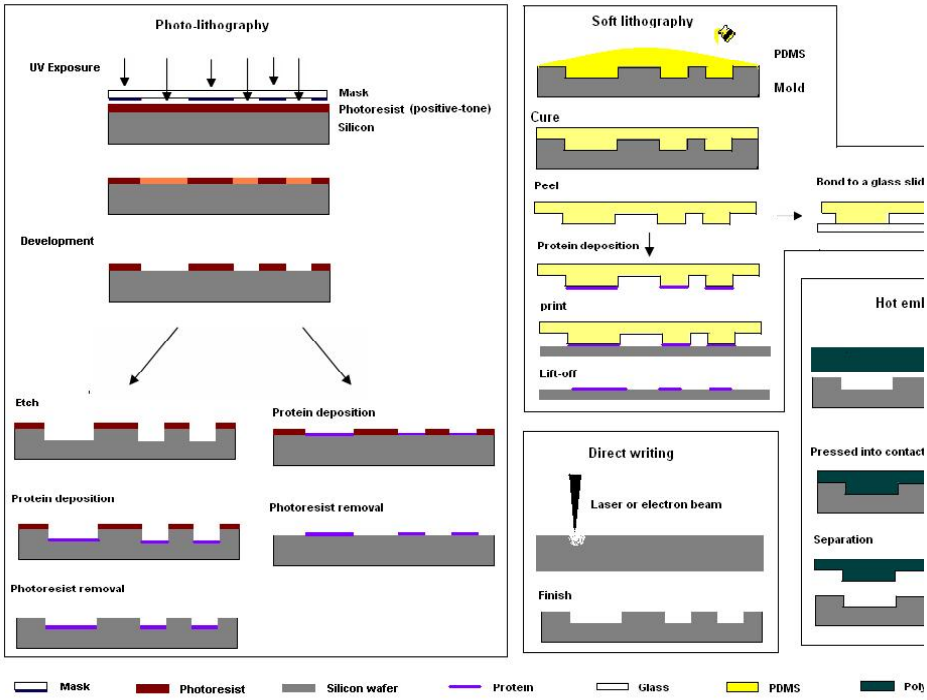

Figure 1.2 Schematics of typical nano and micro fabrication techniques: Photolithography, soft lithography, hot embossing and direct writing.

1.2.2 Electro-beam (E-beam) lithography

Electro-beam lithography has been the primary technique for defining, patterning and connecting experimental structures at the nanoscale [20]. E-beam lithography uses a

narrow electron beam to generate patterns. The extremely short quantum mechanical wavelength of high energy electrons allows it to overcome the diffraction limit, creating single surface features about 3-5 nm in size. This limit increases to 30-40 nm for large area surface patterning [18, 21, 22]. E-beam lithography allows computer-controlled direct pattern writing onto resist-coated substrates without an expensive physical mask. It has some drawbacks as well, such as its high initial capital expense, and slow writing speed due to its point-by-point exposure method.

1.2.3 Soft lithography

Soft lithography is developed for the fabrication of relatively large microstructures (> 50 um) in biological applications [23, 24]. It represents a group of surface patterning techniques including the micro contact printing, microfluidic patterning, and stencil patterning. One key feature of soft lithography is the use of elastomeric materials, most commonly poly (dimethylsiloxane) (PDMS), to replicate patterns from a master by molding. PDMS is inexpensive, biocompatible, highly gas permeable, amenable to surface modification, and optically transparent [25]. Soft lithography enables high volume production of disposable devices and lowers the cost for frequent design changes common in biological research.

Soft lithography starts with making masters for PDMS molding. The master can be either a silicon master or a SU-8 mold made from photolithography, with SU-8 mold being the more popular choice. SU-8 is a transparent negative-tone photoresist originally designed for the MEMS industry. It features a high aspect ratio, good mechanical strength, excellent chemical resistance, biocompatibility and low cost. The process of making a SU-8 mold is simple: spin coat, expose, and develop. To mold PDMS devices, the PDMS oligomer and crosslinking prepolymer are mixed well and

poured onto the SU-8 mold. Negative pressure is applied for removal of air bubbles introduced by mixing. The PDMS precursor mixture is allowed to cure at 65˚C overnight, after which the PDMS sheet can then be peeled off the mold. This micro featured PDMS slab is then ready for use as a stamp for micro contact printing or can be sealed against a substrate for microfluidic applications.

Micro contact printing (uCP) uses a PDMS stamp to pattern chemical molecules, such as proteins or alkanethiolates, onto silicon, glass, gold [26], PDMS [27] and many other plastic substrates. Proteins are deposited or passively absorbed onto the PDMS stamp then brought into contact with the substrate surface for several minutes. Upon lifting of the stamp, the protein pattern is left on the surface. Printing of cell adhesive proteins will result in cell attachment only at defined areas. uCP is capable of transferring patterns with features of 1 um dimensions and with an edge roughness of < 100 nm [23]. This resolution is limited by the stamp distortion during its contact with the substrate, and the surface diffusion of low molecular weight inks [28].

Microfluidic patterning combines a channel system with laminar flow to deliver chemical molecules in solution or cells in suspension to a restricted area. When a PDMS sheet with features is sealed to a glass slide, water-tight flow pathways are formed. This seal is reversible. Proteins or cells can be patterned onto the glass slide by forcing the solution flow through these fluidic channels. It should be noted that the laminar flow in microscale channels allows patterning of several different fluids in parallel to each other in one channel [18]. This phenomenon is also used for gradient generation and toxicological assessment, which are further explained later in this chapter.

Stencil patterning of cells utilizes a thin piece of PDMS sheet with through holes (stencil) to confine protein solution or cell suspensions within defined boundaries. The stencil works as a physical barrier to avoid contact of cell or protein solution with the substrate except at open areas in the stencil. With multi openings on the stencil, multi types of cells can be seeded onto the same piece of substrate for co-cultures. Stencils can be made out of other biocompatible materials as well, but a good seal between the stencil and the substrate is required to avoid cell or chemical cross-contamination.

1.2.4 Hot embossing

Hot embossing is also called thermal imprinting. This technique is capable of manufacturing features in the thermoplastic polymers with dimensions as small as 10 nm [29]. Hot embossing is capable of manufacturing microfeatures with polymer substrates such as polymethyl methacrylate (PMMA) [30], polycarbonate, cyclo-olefin copolymer (COC) [31] and polyimide [29]. For embossing, a silicon or hard polymer mold is pressed into thermoplastic materials at a temperature higher than the material's glass transition temperature (Tg), forming a relief of its feature in the plastic. The material surface is textured and separated from the mold once the polymer is cooled below the Tg [28]. The major advantages of hot embossing include its very low cost, capability for volume production of disposable devices, and ability to form 3D features that are difficult to produce in silicon [29].

1.2.5 Laser micromachining

Lasers can be used for both laser ablation and laser polymerization. Laser ablation combines evaporation and melt expulsion to remove metals, ceramics [32], glass, silicon and plastics materials, while laser polymerization builds three-dimensional

microstructures through laser induced polymerization of organic-inorganic hybrid biomaterials [33]. Laser ablation can produce surface features in the 5-500 um range with submicron accuracy [34]. Coupled with a microlithographic projection technique, laser micromachining with a metal mask can generate fine microstructures at the micron and submicron level by focusing the laser beam exiting the mask onto the polymer target surface via an optical setup for a reduction of the mask pattern [34, 35]. The high-relief topology of the laser lithographed substrates can also be utilized as a master/mold for PDMS stamps for microcontact printing and spatial patterning of cell adhesion proteins.

Multiphoton absorption is a non-linear optical phenomenon where two or more low energy photons are absorbed instead of a high energy photon [36]. Since this process requires an intense flux of excitation photons, optical absorption, and consequent laser ablation or polymerization, are tightly confined to the vicinity of focus with a micrometer resolution [37]. Using this technique, Giridhar et al were able to drill a subsurface tunnel into glass substrate with a high power femtosecond pulsed laser. Multiphoton absorption induced polymerization of organic-inorganic hybrid biomaterials is also used to fabricate microscopic 3D topographies, such as barriers and growth lanes, and microstructured medical devices [33]. Polymerization can be done in situ within dissociated neuron cell cultures without compromising cell viability [38]. In a different application, Costantino and coworkers added fluorescent dyes to UV-cured resins and used two-photon optical lithography to make spatial landmarks to quantify molecular transport, cell growth and migration [39].

Laser micromachining is automatic, fast, cheaper than hot embossing [40], and is capable of causing no or very little thermal effects and allows a very clean cut surface

[35]. The direct writing of subsurface features with multi-photon absorption is unique among available nano and micro fabrication methods.

1.3 Materials for miniature cell culture devices

Design considerations in material selection for a miniature cell culture system may include biocompatibility, capability for surface modification that allow cell attachment, chemical resistance to working fluids, ease of fabrication or processing, durability, and cost.

Silicon and glass are traditional substrates used for micro and nanofabrication. However, they are fragile, and the processes for patterning silicon and glass surfaces, such as photolithography and E-beam lithography, are expensive. Many ceramics, such as Titania ceramic (Titanium Dioxide), are very biocompatible implant materials and can be easily shaped by molding [41]. Gold or gold-coated substrates are often used for cell culture in cell-based biosensors for easy detection of electrical signals [42]. Titanium alloy is a material with good biocompatibility, but poor machinability [43]. Nature and synthetic polymers, especially plastics, are the most popular material for fabricating cell culture devices. Plastics are usually durable, optically transparent, relatively inexpensive, and thus suitable for disposable biomedical devices. They can be micro-machined by soft lithography, hot embossing, direct laser machining and other techniques. Flexible plastic substrates used in soft lithography include PDMS, poly(ethylene-dioxythiophene)/polystyrene sulfonate (PEDT/PSS) [44], polymeric films. Polystyrene, PMMA, polycarbonate, Plexiglas®, and polyethylene are the common plastics used for fabricating cell culture devices using hot embossing. Plastics are seldom used in photolithography due to the difficulty to achieve a good contact between mask and the substrate. It should be noted that surface modification

to promote cell adhesion on the surface of all these materials is usually required to support cell proliferation and function.

Materials used for three dimensional cell cultures within micro cell culture devices have different requirements for physical properties (such as mechanical strength), as well as chemical properties. There are two types of biomaterial for 3D cell culture, porous polymers and hydrogels. Porous polymers such as polylactic acid (PLA), polyglycolic acid (PGA), poly (lactic-co-glycolic acid) (PLGA) are constructed with various pore sizes to house cell cultures. Hydrogels are three-dimensionally cross-linked macromolecules of hydrophilic polymers. They are soft in texture and easy to handle at microliter scale. "Naturally based" hydrogels such as Matrigel (made of native extracellular matrix proteins), collagen (the major extracellular matrix protein) and hyaluronic acid provide endogenous signals that promote the cellular interactions that underlie tissue formation. Hydrogels to mimic the extracellular matrix can be created from synthetic molecules such as poly (ethylene glycol), polyglycolide, polylactide, acrylamide derivatives, calcium alginate and agarose, [45, 46]. These polymers are cross-linked using ultraviolet ray, radioactive ray, chemical cross-linking agent, ion solutions, or via temperature control for thermo-responsive hydrogels to reach a three-dimensional form. The advantages of synthetic gels include their consistent composition and predictable manipulation of properties, but they lack functional sites to interact with soluble or cell-surface proteins [47]. Proteins and positive charged components are often added into the composition to support cell-gel interactions. Cells are usually incubated within the polymer during this process and remain encapsulated after the gel is formed.

Table 1.1 Examples of potential endocrine disruptors

Organochlorines	Dichlorodiphenyltrichloroethane (DDT) [48] DDE (derivatives Of DDT) [49] Dieldrin [50] Methoxychlor (MXC) [51]
Industrial Chemical	Polychlorobiphenyls (PCBs) [52] Brominated Diphenylether (PBDP) [53] Trichlorobenzene (TCB, fabrics Additives) [54] Phthalate Esters [55] 2-hydroxy-4-methoxy-benzophenone (HMBP, photostabilizer) [56] 2,2-dimethoxy-2-phenyl-acetophenone (DMPA, photoinitiator) [56]
Industrial Contaminants	Dioxin-TCDD[57, 58]
Food Additives	Butylated Hydroxyanisole (BHA) [59] Butylated Hydroxytoluene (BHT, inhibitor) [59]
Herbal Estrogens	Daidzein [60] Genistein [61, 62] Lignans [63]
Heavy Metals	Cadmium [64] Arsenic [65]

1.4 Biological problem of interest: estrogenic endocrine disruptors

Endocrine disruptors (EDs) are environmental or man-made xenobiotic chemicals that are hormonally active They might disrupt the endocrine system of humans and the wildlife [66]. EDs affect a variety of biochemical and physiological processes that are regulated by critical hormonal signaling systems. Consequences of ED action may include disruption of normal sexual differentiation, sexual maturation, gonad function, reproduction, metabolism, digestion, and growth. In laboratory studies EDs caused developmental and reproductive problems in animals, fish and other wildlife [66]. However, their impact on human beings is still unclear due to limited human studies. Recent research showed that prenatal phthalate exposure at environmental levels can adversely affect male reproductive development in humans, with a decrease in

anogenital distance among male infants [67]. But such results were usually doubted and considered as “not conclusive” due to small number of subjects.

Human and environmental exposure to EDs, however, is undoubtly occurring with the widespread accumulation of ED chemicals in the environment. The list of chemicals that could act as EDs is extensively long. Table 1.1 summarizes a very small portion of this list with compounds that have been proven to interact with estrogen receptors. In addition, most EDs (such as DDT and PCBs) are persistent and refractory with slow transformation and degradation in the body as well as in the environment. They tend to be retained in the body and environment for decades. As the chemicals bio-accumulate in the body through diet and environmental exposure, their effects are consequently bio-amplified. It is important to point out that endocrine disruption can occur at levels far lower than those normally associated with toxicants. And these different chemicals at very low level may act together or modulate each other, resulting in synergistic effects [68]. There has been uncertainty and concerns about the health risks associated with both general population exposure and occupational exposure to a variety of EDs at various levels. On the other hand, the adverse effects of EDs are not obvious, advance slowly, and may take several generations to be observed and diagnosed. It is necessary to promote public awareness of the risk of EDs exposure. Production and disposal of potential EDs should also be monitored and regulated.

The Congress of the United States passed the Food Quality Protection Act in 1996, requiring that Environmental Protection Agency (EPA) initiate Endocrine Disruptor Screening Program (EDSP) to screen pesticide chemicals and environmental contaminants for their potential endocrine disrupting capabilities. The progress of the EDSP, however, is slow, partially due to the lack of standard methods and procedures

for evaluating a chemical's endocrine disrupting impacts. Currently, there are no standardized approaches for determining whether a particular compound has ED activity. In vivo animal models are perhaps the best approaches available, but they are expensive, time consuming, and fail to produce direct insights into the molecular basis of ED action. Furthermore, it is not always possible to accurately predict human responses from animal models. Though these in vitro studies can give useful data, they may not provide conclusive information about the response in living animals. For example, the active compound may be a metabolite which may not be present in many in vitro assays [69].

This thesis will describe the development in vitro systems to study the toxicity of estrogenic endocrine disruptors. Chapter two describes the creation of a stable dual cell-line green fluorescence protein (GFP) expression system, and the application of this system to detect EDs and to evaluate possible synergistic effects between EDs. This system is capable of addressing tissue specific effects in mammary and endometrial cultures to estrogenic EDs, selective estrogen receptor modulators (SERMs) and antiestrogens. Chapter three describes the discovery of endocrine disrupting contaminates from plastic tubing used in microfluidic cell culture systems. Surface modification and coatings were tested for their effect on contaminant leaching, as well as chemical loss due to surface adsorption. To overcome such problems, in chapter four, a peristaltic micropump was developed to drive the recirculation fluid flow instead of the traditional peristaltic pump which often uses a significant length of plastic tubing. The fabrication of a silicon based microCCA, a physiologically related cell co-culture device, with standard photolithography is also described in chapter four. Results from microCCA device to study EDs and antiestrogens are presented. Chapter five describes a disposable PDMS microCCA

setup with 3D cell culture within hydrogels, which is more physiologically realistic than traditional 2D cell cultures. The photo-curable nature of Poly (ethylene glycol) (PEG) hydrogels is an innovational approach to pattern multi-type of cells within a closed cell culture system. Finally, the overall results of this project is summarized and discussed, with suggestions and recommendations for future work presented and evaluated.

REFERENCES

1. Bhatia, S.N., et al., *Effect of cell-cell interactions in preservation of cellular phenotype: cocultivation of hepatocytes and nonparenchymal cells.* Faseb J, 1999. **13**(14): p. 1883-900.
2. Bhatia, S.N., et al., *Microfabrication of hepatocyte/fibroblast co-cultures: role of homotypic cell interactions.* Biotechnol Prog, 1998. **14**(3): p. 378-87.
3. Nollevaux, G., et al., *Development of a serum-free co-culture of human intestinal epithelium cell-lines (Caco-2/HT29-5M21).* BMC Cell Biol, 2006. **7**: p. 20.
4. Langenbach, R., et al., *Maintenance of adult rat hepatocytes on C3H/10T1/2 cells.* Cancer Res, 1979. **39**(9): p. 3509-14.
5. Bhandari, R.N., et al., *Liver tissue engineering: a role for co-culture systems in modifying hepatocyte function and viability.* Tissue Eng, 2001. **7**(3): p. 345-57.
6. Bhatia, S.N., M.L. Yarmush, and M. Toner, *Controlling cell interactions by micropatterning in co-cultures: hepatocytes and 3T3 fibroblasts.* J Biomed Mater Res, 1997. **34**(2): p. 189-99.
7. Bhatia, S.N., et al., *Probing heterotypic cell interactions: hepatocyte function in microfabricated co-cultures.* J Biomater Sci Polym Ed, 1998. **9**(11): p. 1137-60.
8. Li, A.P., C. Bode, and Y. Sakai, *A novel in vitro system, the integrated discrete multiple organ cell culture (IdMOC) system, for the evaluation of human drug toxicity: comparative cytotoxicity of tamoxifen towards normal human cells from five major organs and MCF-7 adenocarcinoma breast cancer cells.* Chem Biol Interact, 2004. **150**(1): p. 129-36.

9. Poulin, P. and F.P. Theil, *Prediction of pharmacokinetics prior to in vivo studies. II. Generic physiologically based pharmacokinetic models of drug disposition.* J Pharm Sci, 2002. **91**(5): p. 1358-70.

10. Sweeney, L., et al., *A Cell Culture Analogue of Rodent Physiology: Application to Naphthalene Toxicology*. Toxicol. in Vitro, 1995. **9**(3): p. 307-316.

11. Sin, A., et al., *The design and fabrication of three-chamber microscale cell culture analog devices with integrated dissolved oxygen sensors.* Biotechnol Prog, 2004. **20**(1): p. 338-45.

12. Viravaidya, K., A. Sin, and M.L. Shuler, *Development of a microscale cell culture analog to probe naphthalene toxicity.* Biotechnol Prog, 2004. **20**(1): p. 316-23.

13. Tatosian, D.A., *Developemnt of a microscale cell culture analog device to study multidrug resistance modulators*, in *Chemical Engineering*. 2007, Cornell university: Ithaca. p. 186.

14. Park, T.H. and M.L. Shuler, *Integration of cell culture and microfabrication technology*. Biotechnol Prog, 2003. **19**(2): p. 243-53.

15. El-Ali, J., P.K. Sorger, and K.F. Jensen, *Cells on chips.* Nature, 2006. **442**(7101): p. 403-11.

16. Takayama, S., et al., *Subcellular positioning of small molecules.* Nature, 2001. **411**(6841): p. 1016.

17. Li, N., A. Tourovskaia, and A. Folch, *Biology on a chip: microfabrication for studying the behavior of cultured cells.* Crit Rev Biomed Eng, 2003. **31**(5-6): p. 423-88.

18. Madou, M.J., *Fundamentals of microfabrication*. 1997, Boca Raton, Fla.: CRC Press. 589 , [22] of plates.

19. Britland, S., et al., *Micropatterning proteins and synthetic peptides on solid supports: a novel application for microelectronics fabrication technology.* Biotechnol Prog, 1992. **8**(2): p. 155-60.

20. Tseng, S. and C. Tsai, *Fabrication of individual aligned carbon nanotube for scanning probe microscope.* Journal of Physics: Conference Series 2005. **10**: p. 186-9.

21. Vieu, C., F. Carcenac, and A. Pepin, *Electron beam lithography: resolution limits and applications* Applied Surface Science, 2000. **164**(1): p. 111-117(7).

22. Norman, J.J. and T.A. Desai, *Methods for fabrication of nanoscale topography for tissue engineering scaffolds.* Ann Biomed Eng, 2006. **34**(1): p. 89-101.

23. Whitesides, G.M., et al., *Soft lithography in biology and biochemistry.* Annu Rev Biomed Eng, 2001. **3**: p. 335-73.

24. Kane, R.S., et al., *Patterning proteins and cells using soft lithography.* Biomaterials, 1999. **20**(23-24): p. 2363-76.

25. McDonald, J.C., et al., *Fabrication of microfluidic systems in poly(dimethylsiloxane).* Electrophoresis, 2000. **21**(1): p. 27-40.

26. Chen, C.S., et al., *Micropatterned surfaces for control of cell shape, position, and function.* Biotechnol Prog, 1998. **14**(3): p. 356-63.

27. De Silva, M.N., R. Desai, and D.J. Odde, *Micro-patterning of animal cells on PDMS substrates in the presence of serum without use of adhesion inhibitors.* Biomed Microdevices, 2004. **6**(3): p. 219-22.

28. Truskett, V.N. and M.P. Watts, *Trends in imprint lithography for biological applications.* Trends Biotechnol, 2006. **24**(7): p. 312-7.

29. Charest, J.L., et al., *Hot embossing for micropatterned cell substrates.* Biomaterials, 2004. **25**(19): p. 4767-75.

30. Kim, J.E., J.H. Cho, and S.H. Paek, *Functional membrane-implanted lab-on-a-chip for analysis of percent HDL cholesterol.* Anal Chem, 2005. **77**(24): p. 7901-7.

31. Becker, H. and C. Gartner, *Polymer based micro-reactors.* J Biotechnol, 2001. **82**(2): p. 89-99.

32. Hao, L., J. Lawrence, and K.S. Chian, *Osteoblast cell adhesion on a laser modified zirconia based bioceramic.* J Mater Sci Mater Med, 2005. **16**(8): p. 719-26.

33. Doraiswamy, A., et al., *Two photon induced polymerization of organic-inorganic hybrid biomaterials for microstructured medical devices.* Acta Biomater, 2006. **2**(3): p. 267-75.

34. Kearsley, A., *Laser micromachining.* Med Device Technol, 2003. **14**(2): p. 18-9.

35. Duncan, A.C., et al., *Laser microfabricated model surfaces for controlled cell growth.* Biosens Bioelectron, 2002. **17**(5): p. 413-26.

36. Zipfel, W.R., R.M. Williams, and W.W. Webb, *Nonlinear magic: multiphoton microscopy in the biosciences.* Nat Biotechnol, 2003. **21**(11): p. 1369-77.

37. Giridhar, M.S., et al., *Femtosecond pulsed laser micromachining of glass substrates with application to microfluidic devices.* Appl Opt, 2004. **43**(23): p. 4584-9.

38. Kaehr, B., et al., *Guiding neuronal development with in situ microfabrication.* Proc Natl Acad Sci U S A, 2004. **101**(46): p. 16104-8.

39. Costantino, S., et al., *Two-photon fluorescent microlithography for live-cell imaging.* Microsc Res Tech, 2005. **68**(5): p. 272-6.

40. Klank, H., J.P. Kutter, and O. Geschke, *CO(2)-laser micromachining and back-end processing for rapid production of PMMA-based microfluidic systems.* Lab Chip, 2002. **2**(4): p. 242-6.

41. Petronis, S., et al., *Microstructuring ceramic scaffolds for hepatocyte cell culture.* J Mater Sci Mater Med, 2001. **12**(6): p. 523-8.

42. Giaever, I. and C.R. Keese, *A morphological biosensor for mammalian cells.* Nature, 1993. **366**(6455): p. 591-2.

43. Murali, M. and S.H. Yeo, *Rapid biocompatible micro device fabrication by micro electro-discharge machining.* Biomed Microdevices, 2004. **6**(1): p. 41-5.

44. Cosseddu, P. and A. Bonfiglio, *Soft lithography fabrication of all-organic bottom-contact and top-contact field effect transistors.* Applied Physics Letters, 2006. **88**(2): p. 23506.1-23506.3.

45. Woerly, S., G.W. Plant, and A.R. Harvey, *Cultured rat neuronal and glial cells entrapped within hydrogel polymer matrices: a potential tool for neural tissue replacement.* Neurosci Lett, 1996. **205**(3): p. 197-201.

46. Dillon, G.P., et al., *The influence of physical structure and charge on neurite extension in a 3D hydrogel scaffold.* J Biomater Sci Polym Ed, 1998. **9**(10): p. 1049-69.

47. Cushing, M.C. and K.S. Anseth, *Materials science. Hydrogel cell cultures.* Science, 2007. **316**(5828): p. 1133-4.

48. Bitman, J., et al., *Estrogenic activity of o,p'-DDT in the mammalian uterus and avian oviduct.* Science, 1968. **162**(851): p. 371-2.

49. Willingham, E., *Endocrine-disrupting compounds and mixtures: unexpected dose-response.* Arch Environ Contam Toxicol, 2004. **46**(2): p. 265-9.

50. Arnold, S.F., et al., *Synergistic activation of estrogen receptor with combinations of environmental chemicals.* Science, 1996. **272**(5267): p. 1489-92.

51. Elsby, R., et al., *Assessment of the effects of metabolism on the estrogenic activity of xenoestrogens: a two-stage approach coupling human liver microsomes and a yeast estrogenicity assay.* J Pharmacol Exp Ther, 2001. **296**(2): p. 329-37.

52. Soto, A., et al., *The E-SCREEN assay as a tool to identify estrogens: an update on estrogenic environmental pollutants.* Environ Health Perspect. , 1995. **1003 Suppl 7**: p. 113-22.

53. Gee, J.R. and V.C. Moser, *Acute postnatal exposure to brominated diphenylether 47 delays neuromotor ontogeny and alters motor activity in mice.* Neurotoxicol Teratol, 2008. **30**(2): p. 79-87.

54. Kitamura, S., et al., *Comparative study of the endocrine-disrupting activity of bisphenol A and 19 related compounds.* Toxicol Sci, 2005. **84**(2): p. 249-59.

55. Harris, C.A., et al., *The estrogenic activity of phthalate esters in vitro.* Environ Health Perspect, 1997. **105**(8): p. 802-11.

56. Wada, H., et al., *In vitro estrogenicity of resin composites.* J Dent Res, 2004. **83**(3): p. 222-6.

57. Legler, J., et al., *Development of a stably transfected estrogen receptor-mediated luciferase reporter gene assay in the human T47D breast cancer cell line.* Toxicol Sci, 1999. **48**(1): p. 55-66.

58. Safe, S., M. Wormke, and I. Samudio, *Mechanisms of inhibitory aryl hydrocarbon receptor-estrogen receptor crosstalk in human breast cancer cells.* J Mammary Gland Biol Neoplasia, 2000. **5**(3): p. 295-306.

59. Jobling, S., et al., *A variety of environmentally persistent chemicals, including some phthalate plasticizers, are weakly estrogenic.* Environ Health Perspect, 1995. **103**(6): p. 582-7.

60. Harris, D.M., et al., *Phytoestrogens induce differential estrogen receptor alpha- or Beta-mediated responses in transfected breast cancer cells.* Exp Biol Med (Maywood), 2005. **230**(8): p. 558-68.

61. Gutendorf, B. and J. Westendorf, *Comparison of an array of in vitro assays for the assessment of the estrogenic potential of natural and synthetic estrogens, phytoestrogens and xenoestrogens.* Toxicology, 2001. **166**(1-2): p. 79-89.

62. Jorgensen, M., et al., *Assaying estrogenicity by quantitating the expression levels of endogenous estrogen-regulated genes.* Environ Health Perspect, 2000. **108**(5): p. 403-12.

63. Lord, R.S., B. Bongiovanni, and J.A. Bralley, *Estrogen metabolism and the diet-cancer connection: rationale for assessing the ratio of urinary hydroxylated estrogen metabolites.* Altern Med Rev, 2002. **7**(2): p. 112-29.

64. Piasek, M., et al., *Assessment of steroid disruption using cultures of whole ovary and/or placenta in rat and in human placental tissue.* Int Arch Occup Environ Health, 2002. **75 Suppl**: p. S36-44.

65. Kaltreider, R.C., et al., *Arsenic alters the function of the glucocorticoid receptor as a transcription factor.* Environ Health Perspect, 2001. **109**(3): p. 245-51.

66. EPA, *Chemical Selection Approach for Initial Round of Screening.* Federal Refister, 2005. **70**(186): p. 56449-56465.

67. Swan, S.H., et al., *Decrease in anogenital distance among male infants with prenatal phthalate exposure.* Environ Health Perspect, 2005. **113**(8): p. 1056-61.

68. Jacobs, M.N. and D.F. Lewis, *Steroid hormone receptors and dietary ligands: a selected review.* Proc Nutr Soc, 2002. **61**(1): p. 105-22.

69. Sugihara, K., et al., *Metabolic activation of the proestrogens trans-stilbene and trans-stilbene oxide by rat liver microsomes.* Toxicol Appl Pharmacol, 2000. **167**(1): p. 46-54.

CHAPTER 2*

DEVELOPMENT OF A STABLE DUAL CELL-LINE GFP EXPRESSION SYSTEM TO STUDY ESTROGENIC ENDOCRINE DISRUPTORS

2.1 Abstract

Environmental estrogenic endocrine disruptors are a health concern. Here we constructed a dual cell-line green fluorescence protein (GFP) expression system to identify and study endocrine disrupting compounds with activities of estrogen receptor agonists or antagonists. Human breast cancer MCF-7 cells and endometrial carcinoma Ishikawa cells were infected with a two tandem estrogen response elements–E4 promoter-GFP reporter gene construct. The use of GFP reporter enabled direct and simple evaluations of cell responses. GFP intensity in stably transfected MCF7-GFP and Ishikawa-GFP cells was dose-responsive to 17-beta-estradiol, diethylstilbestrol, 2-hydroxyestradiol, and environmental toxins bisphenol A, genistein and o-p'-DDT. Raloxifene and tamoxifen were effective antiestrogens in MCF7-GFP cells, but acted as partial estrogen receptor agonists in Ishikawa-GFP cells at concentrations of 0.1 nM and above. No synergistic effect was observed in chemical combinations between organochlorine pesticides methoxychlor, o-p'-DDT, p-p'-DDT, nor between estradiol and estrone. In summary, for the first time the effects of estrogen receptor agonists or antagonists were compared between mammary and endometrial cancer cells both stably expressing identical plasmids with GFP reporter genes under the control of tandem estrogen response elements. This dual cell-line system provides a rapid

[1] This chapter is based on “Development Of A Stable Dual Cell-Line GFP Expression System To Study Estrogenic Endocrine Disruptors” by Hui Xu, W. Lee Kraus, and Michael L. Shuler, Biotechnol Bioeng 101(6):1276-1287, 2008

method and sensitive assay to identify environmental estrogens, antiestrogens, selective estrogen receptor modulators and to study their tissue specific effects and chemical interactions. Such a system is especially useful for direct and parallel toxicity assessments with a microfluidic cell culture device.

2.2 Background and introduction

Since the last decade, there has been growing concerns that estrogenic pollutants in the environment, such as dichlorodiphenyltrichloroethane (DDT) and bisphenol A (BPA), may mimic natural hormone estrogens, interfere with the normal endocrine system, and elicit adverse health issues in both humans and wildlife [1]. Exposure to estrogenic endocrine disruptor (ED) chemicals in humans may adversely influence female fecundity and fertility, cause developmental and reproductive diseases, and increases the incidence of estrogen-related cancers [2-4]. These concerns have been heightened by the possibility that mixtures of weak EDs may exhibit complex synergistic interactions [5]. Examples of known environmental EDs include pesticides DDT, methoxychlor (MXC) [6, 7], plasticizers such as phthalate esters and BPA [8-10], food antioxidants butylated hydroxyanisole (BHA) [11], and herbal estrogens such as genistein and daidzein in various beans.

Estrogens are essential hormones in regulating the development and functions of the reproduction, nervous, skeletal and the cardiovascular systems. Long-term estrogen signaling occurs primarily through the direct binding of liganded estrogen receptors (ERs) to specific DNA sequences in the genome (estrogen response elements, or EREs) or the indirect binding via interactions with other classes of DNA bound transcription factors, such as activating protein 1 (AP1) [12-14]. This binding consequently recruits co-activators and modulates transcription of downstream target genes that regulate cell

proliferation, energy production and survival [12, 14]. The actions of estrogen vary in different target tissues.

A variety of in vivo and in vitro assays and in silico models have been developed in these years for screening of potential ED compounds and their mixtures. Environmental assays examine fish gonadal recrudescence and frog metamorphosis [15]. Rodent uterotrophic assays determine growth of the uterus gravimetrically [16], and the multigenerational tests assesses long-term toxicity of pollutants [17]. However, in vivo animal assays are costly and time consuming. It is also difficult to extrapolate human responses accurately from animal models. Computational tools, such as the nuclear receptor quantitative structure–activity relationship (QSAR) [18] and molecular docking [19, 20], attempt to predict endocrine disrupting activities basing on chemical structures. But the predictability of such tools is constrained by the limited structural similarity of estrogenic EDs. And predictions derived from computational analysis still require conventional bioassays to verify or obtain the results.

Recently DNA microarrays have been used to recognize the pattern of gene transcription in target cells stimulated by estrogens, which is then used to identify potential estrogenic compounds [21-23]. However, microarray requires careful sample preparation and hybridization, as well as complex data analysis. Hormone receptor binding assays measure the affinity of a compound to ER, but provide no specific information about its agonist or antagonist effects. Cell proliferation test (E-Screen) identify estrogenic chemicals by their proliferative effects, yet it suffers from lack of specificity [24], lengthy test times (5 to 6 days) and inability to produce direct insights into the molecular basis of chemical toxicity.

Methods employing reporter gene expression systems for estrogenicity measurements are typically fast and sensitive [25]. Yeast-based assays are simple, yet only provide limited information about responses in human cells. In human cell line based assays, luciferase (Luc) [25, 26] or chloramphenicol acetyltransferase (CAT) [27] reporter genes offer significant sensitivity. However, quantification of enzyme activities requires cell lysis and addition of enzyme substrates, which are costly and difficult to perform on microfluidic cell culture devices. Green fluorescence protein (GFP) is a real time quantitative reporter with high levels of brightness and photostability [28]. It allows easy and direct quantification with a fluorescence microscope or a spectrofluorometer. GFP can be introduced into target cells by transient or stable transfection. Transient transfection based assays require repeated cell transfection before each assay, while stably transfected cell lines, on the other hand, are ready to use, cost effective, and generate more consistent results.

The effects of estrogens and antiestrogens are tissue specific [29]. Mammary tissue and endometrial tissue are the main targets of estrogens. However, their responses to EDs haven't been compared side by side in a transcription assay with stably transfected cell lines. Only a few stably transfected human mammary cell lines have been reported. Most of them used Luc or CAT as reporters. The only two reported cell lines using GFP as the reporter [9, 30], however, are not readily available.

Our motivation for this work arises from a novel in vitro system, termed as microscale cell culture analog (microCCA), to evaluate the efficacy and toxicity of potential pharmaceuticals and environmental toxins [31-33]. The device is 2.5 cm x 2.5 cm in size on a silicon wafer. Multiple human cell lines, such as the mammary, endometrial,

liver cells and fat cells, can be cultured on the device in separate yet interconnected organ chambers. Cell culture medium (200 ul) is re-circulated through them as a blood surrogate. The physical microCCA system is a direct analog to a Physiologically Based Pharmacokinetic (PBPK) modeling [34]. Chamber size is calculated to provide liquid residence time similar to that in the tissue or organ. Reaction rates in flow limited models are determined by residence time. The relative size of compartments is set by the ratio of organ sizes. MicroCCA provides a more physiology-related dynamic environment for assessments of chemical toxicity in multiple cell lines simultaneously. It is developed to address the issues of reactive metabolite formation and tissue-tissue interaction through exchange of metabolites. The MicroCCA is a relatively complex system compared to traditional cell cultures due to its compact size, multi types of cell culture and the microfluidic system. Because of the difficulty to dislodge cells and separate them from one population from another, on-chip quantification of Luc/CAT activities in each individual type of cells is inconvenient. Instead, cell lines with estrogen-stimulated GFP expressions are preferred. While such cell lines may be used in a microCCA, they can be used advantageously in other assay systems such as multiwall, static cultures.

We report here the development of two stably transfected GFP reporter cell lines, MCF7-GFP and Ishikawa-GFP, to detect, quantify and study estrogenic and antiestrogenic compounds. The parent cell lines are MCF7-BOS [35, 36], a subline of MCF-7 human breast cancer cell line, and Ishikawa [37, 38], an endometrial adenocarcinoma cell line. We investigated how these cells respond to 17β-estradiol (E2), natural and synthetic hormones, pesticides and their mixtures, and how steroid starvation affects such responses. In addition, we examined the tissue-specific effects of several known antiestrogens. Our results indicated that both cell lines responded

promptly and specifically to estrogenic chemicals. Although tamoxifen and raloxifene acted as ER antagonists in MCF7-GFP cells, they both exhibited ER-mediated estrogenic activity in Ishikawa-GFP cells. Finally, no synergistic interaction was observed between tested weak estrogenic chemicals. The dual cell-line system provides a fast, direct and high throughput method to identify ER agonists, antagonists or selective ER modulators (SERMs), as well as to study possible chemical interactions between them.

2.3 Materials and methods

2.3.1 Chemicals and reagents

E2, estrone (E1), 2-hydroxyestradiol (2-OHE2), Bisphenol A (BPA), ICI 182,780 (Fulvestrant, ICI), 4-hydroxy tamoxifen (Tam), raloxifene hydrochloride (Ral), methoxychlor (MXC), genistein (GEN), diethylstilbestrol (DES), o-p'-DDT, p-p'-DDT, puromycin, and polybrene were purchased from Sigma (St. Louis, MO). Fetal bovine serum (FBS) and charcoal-dextran stripped fetal bovine serum (CDFBS) with reduced steroid levels were from Hyclone (Logan, UT). FuGene 6® transfection reagent was from Roche Applied Science (Indianapolis, IN).

2.3.2 Cell culture

MCF7-BOS cells were kindly provided by Dr. Ana Soto and Dr. Carlos Sonnenschein (Tufts University School of Medicine, Boston, MA). These cells were maintained in Dulbecco's Modified Eagle's Medium (DMEM) (MP Biomedicals, Solon, OH) supplemented with 5% heat inactivated FBS. Heat inactivated FBS was prepared by heating FBS in a 57℃ water bath for 30 minutes followed by a filtration through a 0.2-micron filter. 293T, an adenoviral transformed human embryonic kidney cell line, was a generous gift from Dr. Volker Vogt (Cornell University, Ithaca, NY). These cells

were maintained in DMEM medium (Sigma, St. Louis, MO) supplemented with 10% FBS. Ishikawa cells were a kind gift from Dr. Myles Brown (Dana-Farber Cancer Institute, Boston, MA). Cells have been maintained in Minimum Essential Medium (MEM) (Invitrogen, Carlsbad, CA) with 10% FBS. All the cells were cultured at 37°C in a humidified, 5% CO_2, 95% atmosphere incubator.

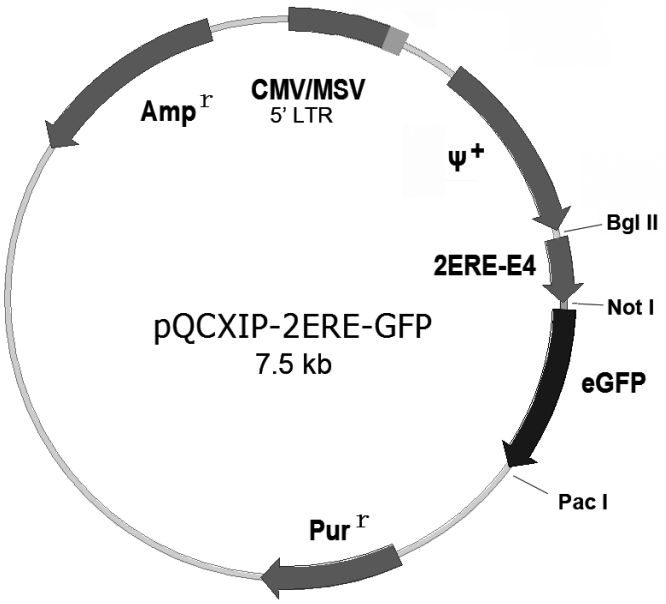

Figure 2.1 Schematic representation of the puromycin-resistant GFP reporter plasmid pQCXIP-2ERE-GFP. In a retrovirus vector pQCXIP-GFP containing a cDNA sequence encoding enhanced GFP, the immediate early CMV promoter ($P_{CMV\ IE}$) was replaced with two tandem estrogen response elements (EREs) upstream of an adenovirus E4 core promoter.

2.3.3 Plasmid construction

The consensus ERE is a 13 base pair inverted repeat sequence (GGTCANNNTGACC) [12, 39]. The retrovirus vector pQCXIP-GFP containing a cDNA sequence encoding enhanced GFP was provided by Dr. Volker Vogt (Cornell University, Ithaca, NY). This plasmid contains a puromycin resistance gene (Pur^r). The immediate early CMV

promoter ($P_{CMV\ IE}$) was removed from pQCXIP-GFP with restriction enzymes BglII and NotI digestion and a fragment containing two tandem EREs and the adenovirus E4 core promoter was ligated in place. The ligation product was pQCXIP-2ERE-GFP (Figure 2.1).

2.3.4 Retrovirus infection of MCF7-BOS and Ishikawa cells

Retrovirus infection was performed by modifying the protocol described by Pear and coworkers [40]. 293T were used as the packaging cell line. 293T cells were cultured in 6 well plates to reach ~80% confluence. Cells were transfected with the plasmid pQCXIP-2ERE-GFP using FuGene 6® transfection reagent. The retroviral supernatant was then harvested 48 h post transfection and filtered through a 0.45 um filter to remove living cells. To infect MCF7-BOS or Ishikawa cells, target cells were seeded into 6 well plates and allowed to attach. 1 ml fresh medium mixed with 1 ml virus-containing supernatant was added into each well 18 h after cell plating. Polybrene was added into the mixture at a final concentration of 4 ug /ml to enhance the efficiency of infection. 48 h later, the virus containing medium was replaced with fresh medium supplemented with 0.5 ug/ml puromycin and 1 nM E2 for the antibiotic selection of successfully transfected cells. This medium was refreshed every 3 days. Cells that survived 7 days' puromycin selection were then expanded in population. After culture with 1 nM E2 for 3 days, GFP positive cells were then sorted out using fluorescence activated cell sorting (FACS) Aria cell sorter (BD-Biosciences, Franklin Lakes, NJ). The cell line based on MCF7-BOS was designated as MCF7-GFP. The cells derived from Ishikawa cells were designated as Ishikawa-GFP. MCF7-GFP and Ishikawa-GFP stock cells were maintained in the same way as their parent cell lines, which have been described in detail earlier.

2.3.5 GFP assay with stably transfected MCF-7 and Ishikawa cells

MCF7-GFP or Ishikawa-GFP cells were seeded into 24-well plates (Costar, Corning, NY) at initial concentrations of 1.6 $x10^5$ cells per well (MCF7-GFP) and 8 x 10^4 cells per well (Ishikawa-GFP) respectively. Cells were allowed to attach overnight. Media were then replaced with 500 ul per well of fresh media supplemented with 5% CDFBS and dosed with chemicals of interest. CDFBS is charcoal/dextran treated FBS with reduced steroid levels. Fluorescence intensity of GFP in each well was then quantified after 48 h. In the GFP assay, chemicals were tested alone for estrogenicity measurements, or tested in the presence of 0.1 nM E2 to assess their antiestrogenic activities. Response was reported as a relative fluorescence using the saturated response at 1 nM or 0.1 nM E2 as the maximal value. Four measurements based on two independent wells dosed at 1 nM or 0.1 nM E2 were made from each set of experiments.

To test the effect of steroid starvation on cell response, cells were preconditioned in culture medium supplemented with 5% CDFBS instead of FBS for 0, 24 or 48 h before being exposed to 0.1 nM E2. GFP responses from cells were then quantified after another 48 h. To investigate possible synergistic activities of estrogenic compounds combinations, compounds were tested alone at designated concentrations, or were mixed 1:1 (v/v) with another chemical of interest at the concentrations of interest.

2.3.6 Optical imaging and data analysis

Cells were observed and imaged under an IMT-2 phase contrast and fluorescence microscope (Olympus America Inc., Center Valley, PA) at 100 X. Fluorescence and transmission images were captured with a Retiga CCD camera (Qimaging, Burnaby,

BC, Canada) in a 12 bit grayscale format, and were analyzed using ImagePro Plus software (Media Cybernetics Inc., Silver Spring, MD). The GFP fluorescence intensity in cells was calculated as the average optical density per pixel of cells. Means and standard errors of the fluorescence intensity were calculated using Origin (OriginLab, MA). Graphs were prepared using Origin with results representing the mean ± standard error of the mean. Best fit curves were generated using logistic fit of the data. The asterisk denotes statistical significance using the Student's t-test ($p < 0.05$).

2.4 Results and discussion

2.4.1 Establishment of an ERE-regulated dual-cell line GFP expression system.

In this work we generated stably transfected mammary and endometrial cell lines to detect estrogen receptor agonistic and antagonistic compounds, demonstrated their capability to identify natural or man-made estrogenic compounds, and studied these compounds' tissue-specific effects and possible synergistic interactions. The parent cell lines were carefully selected. MCF7-BOS is one of the most responsive cell lines for E-screen assay [35]. Ishikawa is a well-differentiated human endometrial adenocarcinoma cell line [38] that is used as a model for uterine tissue [37, 41]. Retrovirus infection of MCF7-BOS or Ishikawa cells with plasmid pQCXIP-2ERE-GFP and an initial selection with puromycin resulted in mixed cell populations with various levels of GFP expression. With fluorescence-activated cell sorting, cells with strong GFP fluorescence were separated from cells with very weak or no GFP fluorescence after a 48 h's treatment with E2. Fluorescent cells were collected as MCF7-GFP and Ishikawa-GFP. Both cell lines had relatively homogeneous levels of GFP expression within each individual cell line. Frozen cell stocks were prepared. For all the experiments, cells were used within ten passages after thawing.

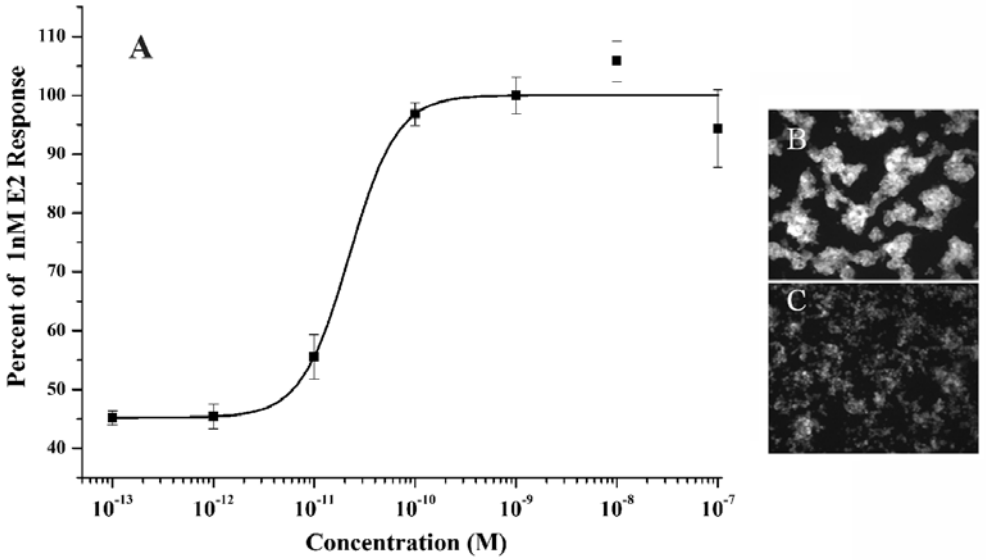

Figure 2.2 (A) Dose response curve of the MCF7-GFP cells to E2. Cells were treated with 17β-estradiol (E2) for 48 h at concentrations from 10^{-13} M to 10^{-7} M at log intervals. Cells responses are presented as % of green fluorescence protein (GFP) activity induced by 1 nM E2. (B) MCF7-GFP cells treated with 1 nM E2 showed a strong expression of GFP. (C) Cells not treated with E2 exhibited only a weak fluorescence background. Cells were imaged at 100 X.

2.4.2 Responses of MCF7-GFP and Ishikawa-GFP cells to estradiol

The sensitivity and responsiveness of transfected cell lines were evaluated with E2. Stable transfectants were treated with E2 for 48 h at concentrations from 10^{-13} M to 10^{-7} M at log intervals. GFP fluorescence within cells was measured with a fluorescence microscope. As described in Materials and Methods, the observed fluorescence was presented as a ratio of measured fluorescence in the well at a given dose to that fluorescence measured for a dose of 10^{-9} M E2. A dose of 10^{-9} M E2 was saturating and maximal. All wells had the same initial cell number. In MCF7-GFP cells, relative GFP fluorescence intensity increased in a dose-response manner from a basal level at 10^{-12} M E2 to a maximal expression at 10^{-10} M E2, but didn't increase further even with higher concentrations of E2 (Figure 2.2). Fifty percent effective concentration (EC50) value was calculated to be approximately 20 pM based on the dose response

curve. Similar responses to E2 were observed in Ishikawa-GFP cells (Figure 2.3) with a slightly higher sensitivity and a lower EC50 value of 9 pM.

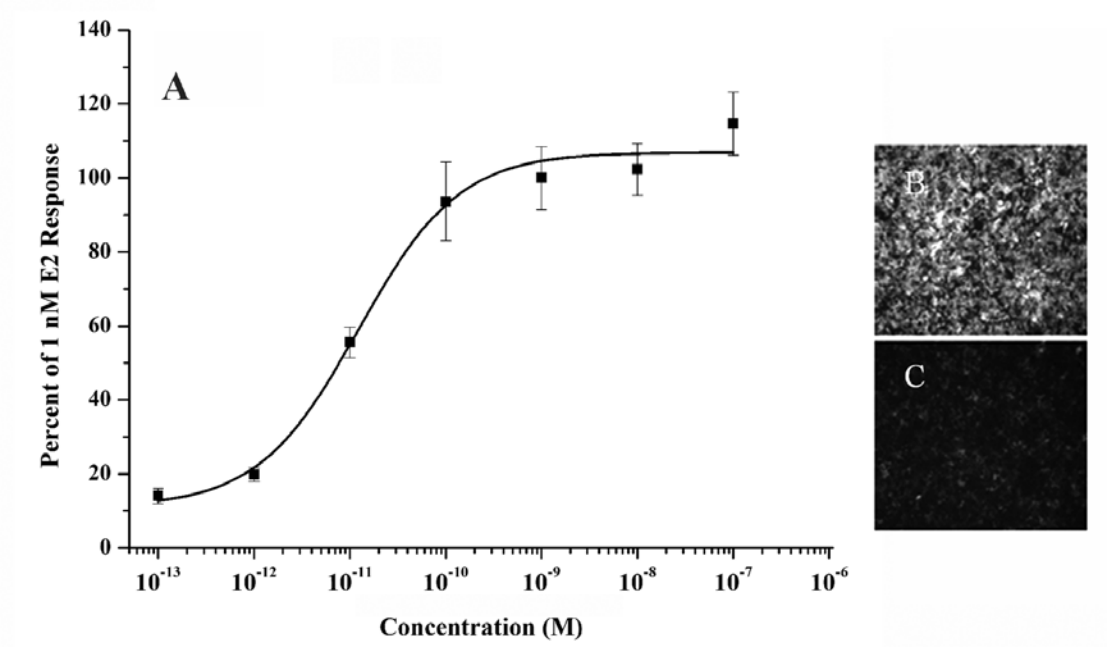

Figure 2.3 (A) Dose response curve of the Ishikawa-GFP cells to E2. Cells were treated with 17β-estradiol (E2) for 48 h at concentrations from 10^{-13} M to 10^{-7} M at log intervals. Cells responses are presented as % of green fluorescence protein (GFP) activity induced by 1 nM. (B) Ishikawa-GFP cells treated with 1 nM E2 showed a strong expression of GFP. (C) Cells not treated with E2 exhibited only a weak fluorescence background. Cells were imaged at 100 X.

To verify that the GFP reporter gene activity was ER-mediated, ICI 182780 was co-administrated with 1nM E2 in both MCF7-GFP and Ishikawa-GFPcultures.ICI 182,780 is a “pure” antiestrogen that down-regulates ER [42, 43]. A pure antiestrogen refers to antiestrogens with high affinity for ER but without any agonist effects. In both cell lines, the induction of GFP by E2 was inhibited in dose-dependent manners by ICI (Figure 2.4), indicating that the binding of E2 to estrogen receptors is essential for expression of the GFP reporter gene.

2.4.3 Effect of steroid starvation on assay sensitivity

Estrogen starvation was performed by preconditioning cells in medium supplemented with steroid-deprived CDFBS. In both MCF7-GFP and Ishikawa-GFP cultures, steroid starvation caused a stronger GFP response to E2 than non-starved cultures (Figure 2.5A, 2.5B). In MCF7-GFP cultures with starvation periods of 0, 1 or 2 days, the ratio of fluorescence in E2 exposed cultures (0.1 nM E2) to untreated controls was 2.2, 2.2, and 1.9, respectively. In contrast the Ishikawa-GFP cultures had a ratio of induced fluorescence (0.1 nM E2) to untreated controls starved for 0, 1 and 2 days as 5.7, 6.7 and 7.2 respectively. The effects of steroid starvation and length of starvation affect Ishikawa-GFP cultures more than MCF7-GFP cultures.

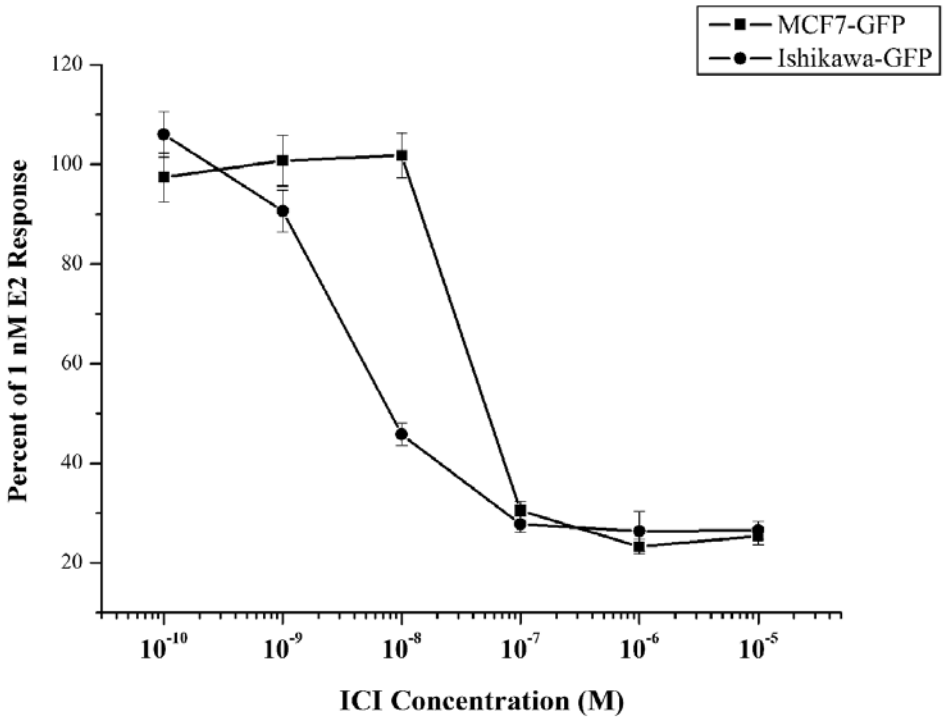

Figure 2.4 Dose responses of MCF7-GFP and Ishikawa-GFP cells to estrogen antagonist ICI 182,780 (ICI) in the presence of 1 nM E2. Cells responses are presented as % of green fluorescence protein (GFP) activity induced by 1 nM E2.

Steroid starvation is used in MCF-7 cell proliferation assays [44] and gene transcription assays [25, 26, 30] to identify estrogenic compounds. The duration of steroid starvation may last one to three days [25, 30, 44] or even seven days [26]. It is suggested that preconditioning in medium with CDFBS up-regulates the expression of estrogen receptors in cells, and consequently increases the cells' sensitivity to estrogens [44]. Our results showed that in Ishikawa-GFP cultures, the ratio of fluorescence intensity between E2 treated cells and the control cells increased slightly (26%) with two days of CDFBS preconditioning. However, in MCF7-GFP cells, despite of the increase of GFP intensity in E2 treated samples, the ratio of fluorescence in treated and control cultures changed little.

In the remainder of this study, the steroid starvation step was omitted from the GFP assays to shorten the duration of the experiments and to allow us to monitor MCF7-GFP and Ishikawa-GFP cells simultaneously. Since the ratio of fluorescence in treated and non-treated controls was relatively constant, the omission of this step has little impact on the experimental response.

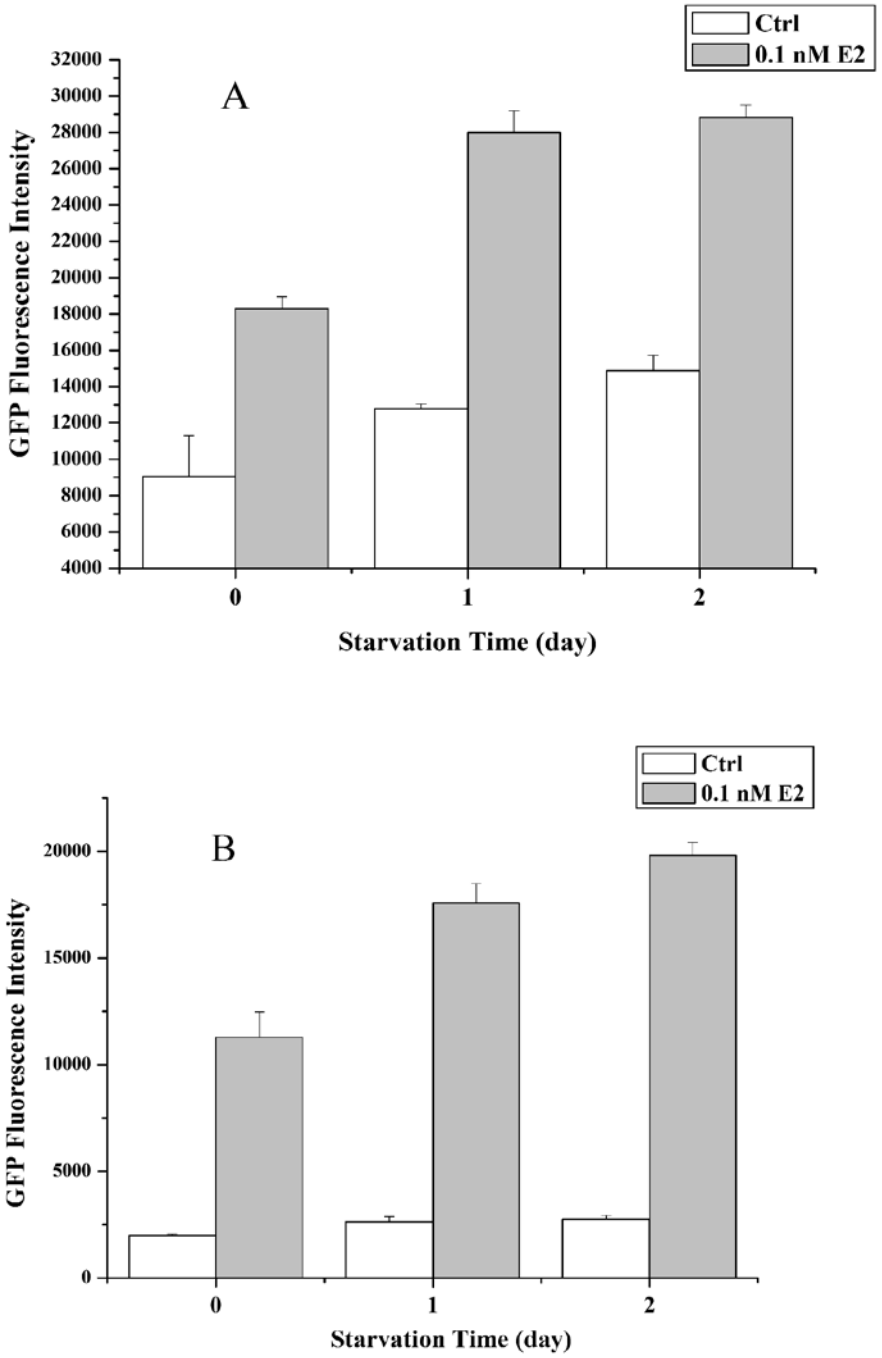

Figure 2.5 The effects of steroid starvation on cells' responses to 17β-estradiol (E2) were investigated in both (A) MCF7-GFP and (B) Ishikawa-GFP cells. Cells were preconditioned in cell culture medium supplemented with charcoal-dextran stripped fetal bovine serum (CDFBS) for 0, 1 or 2 days before being exposed to 0.1 nM E2. Fluorescence intensity of GFP was measured after 48 h of incubation. The data are reported as fluorescence units (FU) per pixel of cells.

2.4.4 Responses to natural or synthetic estrogens, environmental EDs, and progesterone

The performance of this assay was evaluated using the natural estrogens E2 , 2-OHE2 and the synthetic estrogens DES. Dose-response data are presented as a percent of their respective 1 nM E2 control response. DES is a synthetic estrogen used earlier in the 20th century to prevent miscarriage. It was banned in 1971 for its teratogenic effects and increased cancer risk is associated with DES exposure. In MCF7-GFP cells, DES displayed a strong estrogenic activity and induced a sharp GFP intensity increase at 10^{-10} M (Figure 2.6A). The fluorescence intensity obtained with 10^{-9} M E2 was achieved with 10^{-9} M DES. Similar results were observed in Ishikawa-GFP cells with a 90% of 10^{-9} M E2 induction achieved with 10^{-10} M DES (Figure 2.6B). These results indicated that DES is a strong estrogen with potency comparable to E2. 2-OHE2 is a major metabolite of E2. 2-OHE2 also induced a dose-dependent increase of GFP intensity with EC50 values of $6.3x10^{-8}$ M in MCF7-GFP cells (Figure 2.6A) and 3.2×10^{-8} M in Ishikawa-GFP cells (Figure 2.6B). The maximal fluorescence intensity obtained with 10^{-9} M E2 was achieved with 10^{-7} M to 10^{-6} M 2-OHE2. Thus, 2-OHE2 appears to be approximately 3,500 times less potent than E2.

Response of this assay to several known estrogenic endocrine disruptors was also examined (Figure 2.6A, Figure 2.6B). BPA is a plastic monomer and plasticizer that is used in the production of many plastic consumer products and papers, and is one of the highest volume chemicals produced worldwide [45]. An increase in GFP intensity was observed with 10^{-6} M BPA in both MCF7-GFP and Ishikawa-GFP cells. Genistein, an isoflavone from plants, stimulated the GFP expression at 10^{-6} M in MCF-7 cells, and at 10^{-7} M in Ishikawa cells. These results demonstrate that those cell lines respond to various chemicals in the expected differential manner.

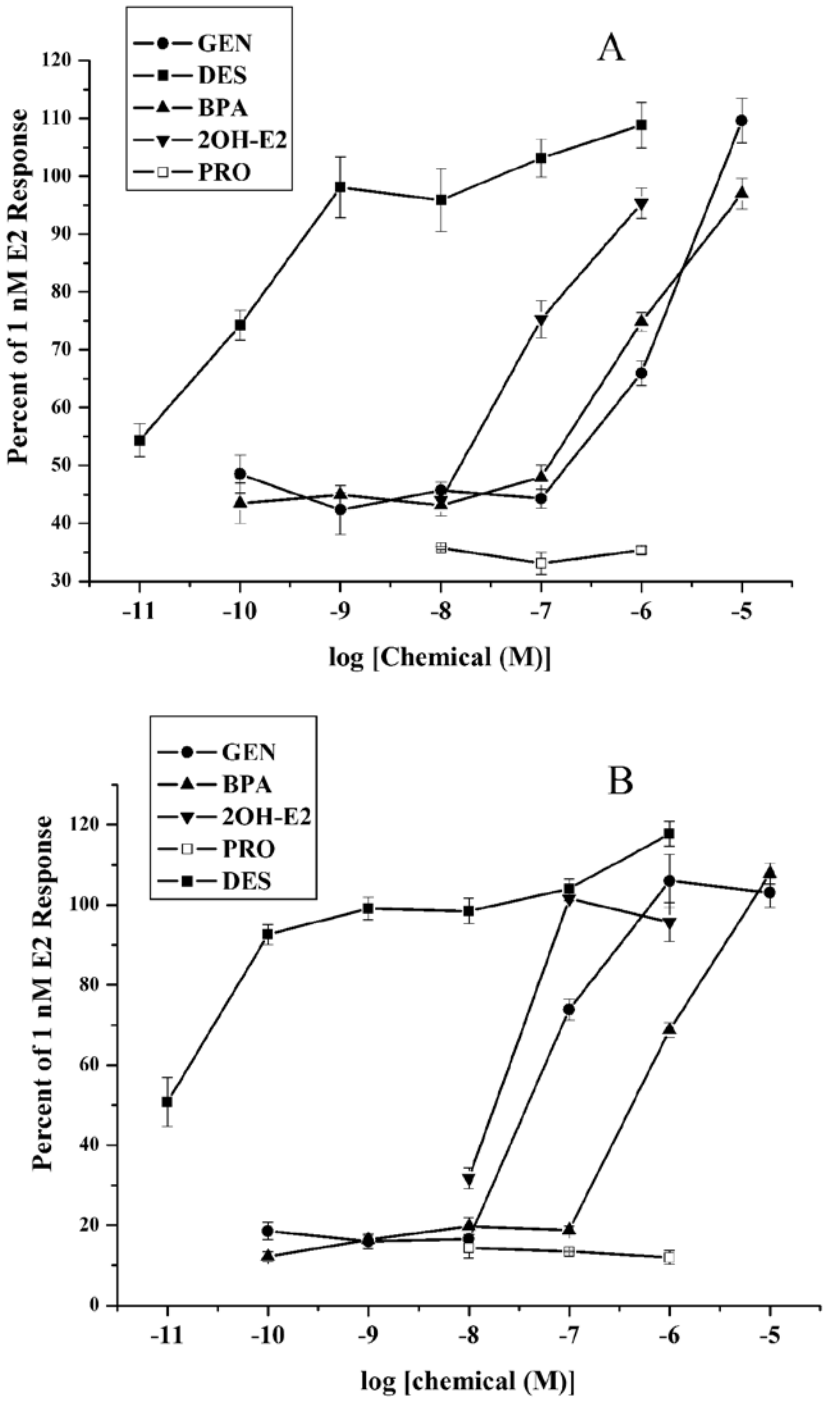

Figure 2.6 Responses of (A) MCF7-GFP and (B) Ishikawa-GFP cells to diethylstilbestrol (DES), 2OH-E2, genistein (GEN), bisphenol A (BPA) and progesterone (Pro). Data are presented as the % of the GFP activity induced by 1 nM 17β-estradiol (E2).

This dual-cell line assay appears to be specific to estrogens. Non-estrogenic hormones, such as progesterone, did not induce GFP expression above the vehicle control in either MCF7-GFP (Figure 2.6A) or Ishikawa-GFP cells (Figure 2.6B) at concentrations from 10^{-8} M to 10^{-6} M.

2.4.5 Comparison of the responsiveness of MCF-7 GFP with Ishikawa-GFP

In this study, both MCF-7 and Ishikawa cells were transfected with identical 2ERE-E4-GFP reporter gene constructs through the same retrovirus infection method. This was done to minimize variations in cell responses caused by different gene expression systems. Estrogenic chemicals tested here (E2, DES, Gen, BPA, 2OH-E2 etc.) generated similar response patterns in both MCF7-GFP and Ishikawa-GFP cells. However, Ishikawa-GFP cells were more sensitive than MCF7-GFP cells with smaller EC50 values. It was also observed that MCF7-BOS cells aggregated when exposed to estrogens, which may partially contribute to the increase of GFP intensity. Such an effect was not observed in Ishikawa cells. These results may represent intrinsic differences between the cells, for example, their distinct gene profiles and different ER expression levels [45]. The retrovirus infection process may introduce variances as well, possibly with various copies of vector fragments being integrated into the genome at different sites.

2.4.6 Tissue-specific effects of tamoxifen and raloxifene

To assess the anti-estrogenic activities of ICI, tamoxifen and raloxifene, MCF7-GFP and Ishikawa-GFP cells were treated with these compounds with or without co-administration of 1 nM E2. In MCF7-GFP cells, none of the compounds alone generated estrogenic activities in the range of 10^{-10} M to 10^{-5} M (data not shown). All three compounds inhibited E2-induced GFP activity in dose response manners as

expected (Figure 2.7A). The GFP fluorescence induction by E2 was completely blocked by all three antiestrogens at concentrations above 10^{-7} M. However, the results in Ishikawa-GFP cells are different. Only ICI, but not tamoxifen and raloxifene, was effective in inhibiting E2-induced GFP expression (Figure 2.7B). ICI alone stimulated no GFP activity. Tamoxifen and raloxifene, on the contrary, acted as estrogen agonists and generated significant estrogenic responses in Ishikawa-GFP cells. Tamoxifen produced a significant GFP intensity increase at concentrations higher than 10^{-10} M. The maximal expression was approximately 36% of the level induced by 10^{-9} M E2. Similar results were observed with raloxifene at 10^{-10} M to 10^{-5} M (Figure 2.7B), with a higher maximal GFP induction being about 60% of the level induced by 10^{-9} M E2.

The role of estrogen receptors in these responses was investigated by examining cell response to tamoxifen or raloxifene in the presence of ICI. It was observed that ICI repressed the estrogenic activities of both tamoxifen and raloxifene at 1 uM in dose response manners (Figure 2.8).

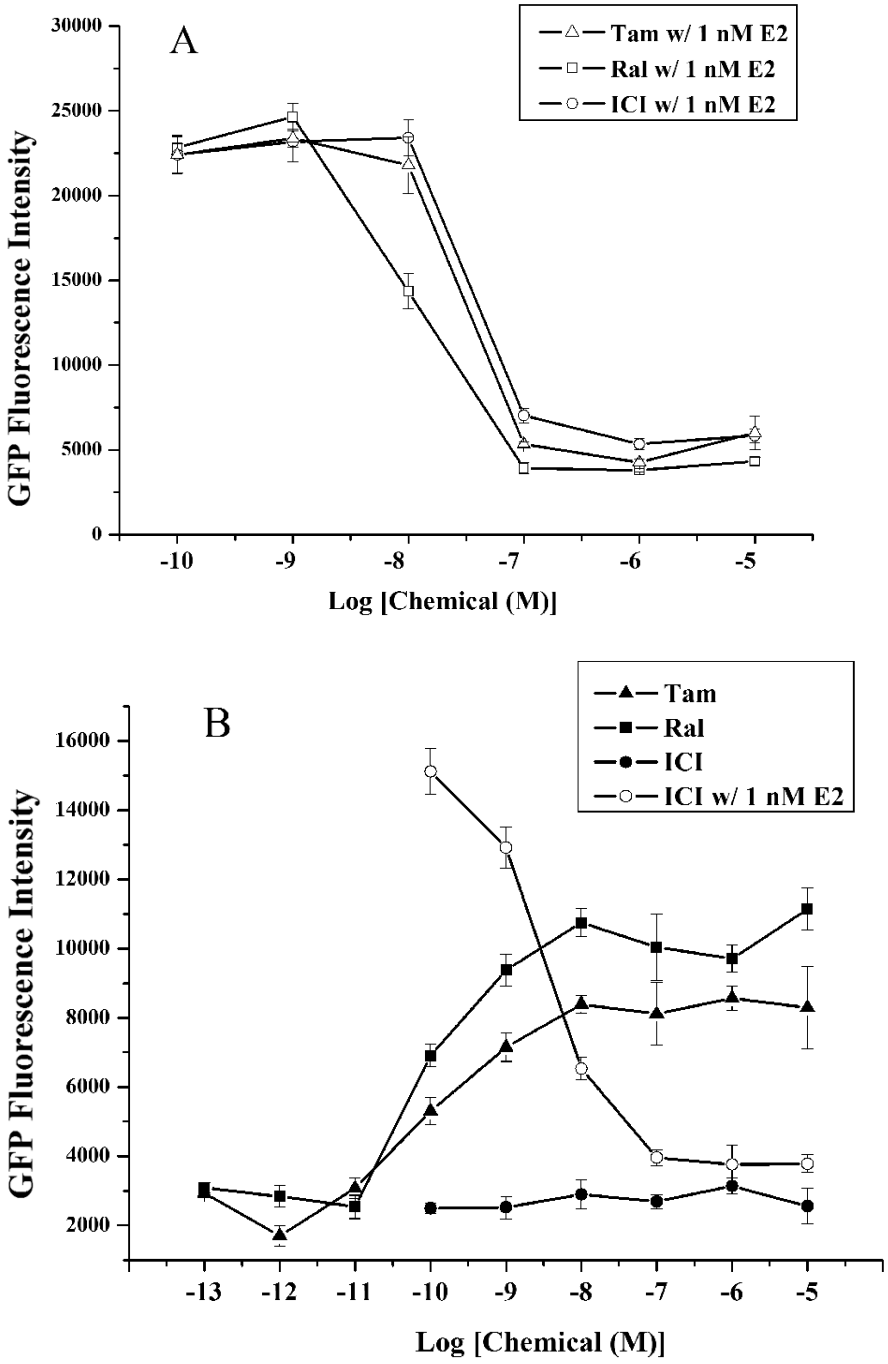

Figure 2.7 GFP responses to estrogen antagonists ICI 182,780 (ICI), tamoxifen (Tam) and raloxifene (Ral) in (A) MCF7-GFP and (B) Ishikawa-GFP cells. Antiestrogens were tested with or without co-administration of 1 nM E2. The data are reported as fluorescence units (FU) per pixel of cells.

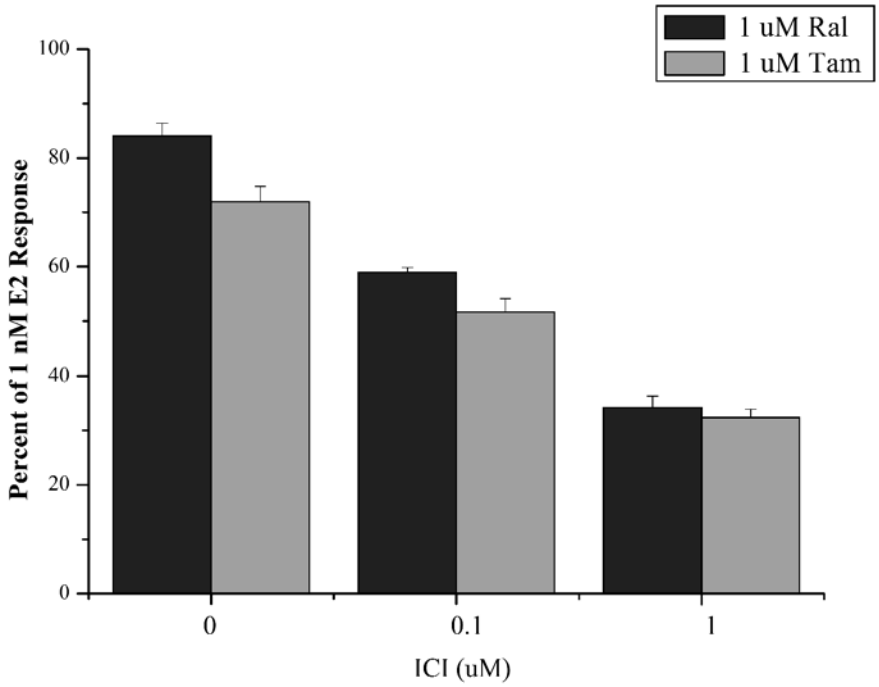

Figure 2.8 The effects of ICI on the GFP activities induced by 1uM raloxifene (Ral) or tamoxifen (Tam) in Ishikawa-GFP cells. 0.1 uM and 1u M ICI was added onto cells treated with Ral or Tam. The GFP fluorescence in cells was measured after 48 h of incubation. Data are presented as the % of the GFP activity induced by 1 nM 17β-estradiol (E2).

The increased risk of endometrial cancer in postmenopausal women under breast cancer therapy has been a concern [37, 46]. The challenge is to discover new SERMs that display ER antagonist activity on estrogen-dependent mammary tumors, but not in endometrial tissue. This dual cell-line system described here can be used as a preliminary screening tool for this purpose. Results from this system showed that ICI was a strong antiestrogen in both breast cancer MCF7-GFP and endometrial Ishikawa-GFP cells (Figure 2.7B). Tamoxifen and raloxifene were antiestrogens in MCF-7 cells but acted as ER agonists in Ishikawa cells, and exhibited partial estrogenic activities.

This conclusion on tamoxifen is consistent with many other studies [47, 48], but the results with raloxifene differ from some studies and many of these former studies are inconsistent with each other. Raloxifene, a compound for osteoporosis treatment, is being tested for breast cancer therapy. It is usually believed that, unlike tamoxifen, raloxifene does not increase the risk of endometrial cancer [37, 46]. Liu and coworkers [49] reported that raloxifene completely inhibited the activity of 1 nM E2 in a ERE-Luc reporter assay. In another work, raloxifene, unlike tamoxifen, did not stimulate the recruitment of co-activators to a subset of estrogen-response genes [37]. Studies with results consistent with ours are also available. Both tamoxifen and raloxifene, but not ICI, stimulated the activity of estrogen-sensitive alkaline phosphatase activity in Ishikawa cells [41]. Raloxifene was also found to stimulate the growth of Ishikawa tumor growth in ovariectomized nude mice [50]. The inconsistency between these studies is caused perhaps by the intrinsic variance of the cells or cell lines, and the reporter gene systems used in each individual study.

ICI inhibited the estrogenic actions of both tamoxifen and raloxifene in almost identical dose response manners (Figure 2.8), indicating that the GFP induction by both chemicals were most likely ER mediated. Raloxifene induced a higher GFP expression than tamoxifen in Ishikawa-GFP cells, implying that raloxifene is a stronger ER agonist than tamoxifen. Together, our data suggested that both tamoxifen and raloxifene have stimulatory effects on ER-ERE mediated gene transcriptions in Ishikawa cells.

2.4.7 Synergistic interactions between weak estrogenic chemicals

Possible synergistic activities between weak estrogenic EDs were investigated by comparing cells' responses to a single compound with cells' responses to chemical

mixtures. We first tested E2 in combination with its metabolite, E1, for possible synergism. The two chemicals were mixed 1:1 (v/v) at designated concentrations, and GFP responses were measured from both MCF7-GFP and Ishikawa-GFP cells. Results were illustrated in Figure 2.9A and Figure 2.9B. The combined effect of E2 and E1 was close to the sum of their individual effects. Interactions between E2 and E1 were additive or slightly less than additive (Figure 2.9A, Figure 2.9B). No synergistic interaction was observed in either cell lines. Organochlorine pesticides, MXC, o-p'-DDT and p-p'-DDT were also tested as endocrine disruptors and for synergistic interactions. MXC is general pesticide used on food crops, ornamentals, livestock, and pets. DDT, a commercial pesticide banned in the 1970's, is a mixture of p-p'-DDT and its inactive isomer o-p'-DDT. Figure 2.10A and Figure 2.10B illustrated responses of MCF7-GFP and Ishikawa-GFP cells to 1 uM MXC, o-p'-DDT, p-p'-DDT or their equimolar binary mixtures. Of these compounds only o-p'-DDT induced a statistically significant response over the control in MCF7-GFP cultures, but both o-p'-DDT and MXC induced significant responses in Ishikawa-GFP cultures.The combinations between these three compounds showed additive GFP activity in MCF7-GFP cells. In Ishikawa-GFP cells, interactions between o-p'-DDT and MXC, or between o-p'-DDT and p-p'-DDT were slightly less than additive.

Since numerous estrogenic agents have been identified in the environment, concerns are being raised about whether synergism occurs in humans exposed to multiple environmental estrogen mimics. Synergistic effect is not uncommon in drug toxicology and may be due to various mechanisms, including receptor interaction and changes in effector mechanisms [51, 52]. However, there have been conflicting reports regarding the existence of synergism between steroidal estrogens and environmental endocrine disruptors. Synergistic effect was observed between E2, E1 and 17α-

Figure 2.9 Transcription activation of GFP in (A) MCF7-GFP cells or in (B) Ishikawa-GFP cells by 0.001 nM E2, 0.1 nM E1, 0.01 nM E1 and their 1:1 (v:v) mixtures, 0.001 nM E2 and 0.1 nM E1 (0.001 nM E2/0.1 nM E1), 0.001 nM E2 and 0.01 nM E1 (0.001 nM E2/0.01 nM E1) . Fluorescence intensity of GFP in cells treated with 0.1 nM E2 (0.1 nM E2) and in the cells receiving solvent only (ctrl) are shown for comparison. The data are reported as fluorescence units (FU) per pixel of cells. Asterisks denote statistical significance of the response of the individual chemical as compared to the perspective vehicle control. * $p < 0.05$.

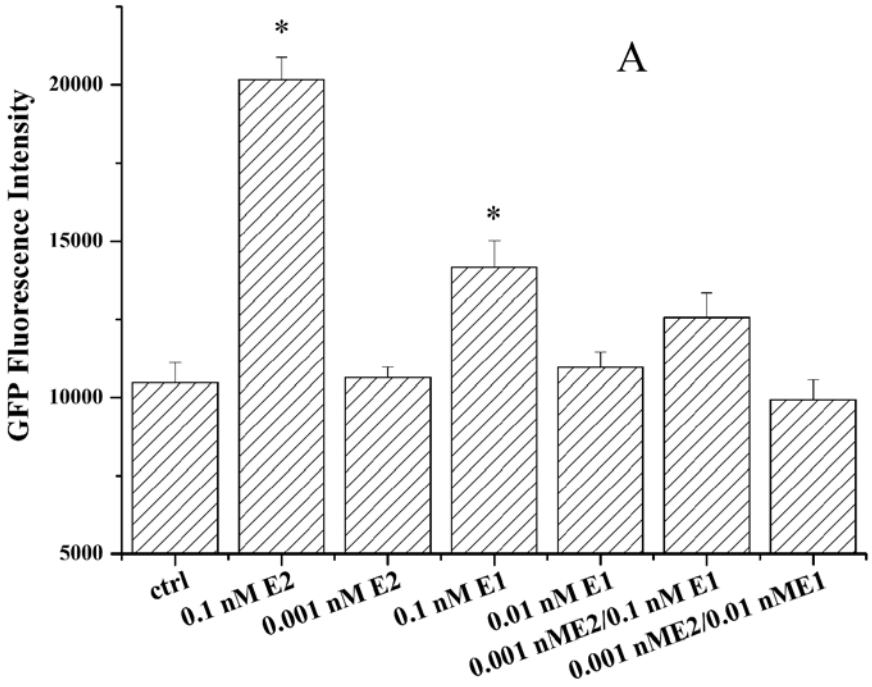
A
GFP Fluorescence Intensity
20000
15000
10000
5000
*
*
ctrl
0.1 nM E2
0.001 nM E2
0.1 nM E1
0.01 nM E1
0.001 nME2/0.1 nM E1
0.001 nME2/0.01 nME1

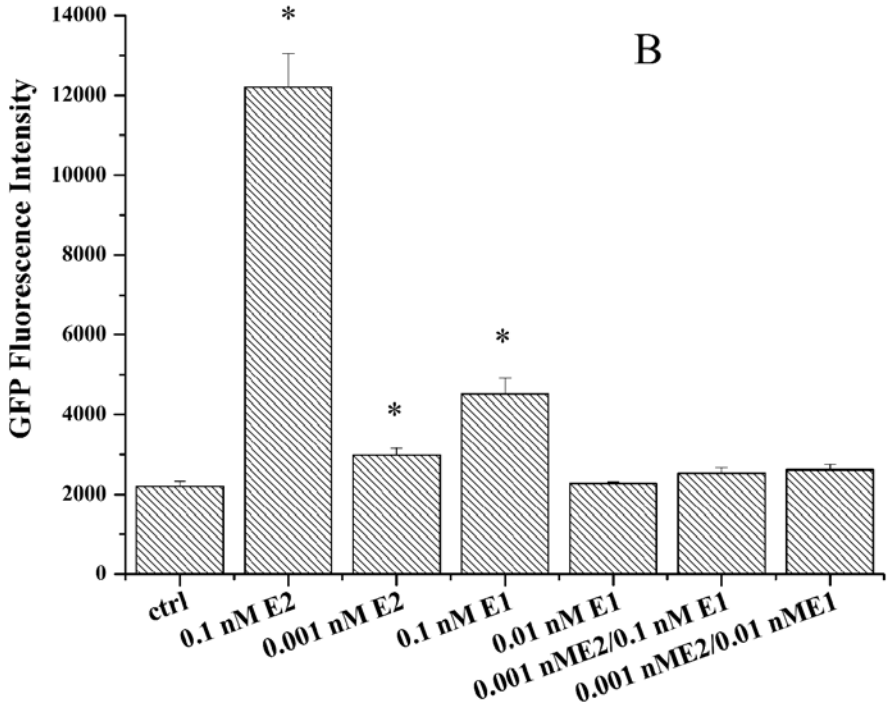
B
GFP Fluorescence Intensity
14000
12000
10000
8000
6000
4000
2000
0
*
*
*
ctrl
0.1 nM E2
0.001 nM E2
0.1 nM E1
0.01 nM E1
0.001 nME2/0.1 nM E1
0.001 nME2/0.01 nME1

Figure 2.10 Transcription activation of GFP in (A) MCF7-GFP cells and (B) Ishikawa-GFP cells by 1 uM methoxychlor (mxc), o-p'-DDT (op), p-p'-DDT (pp) and their equimolar binary mixtures of p-p'-DDT and o-p'-DDT (op/pp), o-p'-DDT and MXC (op/mxc), p-p'-DDT and MXC (pp/mxc). Fluorescence intensity of GFP in cells treated with 1 nM E2 (1 nM E2) and in the cells receiving solvent only (ctrl) are shown for comparison. The data are reported as fluorescence units (FU) per pixel of cells. Asterisks denote statistical significance of the response of the individual chemical as compared to the perspective vehicle control. * $p < 0.05$.

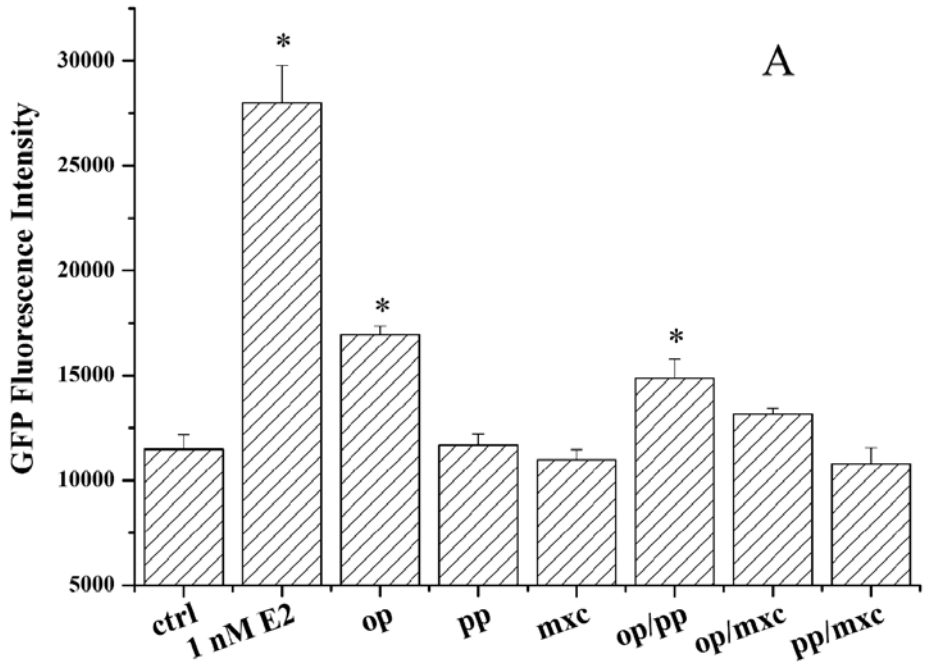
A
GFP Fluorescence Intensity
30000
25000
20000
15000
10000
5000
*
*
*
ctrl
1 nM E2
op
pp
mxc
op/pp
op/mxc
pp/mxc

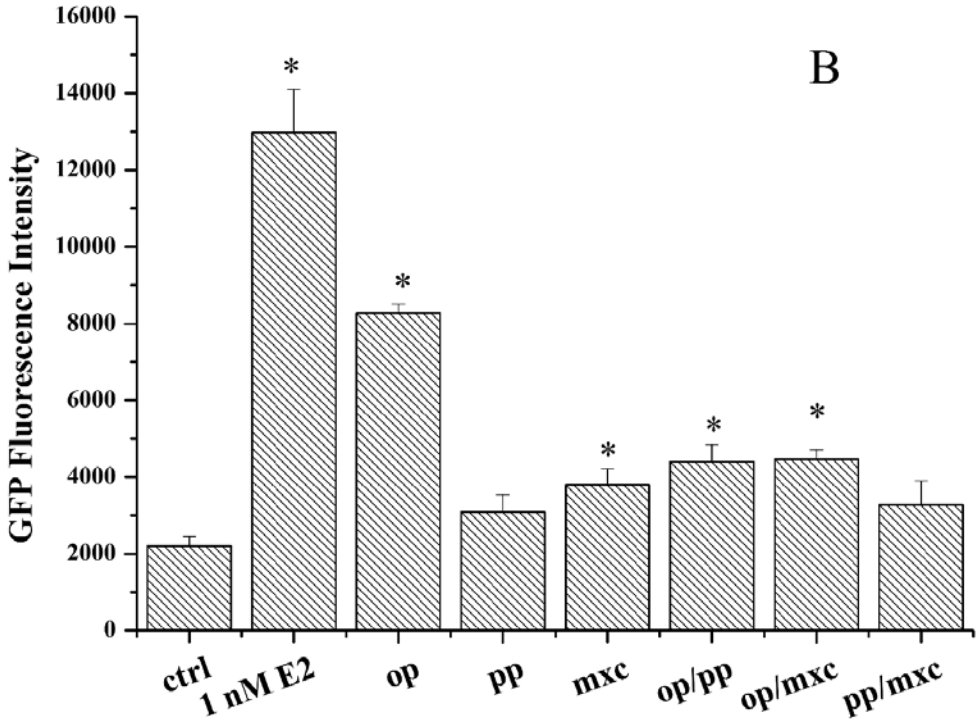
B
GFP Fluorescence Intensity
16000
14000
12000
10000
8000
6000
4000
2000
0
*
*
*
*
*
ctrl
1 nM E2
op
pp
mxc
op/pp
op/mxc
pp/mxc

estradiol [53], and with environmental chemicals such as dieldrin, endosulfan and toxaphene [5, 54]. It was also observed with endocrine-disrupting chemicals that interact with nuclear receptors other than ERs [54, 55]. But many other studies reported only additive effects between dieldrin and toxaphene [56], and organochlorine pesticides [57]. In this study we repeated some of these experiments with the same or similar compounds and concentrations with our dual-cell line GFP expression system. No evidence of synergistic activity was detected between MXC, o-p'-DDT, p-p'-DDT, nor between E2 and E1. However, since we only studied limited combinations of chemicals at specified concentrations, possible synergistic effect cannot be excluded. We suggest that estrogenic interactions of weakly estrogenic chemicals may be highly dependent on assays, including choices of cell lines, chemicals and doses.

2.5 Concluding remarks

Unlike most reported transcription assays that study chemical responses only in one cell line, this dual cell line system allows simultaneous investigations in both mammary and endometrial cells with a same gene transcription system. This is of great importance in the study of estrogens, antiestrogens or SERMs that can act in a tissue-specific manner. The two most notable observations in this study was the differential response (tissue specific) to tamoxifen and raloxifene and the lack of synergistic interactions of estrogenic chemicals.

The use of GFP in this dual-cell line system offer many advantages. Quantification of other reporters such as Luc and CAT require cell lysis and enzyme substrate, which make it difficult to perform on modern microfluidic cell culture devices, especially on microCCA with multi types of cell cultures. GFP is a photostable fluorophore for

analytical measurements, requires no cofactors or substrates for fluorescence to occur, and can be easily monitored in situ without cell disruption [58]. These stable cells with GFP as a reporter enable label-free and direct quantification of cell responses on compact microfluidic biosensors, such as microCCA chip devices. The simplicity of such an assay facilitates high throughput screening, whether in a traditional static or well-based assay or in a flow based microfluidic system.

The EC50 value of E2 following a 48 h exposure was approximately 9 pM in Ishikawa-GFP cells, similar to that observed in other GFP assays [9, 30], but are slightly larger than the EC50s measured in some Luc-based assays (6 pM, Legler et al., 1999; 3 pM, Wilson et al., 2004). As an enzymatic assay, Luc activity detection was usually more sensitive and rapid than protein expression, such as GFP [58, 59]. While steroid starvation may increase potentially the sensitivity of transcription assay, it was omitted in our measurements as we observed only modest increase in response even after two day starvation. Another factor that influences the sensitivity of an assay is the number of copies of ERE in the plasmid, where more copies of ERE are likely to increase the sensitivity of the reporter assay. 3 x ERE were used in the two Luc reporter assays mentioned above, while we used 2 x ERE in our dual-cell line system. A lower number of copies of ERE, however, reduces ligand-independent activities [60].

We believe that this GFP-based transcription assay will contribute to improved screening of estrogen, antiestrogen and SERMs compounds. It is a simple and stable aid in clarifying toxicological mechanism of chemical actions, and to address tissue-specific effects in mammary and endometrial tissues. In our laboratory this dual-cell

line assay is currently used with microCCA devices to identify estrogenic and antiestrogenic compounds. Liver cells cultured on the same chip devices enable the identification of pro-estrogens or pro-antiestrogens, which are activated by liver metabolism, and are most likely to be overlooked in a traditional static cell culture system. We also developed and are currently characterizing cell lines transfected with an AP1-E4-GFP construct. Future research with all these cell lines and the microCCA would facilitate identification of ER agonists and antagonists that act through both ER-ERE and ER-AP1 pathways. Such a system should lead to a clearer picture of crosstalk between these pathways. Dual cell lines should be an important tool in the study of how estrogen receptor modulators behave in a tissue-specific manner.

REFERENCES

1. Price, T.M., S.K. Murphy, and E.V. Younglai, Perspectives: the possible influence of assisted reproductive technologies on transgenerational reproductive effects of environmental endocrine disruptors. Toxicol Sci, 2007. **96**(2): p. 218-26.
2. Swan, S.H., et al., Decrease in anogenital distance among male infants with prenatal phthalate exposure. Environ Health Perspect, 2005. **113**(8): p. 1056-61.
3. Buck Louis, G.M., C.D. Lynch, and M.A. Cooney, Environmental influences on female fecundity and fertility. Semin Reprod Med, 2006. **24**(3): p. 147-55.
4. Hileman, B., Bisphenol A may trigger human breast cancer. Chemical and Engineering News (CEN), 2006. **84**(50): p. 10.
5. Arnold, S.F., et al., Synergistic activation of estrogen receptor with combinations of environmental chemicals. Science, 1996. **272**(5267): p. 1489-92.
6. Bitman, J., et al., Estrogenic activity of o,p'-DDT in the mammalian uterus and avian oviduct. Science, 1968. **162**(851): p. 371-2.
7. Metcalf, J.L., S.C. Laws, and A.M. Cummings, Methoxychlor mimics the action of 17 beta-estradiol on induction of uterine epidermal growth factor receptors in immature female rats. Reprod Toxicol, 1996. **10**(5): p. 393-9.
8. Harris, C.A., et al., The estrogenic activity of phthalate esters in vitro. Environ Health Perspect, 1997. **105**(8): p. 802-11.
9. Kuruto-Niwa, R., S.Teraob, and R. Nozawaa, Identification of estrogenic activity of chlorinated bisphenol A using a GFP expression system Environmental Toxicology and Pharmacology 2002. **12**(1): p. 27-35.
10. Howdeshell, K.L., et al., Bisphenol A is released from used polycarbonate

animal cages into water at room temperature. Environ Health Perspect, 2003. **111**(9): p. 1180-7.

11. Jobling, S., et al., A variety of environmentally persistent chemicals, including some phthalate plasticizers, are weakly estrogenic. Environ Health Perspect, 1995. **103**(6): p. 582-7.
12. Kumar, V. and P. Chambon, The estrogen receptor binds tightly to its responsive element as a ligand-induced homodimer. Cell, 1988. **55**(1): p. 145-56.
13. Kushner, P.J., et al., Estrogen receptor pathways to AP-1. J Steroid Biochem Mol Biol, 2000. **74**(5): p. 311-7.
14. Warner, M., S. Nilsson, and J.A. Gustafsson, The estrogen receptor family. Curr Opin Obstet Gynecol, 1999. **11**(3): p. 249-54.
15. O'Connor, J.C., et al., Evaluation of Tier I screening approaches for detecting endocrine-active compounds (EACs). Crit Rev Toxicol, 2002. **32**(6): p. 521-49.
16. Owens, W. and H.B. Koeter, The OECD program to validate the rat uterotrophic bioassay: an overview. Environ Health Perspect, 2003. **111**(12): p. 1527-9.
17. Hoshino, N., M. Iwai, and Y. Okazaki, A two-generation reproductive toxicity study of dicyclohexyl phthalate in rats. J Toxicol Sci, 2005. **30 Spec No.**: p. 79-96.
18. Jacobs, M.N., In silico tools to aid risk assessment of endocrine disrupting chemicals. Toxicology, 2004. **205**(1-2): p. 43-53.
19. Pike, A.C., et al., Structural aspects of agonism and antagonism in the oestrogen receptor. Biochem Soc Trans, 2000. **28**(4): p. 396-400.
20. Brzozowski, A.M., et al., Molecular basis of agonism and antagonism in the oestrogen receptor. Nature, 1997. **389**(6652): p. 753-8.

21. Francois, E., et al., DNA microarrays for detecting endocrine-disrupting compounds. Biotechnol Adv, 2003. **22**(1-2): p. 17-26.

22. Fujimoto, N., et al., Identification of estrogen-responsive genes in the GH3 cell line by cDNA microarray analysis. J Steroid Biochem Mol Biol, 2004. **91**(3): p. 121-9.

23. Wang, D.Y., et al., Identification of estrogen-responsive genes by complementary deoxyribonucleic acid microarray and characterization of a novel early estrogen-induced gene: EEIG1. Mol Endocrinol, 2004. **18**(2): p. 402-11.

24. Dickson, R.B. and M.E. Lippman, Growth factors in breast cancer. Endocr Rev, 1995. **16**(5): p. 559-89.

25. Legler, J., et al., Development of a stably transfected estrogen receptor-mediated luciferase reporter gene assay in the human T47D breast cancer cell line. Toxicol Sci, 1999. **48**(1): p. 55-66.

26. Wilson, V., K. Bobseine, and J. Gray LE, Development and characterization of a cell line that stably expresses an estrogen-responsive luciferase reporter for the detection of estrogen receptor agonist and antagonists. Toxicol Sci. , 2004. **81**(1): p. 69-77.

27. Byford, J.R., et al., Oestrogenic activity of parabens in MCF7 human breast cancer cells. J Steroid Biochem Mol Biol, 2002. **80**(1): p. 49-60.

28. Tsien, R.Y., The green fluorescent protein. Annu Rev Biochem, 1998. **67**: p. 509-44.

29. Baumann, C.K. and M. Castiglione-Gertsch, Estrogen receptor modulators and down regulators: optimal use in postmenopausal women with breast cancer. Drugs, 2007. **67**(16): p. 2335-53.

30. Miller, S., et al., A rapid and sensitive reporter gene that uses green fluorescent

protein expression to detect chemicals with estrogenic activity. Toxicol Sci, 2000. **55**(1): p. 69-77.

31. Sin, A., et al., The design and fabrication of three-chamber microscale cell culture analog devices with integrated dissolved oxygen sensors. Biotechnol Prog, 2004. **20**(1): p. 338-45.
32. Viravaidya, K., A. Sin, and M.L. Shuler, Development of a microscale cell culture analog to probe naphthalene toxicity. Biotechnol Prog, 2004. **20**(1): p. 316-23.
33. Shuler, M.L. and H. Xu, Novel cell culture systems: nano and microtechnology for toxicology, in Computational Toxicology: Risk Assessment For Pharmaceutical and Environmental Chemicals, S. Ekins, Editor. 2007, John Wiley & Sons: New York. p. 693-724.
34. Gerlowski, L.E. and R.K. Jain, Physiologically based pharmacokinetic modeling: principles and applications. J Pharm Sci, 1983. **72**(10): p. 1103-27.
35. Soto, A., et al., The E-SCREEN assay as a tool to identify estrogens: an update on estrogenic environmental pollutants. Environ Health Perspect. , 1995. **1003 Suppl 7**: p. 113-22.
36. Villalobos, M., et al., The E-screen assay: a comparison of different MCF7 cell stocks. Environ Health Perspect, 1995. **103**(9): p. 844-50.
37. Shang, Y. and M. Brown, Molecular determinants for the tissue specificity of SERMs. Science, 2002. **295**(5564): p. 2465-8.
38. Nishida, M., The Ishikawa cells from birth to the present. Hum Cell, 2002. **15**(3): p. 104-17.
39. Hewitt, S.C. and K.S. Korach, Estrogen receptors: structure, mechanisms and function. Rev Endocr Metab Disord, 2002. **3**(3): p. 193-200.
40. Pear, W.S., M.L. Scott, and G.P. Nolan, Rapid production of high titer, helper-

free retroviruses using transient transfection, in Methods in Molecular Medicine:Gene therapy protocols, P.D. Robbins, Editor. 1997, Humana Press: Totowa, NJ. p. 41-57.

41. Simard, J., et al., Blockade of the stimulatory effect of estrogens, OH-tamoxifen, OH-toremifene, droloxifene, and raloxifene on alkaline phosphatase activity by the antiestrogen EM-800 in human endometrial adenocarcinoma Ishikawa cells. Cancer Res, 1997. **57**(16): p. 3494-7.
42. Howell, A., et al., ICI 182,780 (Faslodex): development of a novel, "pure" antiestrogen. Cancer, 2000. **89**(4): p. 817-25.
43. Wakeling, A.E., M. Dukes, and J. Bowler, A potent specific pure antiestrogen with clinical potential. Cancer Res, 1991. **51**(15): p. 3867-73.
44. Payne, J., et al., Improving the reproducibility of the MCF-7 cell proliferation assay for the detection of xenoestrogens. Sci Total Environ, 2000. **248**(1): p. 51-62.
45. Paech, K., et al., Differential ligand activation of estrogen receptors ERalpha and ERbeta at AP1 sites. Science, 1997. **277**(5331): p. 1508-10.
46. Swaby, R.F., C.G. Sharma, and V.C. Jordan, SERMs for the treatment and prevention of breast cancer. Rev Endocr Metab Disord, 2007. **8**(3): p. 229-39.
47. Shah, Y.M., et al., Selenium disrupts estrogen receptor (alpha) signaling and potentiates tamoxifen antagonism in endometrial cancer cells and tamoxifen-resistant breast cancer cells. Mol Cancer Ther, 2005. **4**(8): p. 1239-49.
48. Menendez, J.A., et al., Inhibition of tumor-associated fatty acid synthase activity antagonizes estradiol- and tamoxifen-induced agonist transactivation of estrogen receptor (ER) in human endometrial adenocarcinoma cells. Oncogene, 2004. **23**(28): p. 4945-58.
49. Liu, H., J.L. Bolton, and G.R. Thatcher, Chemical modification modulates

estrogenic activity, oxidative reactivity, and metabolic stability in 4'F-DMA, a new benzothiophene selective estrogen receptor modulator. Chem Res Toxicol, 2006. **19**(6): p. 779-87.

50. Barsalou, A., et al., Growth-stimulatory and transcriptional activation properties of raloxifene in human endometrial Ishikawa cells. Mol Cell Endocrinol, 2002. **190**(1-2): p. 65-73.
51. Bader, Y., et al., Synergistic effects of deuterium oxide and gemcitabine in human pancreatic cancer cell lines. Cancer Lett, 2008. **259**(2): p. 231-9.
52. Mahmood, I. and M.D. Green, Drug interaction studies of therapeutic proteins or monoclonal antibodies. J Clin Pharmacol, 2007. **47**(12): p. 1540-54.
53. Arnold, S.F., et al., Synergistic responses of steroidal estrogens in vitro (yeast) and in vivo (turtles). Biochem Biophys Res Commun, 1997. **235**(2): p. 336-42.
54. Willingham, E., Endocrine-disrupting compounds and mixtures: unexpected dose-response. Arch Environ Contam Toxicol, 2004. **46**(2): p. 265-9.
55. Crofton, K.M., et al., Thyroid-hormone-disrupting chemicals: evidence for dose-dependent additivity or synergism. Environ Health Perspect, 2005. **113**(11): p. 1549-54.
56. Ramamoorthy, K., et al., Estrogenic activity of a dieldrin/toxaphene mixture in the mouse uterus, MCF-7 human breast cancer cells, and yeast-based estrogen receptor assays: no apparent synergism. Endocrinology, 1997. **138**(4): p. 1520-7.
57. Mumtaz, M.M., et al., Gene induction studies and toxicity of chemical mixtures. Environ Health Perspect, 2002. **110 Suppl 6**: p. 947-56.
58. Justus, T. and S.M. Thomas, Evaluation of transcriptional fusions with green fluorescent protein versus luciferase as reporters in bacterial mutagenicity tests. Mutagenesis, 1999. **14**(4): p. 351-6.

59. Sprangers, M.C., et al., Quantifying adenovirus-neutralizing antibodies by luciferase transgene detection: addressing preexisting immunity to vaccine and gene therapy vectors. J Clin Microbiol, 2003. **41**(11): p. 5046-52.

60. Kraus, W.L., M.M. Montano, and B.S. Katzenellenbogen, Identification of multiple, widely spaced estrogen-responsive regions in the rat progesterone receptor gene. ol Endocrinol, 1994. **8**(8): p. 952-69.

CHAPTER 3*

QUANTIFICATION OF CHEMICAL - POLYMER SURFACE INTERACTIONS IN MICROFLUIDIC CELL CULTURE DEVICES

3.1 Abstract

Microfluidic cell culture devices have been used for drug development, chemical analysis and environmental pollutant detection. Due to the decreased fluid volume and increased surface area to volume ratio, interactions between device surfaces and the fluid is a key element that affects the performance and detection accuracy of microfluidic devices, particularly if fluid is recirculated by a peristaltic pump. However, this issue has not been studied in detail in a microfluidic cell culture environment. In this study, chemical loss and contaminant leakage from various polymer surfaces in a microfluidic setup were characterized. The effects of hydrophilic coating with Poly (vinyl alcohol), Pluronic® F-68 and multi-layer ionic coating were measured. We observed significant surface adsorption of estradiol, doxorubicin, and verapamil with PharMed® BPT tubing, while PTFE/BPT and stainless steel/BPT hybrid tubing caused less chemical loss in proportion to the fraction of BPT tubing in the hybrid system. Contaminants leaching out of the BPT tubing were found to be estrogen receptor agonists as determined by estrogen induced green fluorescence expression in an estrogen responsive Ishikawa cell line. These contaminants also caused interference with an estradiol ELISA assay. Stainless Steel/BPT hybrid tubing caused the least interference with ELISA. In summary, polymer surface and chemical interactions inside microfluidic systems should not be

[1] This chapter is based on "Quantification of Chemical - Polymer Surface Interactions In Microfluidic Cell Culture Devices" by Hui Xu and Michael L. Shuler, Biotechnol Prog, 25(2):543-51, 2009

neglected and require careful investigations when results from a microfluidic system are compared with results from a macro scale cell culture setup.

3.2 Introduction

The development of microfluidic cell culture devices has been rapid in the areas of bioprocessing, drug development, toxicology assessment and clinical diagnosis[1, 2]. Minimization of device size lowers device cost, decreases chemical usage and waste production, and potentially accelerates interactions between chemicals and cells or sensors due to decreased diffusion distances. In addition, introduction of flow into cell culture devices allows dynamic and precise control over cellular and subcellular micro environment, provides physiology-related shear forces, and enables continuous feeding of cells [3-5].

Materials used for microfluidic cell culture devices may be glass, silicon, ceramics, metal, plastics or polymer hydrogels [5-10]. However, disposable plastic materials are most popular because of their low cost and disposable nature, which significantly reduces preparation and cleanup time, avoids cross-contamination, and makes devices lightweight and portable. Examples of such materials include polystyrene, polyethylene, polycarbonate, silicon, Polydimethylsiloxane (PDMS) and Poly(methyl methacrylate) (PMMA, Plexiglas®) [11].

Flow systems typically use peristaltic or diaphragm pumps. Peristaltic pumps are especially useful since the moving parts are not in contact with the fluid. However, the operation of a peristaltic pump usually requires flow through soft plastic tubing. Popular tubing materials used in pharmaceutical and biotechnology applications with a peristaltic pump include silicone, polyvinyl chloride (PVC), and polypropylene-based

PharMed® BPT. The latter one is widely used with cell culture due to its durability, good chemical resistance and excellent biocompatibility.

Interactions between polymers and chemicals have been extensively investigated in macro-scale devices for bioprocessing and pharmaceutical manufactures. Non-specific surface adsorption caused chemical loss have been characterized. For example, adsorption of protein onto PDMS, PMMA [12, 13] are significant. And loss of linoleic acid or cholesterol onto polyethylene cell culture medium storage bag [14] and polypropylene cell culture devices have been found to affect cell growth negatively [15]. A second concern regarding polymer-fluid interactions is the leakage of plasticizer and additives from polymers. Bisphenol A (BPA) leaks from used polycarbonate into water to levels of 310 ug per L [16]. And di-(2-ethylhexyl phthalate) (DEHP) migration from PVC films used extensively in food packaging has raised health concerns [17]. These interactions are influenced by temperature, type of solution, pH, etc. Deposition of hydrophilic polymers such as poly (ethylene glycol) (PEG) and poly (vinyl alcohol) (PVA) onto polymer surfaces is the most common method to both minimize non-specific adsorption and to decrease migration of contaminant from polymers [12, 17, 18].

Despite extensive previous work on characterizing chemical-polymer interactions at macro-scale, few studies have quantified such interactions in a dynamic microfluidic cell culture environment. One of the key characteristics of microfluidic devices is the high surface area to volume ratio. Many microfluidic cell culture devices try to reproduce in vivo like cellular micro environment where the physiological value of liquid to cell volume ratio is about 0.5; this ratio in traditional cell culture flasks and dishes is from 200 to 300. As a result, interactions between fluid and device surface

are amplified in a microfluidic system. Chemical loss due to surface adsorption and migration into polymer matrix should increase in high surface area to volume systems. In addition, potential leaching of chemicals from tubing is also of great concern than in traditional large-scale bioreactors. For example, significant loss of hydrophobic compounds such as Nile Red and dodecyl sulfate was significant due to either absorption[19] or adsorption[20] within PDMS microfluidic structures.

Our group has developed microscale cell culture analog (microCCA), also called “Body-on-a-Chip” devices, to evaluate the efficacy and toxicity of potential pharmaceuticals and environmental chemicals [4, 5, 21]. A microCCA device is a simplified and minimized model of the human body, using mammalian cell cultures to represent key functions of specific organs. Multiple human cell lines, such as the human mammary, endometrial and liver cells, are cultured in respective organ chambers. These chambers are designed to embody the structure of a Physiologically Based Pharmacokinetic (PBPK) model [22] using living cells in a bioreactor compartment instead of differential equations. Cell culture medium (total volume of 200 ul) is recirculated inside a closed-loop system consisting of a microCCA silicon chip sandwiched between two Plexiglas® housing pieces, a small medium reservoir, and a 55 cm long BPT tube that connects the reservoir and the chip together. About 20 cm of tubing is embedded in a peristaltic pump to drive flow. Cells have been successfully cultured on the device for up to 96 h with good cell viability. In proof-of-concept studies, a microCCA was used to test potential mechanisms of toxicity of naphthalene on lung cells [4, 5]. A hypothetical mechanism where lung toxicity was due to conversion of naphthalene in the liver to naphthoquinone and the circulation of naphthoquinone from the liver to other tissue compartments was found to be plausible. Further, it was demonstrated that fat provided partial protection of lung cells from

death and glutathione depletion when challenged with naphthalene or naphthoquinone [23]. Current applications include selection of drug resistance modulators [24], drug screening for cancer therapy, and toxicity assessments of environmental hormones. It is in this latter application that chemical leaching and adsorption are especially problematic.

Most hormones are very potent and the concentrations required for the body to respond are very low (nM to uM) compared to many other chemicals (uM to mM). In addition, most hormones, such as estrogens, are hydrophobic compounds. Consequently, the non-specific interactions between hydrophobic compounds with hydrophobic polymer surfaces cannot be overlooked. Furthermore, contaminates leaked from polymers will accumulate in a closed-loop recirculation system, and are more likely to influence or alter experimental outcomes.

In this study chemical adsorption and contaminant leakage from polymer surfaces were characterized using HPLC, enzyme-linked immunosorbent assay (ELISA) and a green fluorescence protein (GFP) based cell line assay. Our results show that 17β-Estradiol (E2), doxorubicin hydrochloride (Dox), and verapamil (VRP) in cell culture media experienced significant loss after long-term contact with plastic BPT tubing. Hydrophilic surface coatings didn't eliminate this problem. Stainless steel (SS) and PTFE hybrid tubes were able to alleviate adsorption. In addition, contaminates released from BPT tubing caused estrogen stimulated cellular responses in human endometrial cells. Interference was also detected in PTFE tubing with or without hydrophilic coatings. Stainless steel hybrid tubing caused the least interference in estradiol ELISA. When microfluidic systems are used for toxicity assessments and for detection of low concentration of chemicals, careful investigation of surface

adsorption and contamination release must be conducted.

3.3 Materials and methods

3.3.1 Chemicals and reagents

E2, Dox, daunorubicin, VRP, benzo-f-quinoline, polybrene, dextran sulfate, PVA and Pluronic® F-68 (PF) were purchased from Sigma (St. Louis, MO). Defined fetal bovine serum (FBS) and charcoal/dextran treated fetal bovine serum (CDFBS) with reduced steroid levels were from Hyclone (Logan, UT). E2 ELISA Kit was from Cayman Chemical (Ann Arbor, MI).

Microbore PharMed® BPT tubing (ID = 0.25 mm) and polytetrafluoroethylene (PTFE) tubing were purchased from Cole-Parmer (Vernon Hills, IL). Stainless steel hypodermic tubing (24G, ID = 0.30 mm) was from Small Parts, Inc (Miami Lakes, FL). The peristaltic pump used in this study was a multi-channel Watson-Marlow 205S pump (Watson-Marlow and Bredel, Baldwinsville, NY). Polystyrene stripwells used as medium reservoirs were purchased from Corning Incorporation (Corning, NY). Molded PTFE/Silicone Liners were from Biotech Solutions (Vineland, NJ).

3.3.2 Ishikawa-GFP cell line maintenance and GFP assay

The development of stable Ishikawa-GFP cell line for quantification of estrogenic compounds has been previously described[25]. In short, a two tandem estrogen response elements (2ERE) – adenoviral E4 promoter – GFP reporter gene construct pQCXIP-2ERE-GFP was introduced into Ishikawa cells through retrovirus infection. Successfully transfected cells were selected out with antibiotic selection and fluorescence activated cell sorting (FACS).The stable transfectant Ishikawa-GFP cell line exhibited increased GFP expression when exposed to estrogens. Ishikawa-GFP

cells were cultured in minimum essential medium (MEM) (Invitrogen, Carlsbad, CA) supplied with 10% FBS and maintained at 37°C in a humidified, 5% CO_2, 95% atmosphere incubator.

For GFP assay, Ishikawa-GFP cells were seeded into 96-well plates (Costar, Corning, NY) at initial concentrations of 1.4 x 10^4 cells per well. Cells were allowed to attach overnight. Frozen medium samples from experiments were thawed. Then 0.2 mM L-glutamine was added to medium samples to compensate for glutamine decomposition during 3 day incubation at 37°C. In addition, medium samples from the experiments assessing the loss of E2 in tubing were diluted 10,000 to avoid the saturation of GFP signals with 0.1 nM or higher concentrations of E2. Prepared medium samples of 100 ul were then added into each well of cell culture after equilibration to 37°C. GFP fluorescence intensities were quantified after 48 h. Cells were observed and imaged under an IMT-2 phase contrast and fluorescence microscope (Olympus America Inc., Center Valley, PA) at 100 X. Fluorescence images were captured with a Retiga CCD camera (Qimaging, Burnaby, BC, Canada) in a 12 bit grayscale format.

3.3.3 Quantification of association of compounds to tubing surfaces

Rather than using a full microCCA system, a simpler system was used for recirculation through a reservoir (Figure 3.1A). Experiments were performed with a Watson-Marlow 205S multi-channel peristaltic pump. Chemicals of interested, 1 uM E2, Dox or VRP, were added into cell culture medium supplied with 10% CDFBS. 200 ul medium per well were then aliquoted into strips wells used as medium reservoirs. The wells were sealed with molded PTFE/silicone liners. Tubing used in this study were 55 cm long BPT tubing, BPT/PTFE hybrid (with 20 cm long BPT tubing and 35 cm long PTFE tubing or BPT/SS hybrid tubing (with 20 cm long BPT tubing and 35

cm long SS tubing) (Figure 3.1B). The 20 cm long soft BPT tubing was necessary to work with the peristaltic pump. The ends of each BPT or BPT hybrid tubing were inserted into the reservoir, and cell culture medium was then recirculated inside the tubing and the reservoir at 3 ul per min for 72 h. All tubes were sterilized by autoclaving for 30 min, rinsed with water for 30 min, and then rinsed again with appropriate medium before the experiments. All experiments were performed inside a humidified, 5% CO_2, 95% atmosphere cell culture incubator at 37°C. When the experiments were done, medium reservoirs were frozen at -20°C until further analysis with HPLC or ELISA.

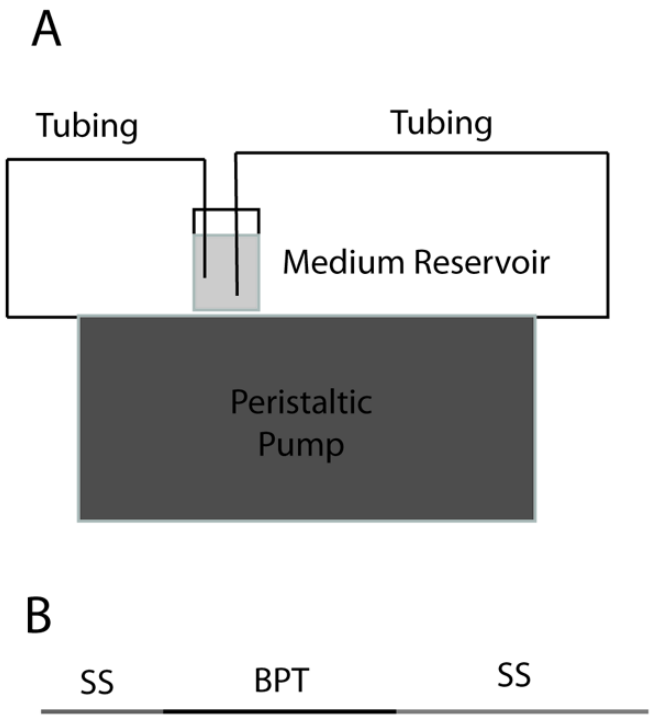

Figure 3.1 Schematic representation of experimental setup (Figure 3.1A), and the stainless steel (SS)/BPT hybrid tubing (Figure 3.1B) as an example of the hybrid tubing used in this study. The lengths of SS tubing and BPT tubing are 35 cm and 20 cm. The ends of the tubes were inserted into a medium reservoir with 200 ul cell culture medium. Flow rate was set at 3 ul per min.

Two types of controls samples were prepared for each set of experiments. Frozen control samples were 500 ul unused medium samples maintained at -20℃ in polypropylene vials. Reservoir only control samples were 200 ul medium samples in the polystyrene reservoirs that were incubated along with the experimental medium samples in the cell culture incubator, but without medium recirculation.

3.3.4 Hydrophilic surface coating

1% (w/v) PVA, 3% (w/v) PF or multi-ionic (MI) layer coating were used to coat the inner surface of various tubing materials. For PVA and PF coating, tubes were first rinsed with sterile Milli-Q water for 30 min at 20 ul per min. 1% PVA or 3% PF was then pumped through the tubes for 10 min and allowed to sit for 25 min. Fluid was then pumped out of the tubes, and air was pumped through the tubing for 30 min. MI coating was adapted from a method described by Johns and Hayes [26]. Tubes were first treated with 0.1 M sodium hydroxide for 4 min, followed with a 4 min rinsing with sterile Milli-Q water. A 5% (w/v) polybrene solution was pumped through the tubes continuously for 2 min and allowed to stand for 15 min before being pumped out. 3% dextran sulfate was then pumped through the tubes for 2 min and allowed to stand for 15 min. Tubing was then rinsed with sterile Milli-Q water for 10 min, followed with appropriate medium rinse for 30 min.

Tubes were sterilized with a dry autoclave run of 30 min before surface coatings. All the coating processes were performed within a cell culture hood to maintain sterility.

3.3.5 Chemical loss in medium droplets placed on top of plastic pieces

Polycarbonate and Plexiglas® were cut into 2 cm x 2 cm square pieces and wipe-

cleaned with 70% ethanol. Plastic pieces were treated with oxygen plasma in an Expanded Plasma Cleaner (Harrick Plasma, Ithaca, NY) for 2 min followed by PF or PVA coatings. 200 ul cell culture media with or without 1 uM E2 were aliquoted onto the plastic pieces and incubated for 24 h in a humidified, 5% CO_2, 95% atmosphere cell culture incubator at 37°C. Medium droplets were aspirated carefully into 1 ml polypropylene tubes (VWR.com, West Chester, PA) and were frozen for further analysis with ELISA.

3.3.6 Quantification of Dox and VRP with reverse-phase HPLC

Dox and VRP were extracted from medium samples with a cold methanol precipitation method described previously in literature [24, 27]. In short, 140 ul ice cold methanol was mixed with 50 ul cell culture medium samples and 10 ul internal standard: 1.6 uM daunorubicin for Dox or 0.33 uM benzo-f-quinoline for VRP. The mixture was mixed well and centrifuged at 4℃ for 10 min at 9000 x g. The supernatants were then transferred into polypropylene screw top HPLC vials (Waters Corp., Milford, MA) for analysis.

Dox and VRP were quantified with a Waters 2690 separation module and a Waters 474 fluorescence detector (Waters Corp., Milford, MA) following the method described in the literature [24, 27, 28]. The column used for Dox was a 150 mm x 4.6 mm Xterra RP C18 column (Waters Corp.; Milford, MA). Fluorescence detection was realized at excitation wavelength of 480 nm and emission wavelength of 560 nm. The mobile phase consisted of 65% 50 mM mono sodium phosphate, 25% acetonitrile and 2% 1-isopropanol, with a flow rate of 1 ml per min. Column used for VRP is a 150 mm x 3.9 mm Novapak column (Waters Corp., Milford, MA). VRP was detected at 276 /310 nm (Ex./Em.) with a mobile phase consisting of 35% acetonitrile and 0.03%

triethylamine, pH = 3.8. Flow rate was set at 0.9 ml per min.

3.3.7 Quantification of E2 and interference factors with ELISA

E2 in medium samples were quantified with an Estradiol ELISA kit (Cayman Chemical, Ann Arbor, Michigan) as instructed. The measurement is based on the competition between estradiol and an estradiol-acetylcholinesterase conjugate for limited amount of estradiol antiserum. The concentration of estradiol-acetylcholinesterase conjugate is held constant, while the amount of estrogen in the samples varies. The antiserum-estradiol complex binds to the IgG mouse monoclonal antibody that was previously attached to the well. After washing, color is developed with Ellman's reagent, and optical absorbance is measured at 412 nm with a VERSAmax microplate reader (Molecular Devices, Sunnyvale, CA).

Medium samples were diluted when necessary in order to be in the detection range of the ELISA test. 300 times dilutions were conducted for medium samples from the experiments for quantifying the loss of E2 in various tubing, where 1 uM E2 was added into the medium at the starting point of the tests.

3.3.8 Ethanol extraction of E2 from tubing surface

Immediately following the experiments quantifying loss of E2 within plastic tubing, tubes were rinsed with 10 ml Milli-Q water to remove loosely adhered chemicals. Each tubing was then connected to a HPLC polypropylene vial (Waters Corp., Milford, MA) filled with 200 ul absolute ethanol, which was recirculated through the tubing overnight at 20 ul per min to extract E2 off the tubing surface.

The extracts were evaporated to dryness in a SpeedVac concentrator (Thermo Savant,

Holbrook, NY), and the remaining residues were re-dissolved completely into 200 ul 1 M phosphate buffer (Cayman Chemical, Ann Arbor, MI). Samples were frozen at -20°C until further analysis. E2 concentrations in the buffer were quantified with ELISA.

3.3.9 Statistical analysis

Four measurements based on two independent tubing were made for each individual experiment condition. Means and standard errors of the measurements were calculated using Origin (OriginLab, MA). Data are presented in the figures as the mean ± standard error of the mean.

3.4 Results and discussions

3.4.1 Loss of E2, Dox and VRP in microbore BPT tubing

Because of the hydrophobic nature of most plastics, they tend to adsorb small hydrophobic molecules such as lipids, proteins, vitamins and hormones onto their surfaces [14, 15]. However, limited studies have been conducted regarding chemical loss in microfluidic devices, inside which such polymer-chemical interactions are expected to be more prominent than in macro-scale fluidic devices due to increased surface area to volume ratio. In this study, losses of three hydrophobic compounds, E2, Dox and VRP in microbore tubes were characterized. These chemicals were selected because they were currently of interest to our lab and were being extensively used in our research projects. MicroCCA was designed based on human physiological parameters, and was a physical representation of a human body. Flow rate of the medium recirculation was calculated based on fluid residence time in individual organs [4, 5, 7]. The external reservoir represents ‘other tissue’ that were not present on the chip. Volume of the reservoir (200 ul) was selected to maintain the same trends

and order of magnitude of chemicals distribution in the tissues of interest. A larger volume of medium would increase volume/surface ratio and make the culture less physiologically realistic. In microCCA, the medium is recirculated constantly through the reservoir, tubing and cell culture chambers, which mimics the blood circulation pattern in the body. Such a system can address issues of reactive metabolite formation and tissue-tissue interaction through exchange of metabolites or signal molecules [4, 7]. Other experimental parameters such as the period of experiments were based on experimental protocols for use of a microCCA. Typical operation time for microCCA is 72 h. This period of 72 h is consistent with prior studies where, for example, 72 h was sufficient for the association of cholesterol and linoleic acid with polytheylene to reach steady-state [14].

Figure 3.2 shows the decreased chemical concentration in the cell culture medium due to recirculation in the BPT tubing. Chemical concentrations were quantified with HPLC. Data are plotted as percent of chemical concentration in the control samples that were kept frozen at -20℃ (frozen controls). All three chemicals, E2, Dox and VRP suffered significant loss due to adsorption to surfaces. For 1 uM E2 and VRP, incubation in polystyrene reservoirs at 37℃ for 72 h caused less than 9% chemical loss. However, recirculation within BPT tubing caused an additional 80% loss of E2. It also caused an additional 91% loss of VRP, leaving the amount of VRP remaining in the cell culture medium lower than the limit of detection with HPLC. For 1 uM Dox, half of the chemical was lost after 72 h at 37℃ in the reservoir, likely due to degradation of Dox because of light sensitive and unstable nature of this compound, as well as surface adsorption to the reservoir. Recirculation through the BPT tubing caused another 32% loss, leaving only 0.18 uM Dox in the cell culture medium after 72 h.

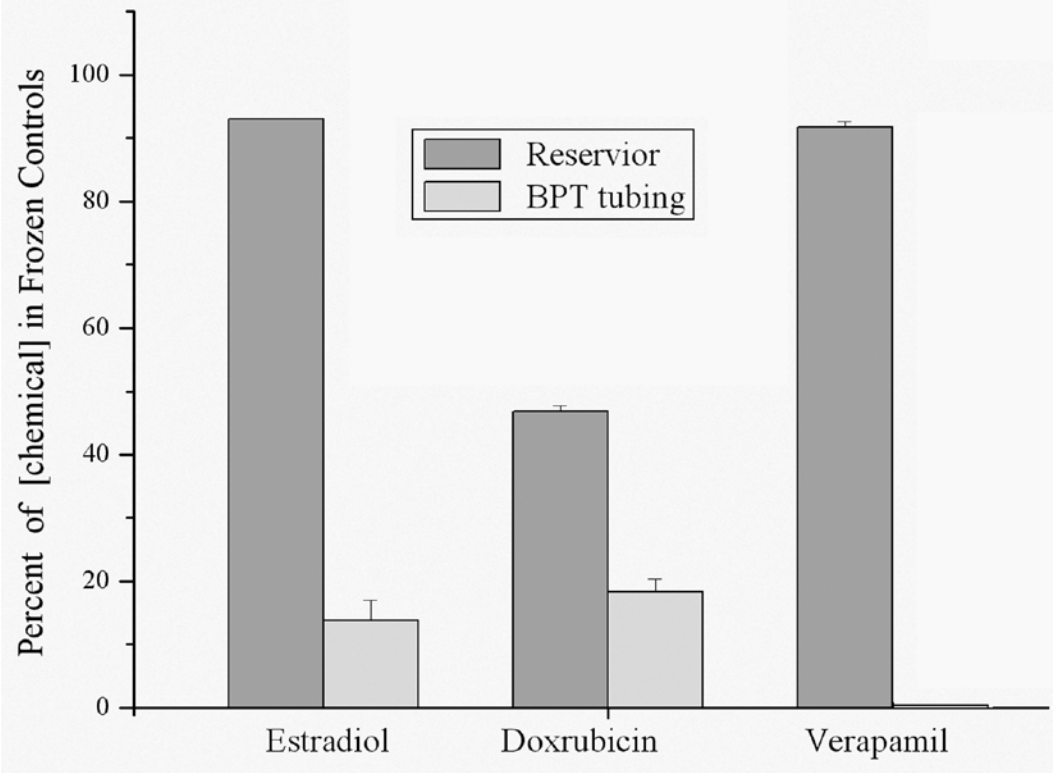

Figure 3.2 Chemical losses in medium after 72 h recirculation within BPT tubing. Data were plotted as the percent of [E2] in control samples that that were frozen and not recirculated through the tubing. The initial concentration of chemicals added into the medium was 1 uM. Verapamil values were undetectable after recirculation through the BPT tubing. A value of 100% corresponds to the measured level in control samples that were frozen and not recirculated through the tubing.

Loss of E2 was also demonstrated with Ishikawa-GFP cell based transcription assay. Ishikawa-GFP is a human endometrial carcinoma cell line with stable estrogen stimulated GFP expression [25]. Natural estrogenic compounds such as E2, and environmental estrogens such as o,p-DDT and BPA bind to estrogen receptors and interact with ERE to initiate GFP expression. Ishikawa-GFP exhibited increased GFP expression to estrogens in a dose-response manner with an EC50 value of 9 pM E2. GFP responses saturated with E2 concentrations higher than 0.1 nM [25]. Such responses are specific to estrogens. Before the GFP assay, 0.2 mM L-glutamine was

added into all medium samples, which were maintained at 37°C for 3 days in the experiments characterizing E2 loss. Since L-glutamine is more labile in solution than other amino acids and its breakdown is accelerated at 37°C, replenishment is important to prevent glutamine from limiting cellular response [29]. The medium samples were never freeze-thawed more than once if the medium was to be used for cell culture.

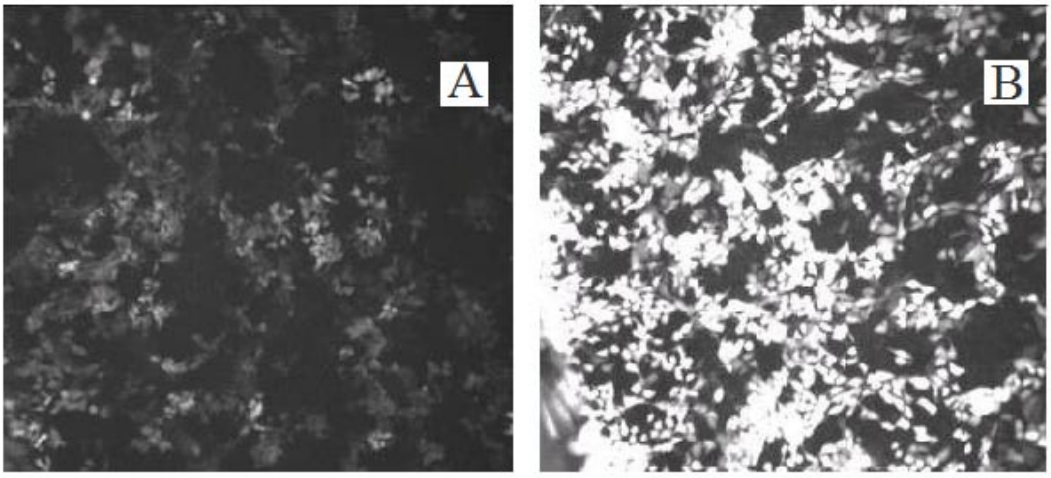

Figure 3.3 Responses of Ishikawa-GFP cell to medium samples supplied with 1 uM estradiol and (A) recirculated within BPT tubing for 72 h, or (B) kept in the reservoirs without contact with the BPT tubing. Medium samples recirculated within BPT tubing induced less GFP expression in Ishikawa-GFP cells, indicating that less estradiol was available to the cells. Cells were imaged at X 100 .

Figure 3.3 presents response of Ishikawa-GFP cells to E2 in medium samples initially spiked with 1 uM E2 before the 3 day recirculation test. Medium samples were diluted 10,000 times to avoid the saturation of GFP responses. It was observed that after recirculation in BPT tubing, medium samples induced significantly less GFP expression (Figure 3.3A) than controls (Figure 3.3B). These results indicate that less E2 was available in the medium after 72 h's recirculation within BPT tubing compared

to samples that were kept in the reservoirs without contact with BPT tubes. This result is consistent with the measurements from HPLC.

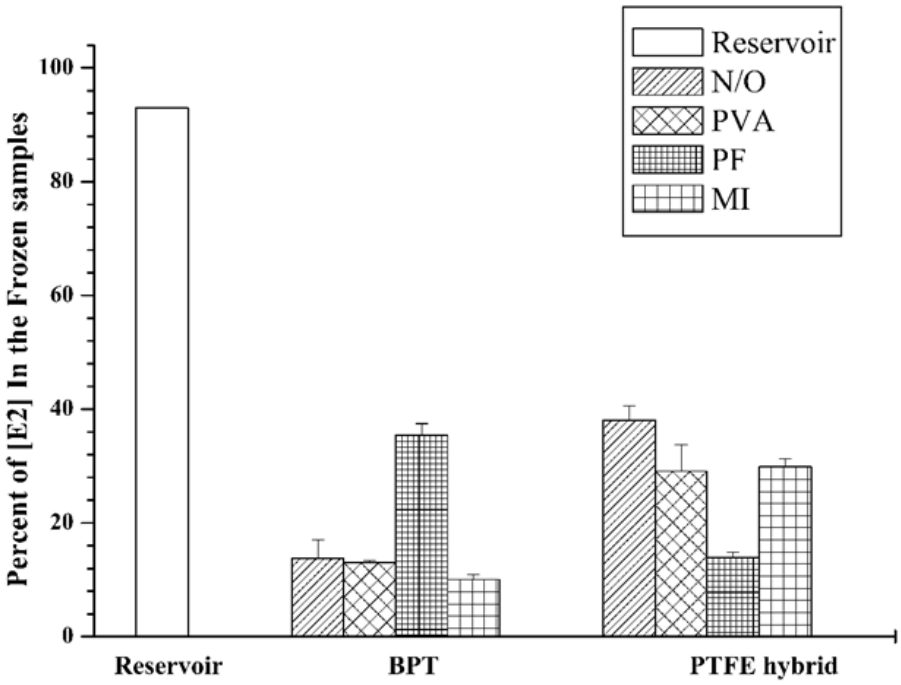

Figure 3.4 Effects on the loss of estradiol (E2) in BPT tubing and BPT/PTFE hybrid tubing with: N/O, no coating; PVA, Poly (vinyl alcohol) coating; PF, Pluronic® F-68 coating; MI, multi-ionic layer coating with polybrene and dextran sulfate. The reservoir control (Reservoir) corresponds to samples that were in the reservoir for 72 h without recirculation in the tubing. A value of 100% corresponds to the measured level in control samples that were frozen and not recirculated through the tubing.

3.4.2 Effects of hydrophilic coating on chemical adsorption

Most disposable labware and medical implements are fabricated from plastics. However their hydrophobic nature can cause issues with non-specific adsorption and

poor fluid wettability. Hydrophilic polymers such as PVA[30], Aerosol™, Geropon™ and Pluronic™ surfactants [30] have been used for surface functionalization of fluidic devices at both macro and micros scales. Multi-ionic (MI) layer, or polyelectrolyte multilayer coating is another popular surface modification method for microchip analytical devices [26]. PVA, Pluronic® F-68 (PF) and MI coating were easy to perform and require no harsh chemicals.

Figure 3.4 showed the effect of PVA, PF and MI hydrophilic coatings on the surface adsorption of E2 in BPT or BPT/PTFE hybrid tubing. The concentrations of E2 detected in the medium were plotted as the percent of amount of E2 in the samples frozen and never placed in the reservoir or re-circulated. With BPT tubing, PF coating decreased the adsorption of E2 significantly and increased the amount of E2 remaining in the reservoir. The effects of PVA or MI coatings, however, were negligible. Without hydrophilic coatings, PTFE/BPT hybrid tubing caused less E2 loss than BPT tubes, leaving three times' higher concentration of E2 in the medium after 72 h recirculation. Coating with PVA, PF and MI, surprisingly, increased surface adsorption of E2, while the effect by PF coating was more prominent. The losses of E2 with different hydrophilic coatings depend on the substrate (i.e. BPT or PTFE), which indicates the stabilities of hydrophilic coatings on BPT or PTFE might not enough during recirculation. The reason of using PTFE/BPT hybrid rather than PTFE tubing alone is that PTFE tubing is rigid while flexible BPT tubing was needed for insertion into the Watson-Marlow 205S peristaltic pump head. However, even at the best situation of PTFE/BPT tubing, only approximately 38% of 1 uM E2 was available in the medium. The loss of about 50% E2 caused by recirculation within plastic tubing, may greatly affect how cells respond to E2 and other hydrophobic compounds. Alternatives to peristaltic pumps that can maintain recirculation at 3 ul per min for extended periods

of times, which allow use of only PTFE tubing, would reduce adsorption.

It was unclear whether E2 losses were due to adsorption onto the tubing surface and migration of E2 into the plastic. To test this hypothesis, E2 on the tubing surface or near-surface was extracted with an overnight ethanol rinse, which was conducted after the tubes were used to recirculate 1 uM E2 medium for 72 h. The concentration of E2 detected in the extraction solution was plotted on the right side of Figure 3.5 (Figure 3.5R), and the quantity of E2 in the medium from Figure 3.4 was re-plotted in Figure 3.5 (Figure 3.5L) for comparison. All data are presented as the percent of E2 concentration in the frozen samples (initially spiked with 1 uM E2). It was observed that, when less E2 was detected left in the medium, a higher concentration of E2 was usually detected in the extraction solutions. And the total amount of E2, $\mathbf{T}_{E2} = [E2]_{medium} + [E2]_{extraction}$, was relatively constant despite the different coating conditions or tubes used. T_{E2} equaled about 50% of the amount of E2 initially added into the cell culture medium. The only exception was for BPT tubing without hydrophilic coating, where the total amount of E2 was measured lower than the other situations. BPT tubing is polypropylene based material with mineral oil and other blend materials. One possible explanation for this observation is that, when BPT tubing was not coated with hydrophilic polymers, mineral oil within the BPT matrix may have increased E2 migration into the tubing matrix; E2 diffused into the bulk polymer would not be extracted efficiently with ethanol. T_{E2} was different from total amount of E2 in the control sample (92%), possibly because of the incomplete extraction from the tubing surface, and again the inefficiency of ethanol rinsing to extract chemicals from the bulk polymer.

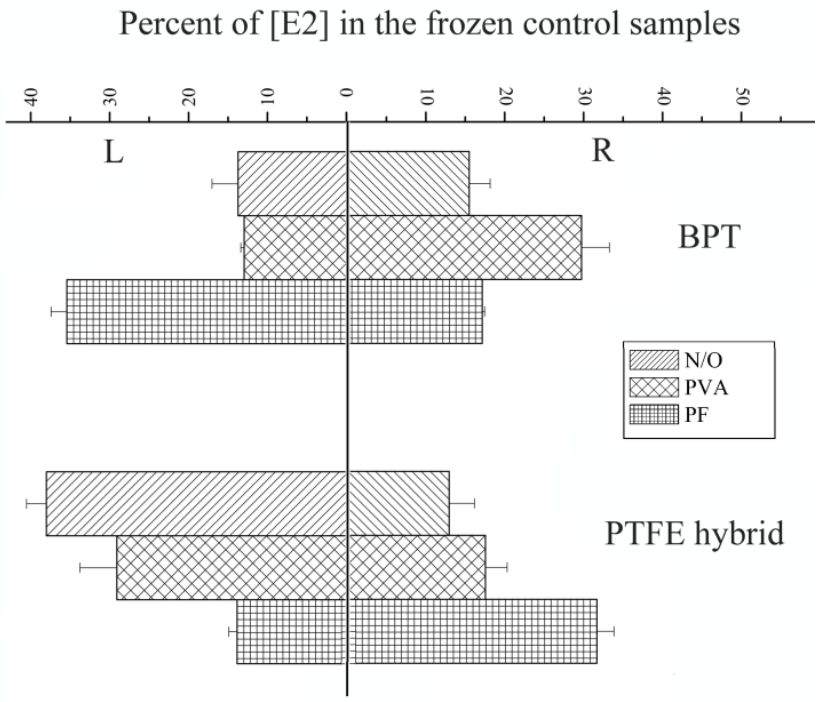

Figure 3.5 Extraction of estradiol (E2) from tubing surface (R). Data were plotted together with the amount of E2 measured in the medium (L) after recirculation within BPT or BPT/PTFE hybrid tubes coated with Poly (vinyl alcohol) (PVA), Pluronic® F68 (PF) or no coating (N/O). A value of 100% corresponds to the measured level of E2 in control samples that were frozen and not recirculated through the tubing.

3.4.3 Chemical leaching from polymer tubing

Manufacture of plastic tubes usually involves the use of solvents, plasticizers, antioxidants and other additives. These additives blended into the tubing material may leach out during autoclaving or normal use. As tubes used in microfluidic devices have small inner diameters (e.g. 0.19 mm), with the increased surface to fluid volume ratio in microbore tubing and microfluidic devices, contaminating chemicals leaching into the fluid may accumulate and cause unwanted interference. The kinetics of chemical leakage can be influenced by pH, temperature, type of solution, surfactants [31] and a variety of environmental parameters. Coating with hydrophilic polymers has been shown to decrease the release of contaminates such as plasticizers [17].

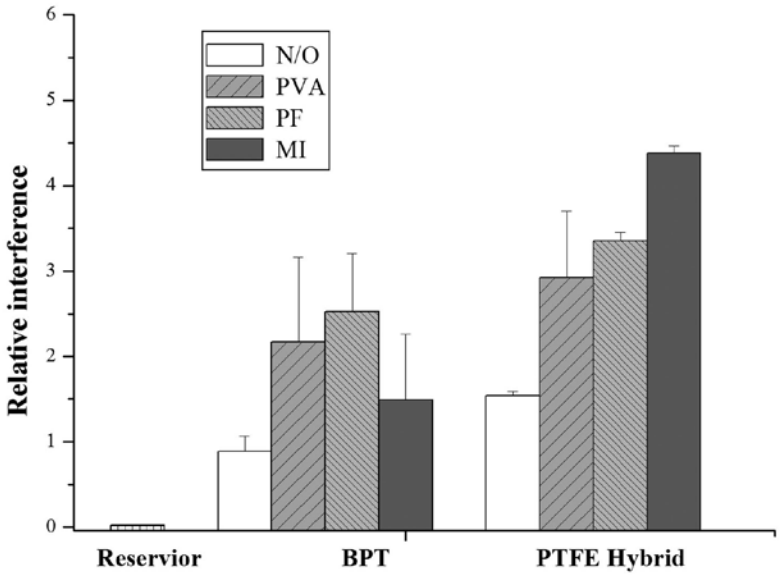

Figure 3.6 Interference with the E2 ELISA assay caused by medium recirculation for 72 h within BPT and PTFE/BPT hybrid tubing with different surface coatings. The interference values were presented as activities relative to the activity of 1nM E2. The reservoir control (Reservoir) corresponds to samples that were in the reservoir without recirculation in the tubing. N/O, no coating; PVA, Poly (vinyl alcohol); PF, Pluronic® F-68; MI, multi-ionic layer coating with polybrene and dextran sulfate.

We used estradiol ELISA to quantify the interference in medium introduced by recirculation inside tubes. As no E2 was added into the medium samples, an activity detected from the ELISA indicates the presence of certain compounds in the samples that interfere with the immunoassay. Although ELISA does not provide direct information for chemical identification, it allows the comparison of the relative amount of interference introduced by different materials and coating conditions. These interferences could be caused by chemicals with structures similar to E2, such as genistein, or any chemicals that alter ligand-antibody binding, including solvent. In this study, ethanol and dimethyl sulfoxide (DMSO) were used to dissolve chemicals; and mineral oil is a component in the BPT tubing. Under our experimental conditions,

ethanol, DMSO or mineral oil in the medium did not cause significant interference (with $p > 0.1$ using the Student's t-test) with the ELISA test with concentrations of 0.1% (v/v) or less (data not shown).

Recirculation of medium within BPT or PTFE/BPT hybrid tubing caused significant interference (Figure 3.6) compared to the condition without recirculation in tubes (reservoir only controls). The interference values were presented as activities relative to the activity of 1nM E2. Hydrophilic coatings with PVA, PF or MI didn't decrease contamination release, but instead caused a higher amount of interference. The antioxidant additive in polymer powder or solutions, such as butylated hydroxytoluene (BHT) in PF powder, which has been found to be weakly estrogenic in a human embryonic kidney fibroblast cell line based assays [32], may be the cause of increased interference in our ELISA measurements. Figure 3.7 presents the different responses of Ishikawa-GFP cells to medium samples (with no addition of E2) without recirculation (Figure 3.7A) or after being recirculated within tubes (Figure 3.7B). The samples that stayed only within the reservoirs didn't induce GFP expression. However, medium after a 72 h's recirculation within BPT tubing caused a significant GFP induction in Ishikawa-GFP cells. The expression of GFP was blocked with ICI 182,780 (Figure 3.7C), which increases degradation and down-regulates estrogen receptors [33]. These results indicates that contaminates were released from BPT tubing, and at least some of these contaminates were able to interact with estrogen receptors and elicit estrogen-like responses in Ishikawa-GFP cells.

The activity of such interference was in the order of 0.1% of the activity of 1uM E2. It was significant when compared to control samples when no E2 was added into the samples. However, it was insignificant and negligible when compared to the amount

of E2 (in the range of 0.1 to 1uM) in samples from the experiments quantifying the loss of E2 in tubing, thus had no effect on those experimental outcomes.

Figure 3.7 Responses of Ishikawa-GFP cells to cell culture medium samples (without addition of estradiol) kept (A) in the reservoir, or (B) recirculated within BPT tubing at 3 ul per min for 72 h. Contaminant leaked from the BPT tubing induced GFP expression in Ishikawa cells (B), which was blocked by 1 uM ICI182,780 (C). Cells were imaged at X 100.

The specific contaminates responsible for such interference have not been fully identified. We excluded the possibility of cross-contamination between tubes as tubes were all individually labeled and those used with E2 and those for experiments without E2 were separated. Based on literature reports, we speculate that these contaminates could be one or a mixture of plasticizers or other additives used to produce polypropylene or polypropylene-based BPT tubing. Various plasticizers used in plastic production, such as tris(2-ethylhexyl)trimellitate (TEHTM), di-isoheptyl phthalate (DIHP) [34] and bisphenol-A [16, 35, 36] have been found to be weak estrogens and induced estrogenic responses in reporter-gene based transcription assays [34, 37].

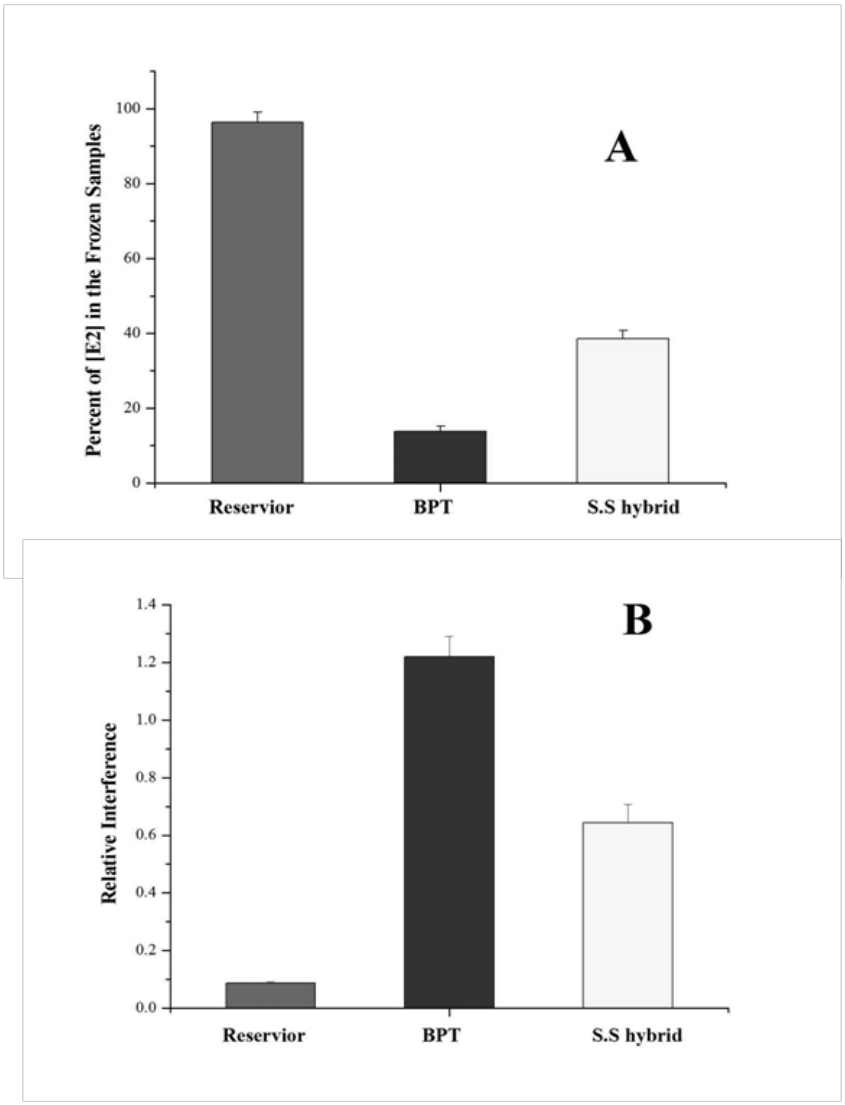

Figure 3.8 Comparison of (A) loss of Estradiol (E2) and (B) release of interference in BPT and stainless steel (SS)/ BPT hybrid tubing. With 1 uM E2 initially added into the medium, three-time higher concentration of estradiol was detected in medium within SS/BPT hybrid tubing compared to that in BPT tubing. The interference from stainless steel hybrid tubing was half of that amount from BPT tubing.

3.4.4 Loss of E2 and release of interference in stainless steel hybrid tubing

Stainless steel tubing is corrosion-resistant, exceptionally tough, relatively flexible, and is ideal for many applications in bioprocessing and analysis such as high pressure liquid chromatography. With stainless steel/BPT hybrid tubing, the adsorption loss of

E2 was decreased, but not eliminated. Three time higher concentration of E2 remained in the medium compared to BPT tubing alone (Figure 3.8A). Chemicals released from stainless steel tubing were also less problematic and caused about 60% less interference in the ELISA assay (Figure 3.8B) than chemicals released from the BPT or PTFE/BPT hybrid tubing.

3.4.5 Loss of E2 and release of interference into medium on top of plastic pieces

In addition to microbore tubing, most microfluidic devices use polymers such as Plexiglas®, PDMS, polycarbonate and other plastics as body or housing materials. In microCCA devices developed in our lab, the silicon microCCA chip is sandwiched between two Plexiglas® or polycarbonate pieces [4, 5, 7]. Medium recirculating inside the channels and cell culture chambers is in direct contact with the Plexiglas® or polycarbonate housing, which may cause chemical loss or contaminations as well as with the tubing. Such effects were quantified by measuring chemical loss and contamination release by placing a drop of medium (200 ul) onto clean plastic pieces. These experiments were performed for a period of 24 h instead of 72 h to minimize medium evaporation and contamination issues.

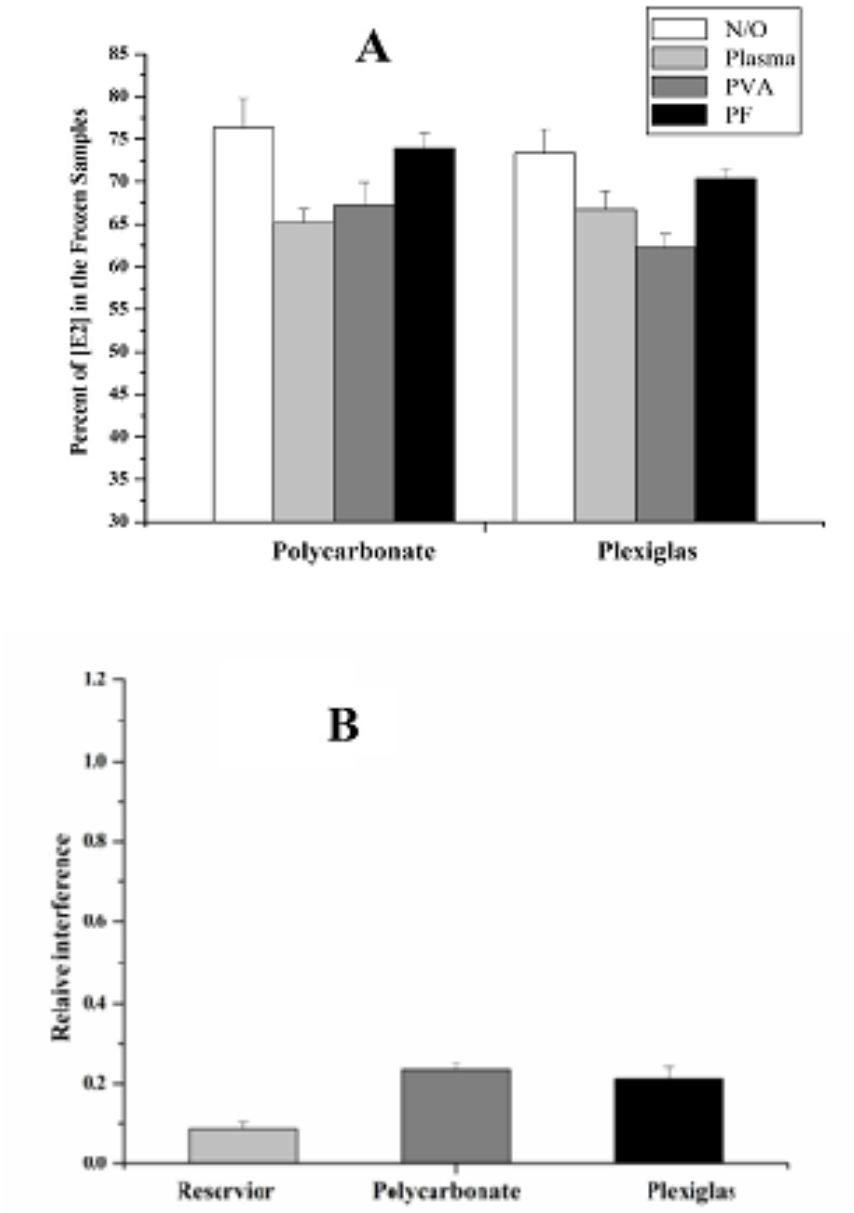

Figure 3.9 (A) Loss of estradiE2) and (B) release of interference from polycarbonate and Plexiglas® pieces. 200 ul media were placed onto square plastic pieces and incubated for 24 h. Plastics were treated with oxygen plasma (Plasma) and coated with Poly (vinyl alcohol) (PVA) or Pluronic® F-68 (PF) or with no surface treatment (N/O) right before the placement of medium drops. Plasma treatment and PVA coating caused more E2 loss compared to the other two conditions. Interference to ELISA caused by all conditions were observed but were minor compared to that from BPT tubing. The interference values were presented as activities relative to the activity of 1nM E2.

Significant losses of E2 were observed on both polycarbonate and Plexiglas® pieces with or without hydrophilic coatings (Figure 3.9A). Although plastic surfaces are usually oxidized and more hydrophilic after oxygen plasma treatment, in this study plasma treatment alone or followed by PVA coating slightly increased the loss of E2 and decreased its amount in the medium compared to no surface treatment (Figure 3.9A). Similar results were observed with PF coating followed by a plasma treatment. Incubations on polycarbonate or Plexiglas® pieces did caused a increase of interference to the ELISA assay, but the interference was much smaller compared to that caused by recirculation in polymer tubing (Figure 3.9B). Since these studies were carried on at static state rather than at a dynamic situation with constant flow, and the incubation time was relatively short, larger chemical loss and contaminant release are expected under microCCA experimental conditions. Plexiglas® and polycarbonate pieces used in this study were both new materials and no obvious difference between new Plexiglas® and polycarbonate was observed here. However, it has been reported that BPA was released from used polycarbonate plastic into waters [16].

3.5 Conclusions

In the present work, chemical losses and contaminant leakage inside a microfluidic cell culture device setup were characterized in both microbore polymer tubing and on selected plastic surfaces. Significant chemical loss (up to about 100%) was observed with E2, DOX and VRP with BPT tubing. The effect of hydrophilic coating on surface adsorption was material-dependent. PTFE/BPT and stainless steel/BPT hybrid tubing were more resistant to surface adsorption than BPT tubing alone. Chemicals leached from BPT tubing caused estrogenic responses in human endometrial cells, and interfered with E2 ELISA assays. Stainless steel was able to decrease this interference. Since the embedded segment of BPT tubing inside the pump is constantly squeezed

and stretched during peristaltic pumping, both chemical release and chemical adsorption are expected to be higher than BPT tubing outside the pump. Less chemical adsorption and contaminant release are expected if 100% PTFE or stainless steel materials are used, which may require the replacement of current peristaltic pump with other micropumps to eliminate the need for soft tubing. Glass or ceramic capillaries are also possible choices for similar applications but they have not been tested in our system due to their fragility.

As a result, chemical loss and contaminant release may alter experimental outcomes, and need be considered when results from microfluidic devices are compared to conventional cultures especially when low concentrations of hydrophobic compounds are studied. For example, chemical loss may affect dose responses and the measurement of EC50 with cells cultured in microfluidic devices. Interference caused by chemical leaching in a microfluidic system should also be carefully examined and eliminated when possible.

We believe that this study should be of general interest especially to researchers working with hydrophobic compounds and microfluidic devices. It is expected that these studies may serve as a guideline for their future studies.

REFERENCES

1. Atencia, J. and D.J. Beebe, Controlled microfluidic interfaces. Nature, 2005. **437**(7059): p. 648-55.
2. Whitesides, G.M., The origins and the future of microfluidics. Nature, 2006. **442**(7101): p. 368-73.
3. Takayama, S., et al., Subcellular positioning of small molecules. Nature, 2001. **411**(6841): p. 1016.
4. Viravaidya, K., A. Sin, and M.L. Shuler, Development of a microscale cell culture analog to probe naphthalene toxicity. Biotechnol Prog, 2004. **20**(1): p. 316-23.
5. Sin, A., et al., The design and fabrication of three-chamber microscale cell culture analog devices with integrated dissolved oxygen sensors. Biotechnol Prog, 2004. **20**(1): p. 338-45.
6. Choi, N.W., et al., Microfluidic scaffolds for tissue engineering. Nat Mater, 2007. **6**(11): p. 908-15.
7. Shuler, M.L. and H. Xu, Novel cell culture systems: nano and microtechnology for toxicology, in Computational Toxicology: Risk Assessment For Pharmaceutical and Environmental Chemicals, S. Ekins, Editor. 2007, John Wiley & Sons: New York. p. 693-724.
8. Leclerc, E., Y. Sakai, and T. Fujii, Microfluidic PDMS (polydimethylsiloxane) bioreactor for large-scale culture of hepatocytes. Biotechnol Prog, 2004. **20**(3): p. 750-5.
9. Wong, A.P., et al., Partitioning microfluidic channels with hydrogel to construct tunable 3-D cellular microenvironments. Biomaterials, 2008. **29**(12): p. 1853-61.

10. Frisk, T., et al., A concept for miniaturized 3-D cell culture using an extracellular matrix gel. Electrophoresis, 2005. **26**(24): p. 4751-8.
11. Kim, J.E., J.H. Cho, and S.H. Paek, Functional membrane-implanted lab-on-a-chip for analysis of percent HDL cholesterol. Anal Chem, 2005. **77**(24): p. 7901-7.
12. Wu, D., et al., Grafting epoxy-modified hydrophilic polymers onto poly(dimethylsiloxane) microfluidic chip to resist nonspecific protein adsorption. Lab Chip, 2006. **6**(7): p. 942-7.
13. Bi, H., et al., Deposition of PEG onto PMMA microchannel surface to minimize nonspecific adsorption. Lab Chip, 2006. **6**(6): p. 769-75.
14. Altaras, G.M., et al., Quantitation of interaction of lipids with polymer surfaces in cell culture. Biotechnol Bioeng, 2007. **96**(5): p. 999-1007.
15. Kadarusman, J., et al., Growing cholesterol-dependent NS0 myeloma cell line in the wave bioreactor system: overcoming cholesterol-polymer interaction by using pretreated polymer or inert fluorinated ethylene propylene. Biotechnol Prog, 2005. **21**(4): p. 1341-6.
16. Howdeshell, K.L., et al., Bisphenol A is released from used polycarbonate animal cages into water at room temperature. Environ Health Perspect, 2003. **111**(9): p. 1180-7.
17. Lakshmi, S. and A. Jayakrishnan, Migration resistant, blood-compatible plasticized polyvinyl chloride for medical and related applications. Artificial Organs, 1998. **22**(3): p. 222-229.
18. Barrett, D.A., et al., Resistance to nonspecific protein adsorption by poly(vinyl alcohol) thin films adsorbed to a poly(styrene) support matrix studied using surface plasmon resonance. Anal Chem, 2001. **73**(21): p. 5232-9.
19. Toepke, M.W. and D.J. Beebe, PDMS absorption of small molecules and

consequences in microfluidic applications. Lab Chip, 2006. **6**(12): p. 1484-6.

20. Ocvirk, G., et al., Electrokinetic control of fluid flow in native poly(dimethylsiloxane) capillary electrophoresis devices. Electrophoresis, 2000. **21**(1): p. 107-15.
21. Viravaidya, K., E. Jan, and M.L. Shuler, Lipid-gel and poly(dimethylsiloxane) film to mimic bioaccumulation in adipocytes. Biotechnol Bioeng, 2004. **86**(6): p. 643-9.
22. Gerlowski, L.E. and R.K. Jain, Physiologically based pharmacokinetic modeling: principles and applications. J Pharm Sci, 1983. **72**(10): p. 1103-27.
23. Viravaidya, K. and M.L. Shuler, Incorporation of 3T3-L1 cells to mimic bioaccumulation in a microscale cell culture analog device for toxicity studies. Biotechnol Prog, 2004. **20**(2): p. 590-7.
24. Tatosian, D.A., Developemnt of a microscale cell culture analog device to study multidrug resistance modulators, in Chemical Engineering. 2007, Cornell university: Ithaca. p. 186.
25. Xu, H., W.L. Kraus, and M.L. Shuler, Development of a stable dual cell-line GFP expression system to study estrogenic endocrine disruptors. Biotechnol Bioeng, 2008. **101**(6): p. 1276-1287.
26. Jones, B.J. and M.A. Hayes, Surface modification methods for enhanced device efficacy and function. Methods Mol Biol, 2006. **339**: p. 49-56.
27. Zhou, Q. and B. Chowbay, Determination of doxorubicin and its metabolites in rat serum and bile by LC: application to preclinical pharmacokinetic studies. J Pharm Biomed Anal, 2002. **30**(4): p. 1063-74.
28. Brandsteterova, E. and I.W. Wainer, Achiral and chiral high-performance liquid chromatography of verapamil and its metabolites in serum samples. J Chromatogr B Biomed Sci Appl, 1999. **732**(2): p. 395-404.

29. Rosenblum, R., Stability of Glutamine in Vitro. Proc Soc Exp Biol Med, 1965. **119**: p. 763-5.

30. Leong, K., Hydrophilic coatings for medical implements. 2003: USA.

31. Rubin, R.J. and P.M. Ness, What Price Progress - an Update on Vinyl Plastic Blood Bags. Transfusion, 1989. **29**(4): p. 358-361.

32. Wada, H., et al., In vitro estrogenicity of resin composites. J Dent Res, 2004. **83**(3): p. 222-6.

33. Wakeling, A.E., Similarities and distinctions in the mode of action of different classes of antioestrogens. Endocr Relat Cancer, 2000. **7**(1): p. 17-28.

34. ter Veld, M.G., et al., Estrogenic potency of food-packaging-associated plasticizers and antioxidants as detected in ERalpha and ERbeta reporter gene cell lines. J Agric Food Chem, 2006. **54**(12): p. 4407-16.

35. Krishnan, A.V., et al., Bisphenol-a - an Estrogenic Substance Is Released from Polycarbonate Flasks during Autoclaving. Endocrinology, 1993. **132**(6): p. 2279-2286.

36. Kang, J.H., D. Aasi, and Y. Katayama, Bisphenol a in the aquatic environment and its endocrine-disruptive effects on aquatic organisms. Crit Rev Toxicol, 2007. **37**(7): p. 607-25.

37. Kuruto-Niwa, R., S.Teraob, and R. Nozawaa, Identification of estrogenic activity of chlorinated bisphenol A using a GFP expression system Environmental Toxicology and Pharmacology 2002. **12**(1): p. 27-35.

CHAPTER 4

DEVELOPMENT OF A SILICON CELL CULTURE ANALOG DEVICE TO STUDY ENDOCRINE DISRUPTORS

4.1 Abstract

The general population is exposed to a variety of environmental chemicals that might inadvertently disrupt the endocrine system of humans and wildlife. However, in vitro assays for rapid screening and in depth understanding of such compounds are limited. In this work, physiologically realistic microCCA devices were developed to help predict in vivo responses to EDs. The silicon microCCA device contained a co-culture of three cell lines: MCF7-GFP (breast origin), Ishikawa-GFP (uterine origin) and HepG2/C3A (liver origin). Recirculation of medium mimicked the time dependent changes in the concentration of a chemical compound and its metabolites. Introduction of the flow also reproduced the microfluidic shear conditions inside a body. In addition, an in-line bubble tip was developed for bubble removal from the microfluidic pathways and to overcome air bubble related device failure that occurred in previous designs. It was found that the BPT tubing previously used with the peristaltic pump for microCCA leached ED like chemicals. A PDMS pneumatic micropump with a pumping rate ~3 ul per min was build to replace the bulky peristaltic pump. The micropump was used together with microCCA devices to detect estrogens. Preliminary results also showed tissue specific responses from uterine and breast derived cell lines.

4.2 Introduction

Estrogens are essential hormones in regulating the development and functions of the reproduction, nervous, skeletal and the cardiovascular systems. Over the last decade, there has been growing concern that estrogenic pollutants in the environment, such as dichlorodiphenyltrichloroethane (DDT) [1] and bisphenol A (BPA), may mimic natural hormone estrogens, interfere with the normal endocrine system, and elicit adverse health issues in both humans and wildlife [2]. Exposure to estrogenic endocrine disruptor (ED) chemicals in humans may adversely influence female fecundity and fertility, cause developmental and reproductive diseases, and increases the incidence of estrogen-related cancers [3-5]. These concerns have been heightened by the possibility that mixtures of weak EDs may exhibit complex synergistic interactions [6].

A variety of in vivo and in silico models have been developed for screening of potential ED compounds and their mixtures. In vivo animal assays, such as environmental assays [7], rodent uterotrophic assays [8] and the multigenerational tests [9], are costly and time consuming. It is also difficult to extrapolate human responses accurately from animal models. Computational tools, such as the nuclear receptor quantitative structure–activity relationship (QSAR) [10] and molecular docking [11, 12] have constrained predictability due to the limited structural similarity of estrogenic EDs. Recently DNA microarrays have been used to recognize the pattern of gene transcription in target cells stimulated by estrogens, which is then used to identify potential estrogenic compounds [13-15]. While a significant advance technology, microarray technology requires careful sample preparation and hybridization, as well as complex data analysis. More importantly, microarray analysis may not be able to address response to mixtures and provides limited opportunities to

probe subcellular mechanisms. Hormone receptor binding assays measure the affinity of a compound to ER, but provide no specific information about its agonist or antagonist effects.

Current in vitro tools for the study of EDs also have their limitations. The cell proliferation test (E-Screen) [16] identifies estrogenic chemicals by their proliferative effects, yet it suffers from lack of specificity, lengthy test times (5 to 6 days) and inability to produce direct insights into the molecular basis of chemical toxicity. Methods employing reporter gene expression systems for estrogenicity measurements are typically fast and sensitive [17]. We reported earlier the development of two stably transfected GFP reporter cell lines, MCF7-GFP and Ishikawa-GFP, to detect estrogenic and antiestrogenic compounds [18]. This dual cell line system enables simultaneous in vitro study of the toxicity effect of ED in both mammary and endometrial tissues. However, cell culture in the in vitro systems described above is usually static, while in vivo the physiological environment cells experience is dynamic due to exchange of compounds between organs and tissues, as well as the mechanical forces generated by recirculation. Also, only one individual cell type is studied at a time in these standard assays (using microwell plates, etc.). The physical and chemical interconnections between different organs are overlooked. As a result, most in vitro systems are incapable of providing useful information about the pharmacokinetics inside a human body, and usually fail to make connections between the toxicity effect and the pharmacokinetic profile of a toxin or a drug.

In this work a novel in vitro system, termed as microscale cell culture analog (microCCA), was developed to evaluate the toxicity of environmental endocrine disruptors. The device is 2.5 cm x 2.5 cm in size on a silicon wafer. Multiple human

cell lines, including the mammary, endometrial and liver cells were cultured on the device in separate yet interconnected organ chambers. Cell culture medium (200 ul) is re-circulated through them as a blood surrogate. The physical microCCA system is a direct analog to a Physiologically Based Pharmacokinetic (PBPK) modeling [19]. Since reaction rates in flow limited models are determined by residence time, size of the chambers is calculated to provide a liquid residence time similar to that in the tissue or organ. The relative size of compartments is set by the ratio of organ sizes. MicroCCA provides a more physiology-relevant dynamic environment for assessments of chemical toxicity in multiple cell lines simultaneously. It was also capable of addressing the issues of response to pro-estrogens with a “liver” compartment to mimic formation of active estrogenic compounds and tissue-tissue interaction through exchange of metabolites. In addition, a home-made bubble tip was described as an in-line debubbler for microCCA. It is a better alternative to commercial debubblers for many microfluidic devices as it has a smaller inner volume and requires no additional tubing connections.

The microCCA was tested with selective estrogen receptor modulators ICI 182,780 and tamoxifen. ICI suppressed GFP expression induced by E2 in both Ishikawa-GFP and MCF7-GFP cells while the effect of tamoxifen was tissue specific. Results from microCCA experiments also suggested the presence of ED chemicals leaching out from polypropylene based tubing (BPT) used with the bulky peristaltic pump. To overcome this problem, a compact micropump is described here for precise control of on-chip perfusion. Incorporation of the compact micropump with microCCA increases its capability for parallel testing at large numbers of samples.

In summary, this work describes an in vitro system that may be able to better predict human response to environmental estrogens and other toxins.

4.3 Materials and methods

4.3.1 Chemicals and reagents

E2, ICI 182,780 (Fulvestrant, ICI), 4-hydroxy tamoxifen (Tam) and raloxifene hydrochloride (Ral) were purchased from Sigma (St. Louis, MO). Fetal bovine serum (FBS) and charcoal-dextran stripped fetal bovine serum (CDFBS) with reduced steroid levels were from Hyclone (Logan, UT). Human plasma fibronectin was acquired from Millipore (Billerica, MA). Multi-well plates were purchased from Corning Life Science (Corning, NY). Single side polished silicon wafers ((100), 500-550 um in thickness, 100 mm in diameter) were obtained from Wafer Works Corporation (San Jose, CA). P20 and Shipley 1813 and 1027 photoresist were purchased from Shipley Company (Marlborough, MA). MIF 300 developer was obtained from Claricut (Somerville, NY).

4.3.2 Cell culture

The construction of stable MCF7-GFP and Ishikawa-GFP cell lines for quantification of estrogenic compounds has been previously described [18]. In short, a two tandem estrogen response elements (2ERE) – adenoviral E4 promoter – GFP reporter gene construct, pQCXIP-2ERE-GFP, was introduced into Ishikawa cells through retrovirus infection. Successfully transfected cells were selected out with antibiotic selection and fluorescence activated cell sorting (FACS). The stable transfectant MCF7-GFP and Ishikawa-GFP cell lines exhibited increased GFP expression when exposed to estrogens.

The parental MCF7-BOS cells were kindly provided by Dr. Ana Soto and Dr. Carlos Sonnenschein (Tufts University School of Medicine, Boston, MA). These cells, as well as MCF7-GFP cells, were maintained in Dulbecco's Modified Eagle's Medium (DMEM) (MP Biomedicals, Solon, OH) supplemented with 5% heat inactivated FBS. Heat inactivated FBS was prepared by heating FBS in a 57℃ water bath for 30 minutes followed by a filtration through a 0.2-micron filter. The parental Ishikawa cells were a kind gift from Dr. Myles Brown (Dana-Farber Cancer Institute, Boston, MA). Ishikawa and Ishikawa-GFP Cells have been maintained in Minimum Essential Medium (MEM) (Invitrogen, Carlsbad, CA) with 10% FBS. HepG2/C3A cells were obtained from the American Type Culture Collection (Manassas, VA), and were maintained in MEM with 1.0 mM sodium pyruvate and 10% FBS. All the cells were cultured at 37°C in a humidified, 5% CO_2, 95% atmosphere incubator.

4.3.3 MicroCCA design and fabrication

4.3.3.1 MicroCCA design

MicroCCA chips were designed based on a simplified PBPK model of the human body (Table 4.1). The body is divided into liver, mammary gland, uterus, fat and the other tissues. Parameters, such as blood flow rate, residence time, etc are obtained from the literature. Physical parameters of each chambers and channels are carefully adjusted and calculated to balance the pressure drop between medium inlet/outlet, to maintain the residence time consistent with in vivo situations.

Table 4.1 Physiological parameters for the PBPK model [20-23]

	Liver	**Mammary**	**Uterine**	**Fat**
Blood fraction (%)	24	1.35	0.62	5.0
Blood Flow rate (mL/s)	23.2	1.31	0.60	4.83
Tissue volume (L)	1.50	0.21	0.09	15.1
Residence time (s)	65	161	158	3124

4.3.3.2 MicroCCA fabrication

The microCCA chips were fabricated at the Cornell Nanofabrication Facility (CNF) using standard photolithography and etching techniques that have been described previously [24]. Briefly, the pattern was first designed with L-Edit Layout Editor (Tanner EDA, Monrovia, CA). The pattern was then directly written onto a 127 mm (5 inch) chrome-coated glass mask via Heidelberg DWL 66 laser writer (Heidelberg Instruments, Germany). A 4 inch diameter, 525 um thick silicon wafer was primed with P20 primer at 300 rpm for 30 sec to promote adhesion for photoresist. Next, the wafer was coated with 1.2 um of Shipley 1813 photoresist at 3000 rpm. A 1 min pre-exposure bake, or soft bake, on a 90°C vacuum hot plate was used to drive the solvent from the resist. The mask pattern was transferred onto the wafer with a 40 sec UV exposure (405 nm) on a Hybrid Technology Group's (HTG) system III-HR contact/proximity mask aligner (San Jose, CA). Resist was developed in a Hamatech-Steag Wafer processor with 300MIF developer for 1 min. Chambers on the chip were etched into the chip via a single chamber (licensed Bosch fluorine process) inductively coupled plasma / reactive ion etcher Unaxis 770 (Unaxia USA Inc., St. Petersburg, FL). Resist hot strip bath was used for stripping photoresist off the wafers with heated AZ 300T (Clariant Corporation, Somerville, NJ). The wafer was then rinsed clean

with DI water and dried. 1 inch x 1 inch individual chips (6 per wafer) were separated with a K&S 7100 Dicing Saw (Kulicke & Soffa Industries Inc., Fort Washington PA) After each use, cells were killed and detached from the device by immersing the microCCA chips into Clorox overnight. The piranha solution consisting of 3:1 ratio of 30% hydrogen peroxide (H_2O_2) and sulfuric acid (H_2SO_4) was used to clean and hydroxylate the silicone substrate surface of the microCCA chip.

4.3.3.3 Fabrication of the housing

Housing was fabricated from plexiglass (McMaster-Carr, New Brunswick, NJ) by Glenn Swann (school of Chemical and Biomolecular Engineering). The size of the top was 4.13 cm x 4.13 cm with a thickness of 0.3 cm. The bottom piece was 4.13 cm x 4.13 cm with a thickness of 0.46 cm. Inlet and outlet holes (D = 0.14 cm) were drilled into the top piece. The beginning part of the holes were enlarged a little (D = 0.17 cm) to facilitate the insertion of plastic tips connected to medium tubing. A 2.55 cm x 2.55 cm chamber with a depth of 0.5 mm was machined into the bottom piece to house the microCCA chip. The size of this chamber was precisely controlled to ensure a good alignment of the inlet/outlet holes with the inlet/outlet on the chip device, yet also allow easy placement of the chip into the chamber. Thread was drilled on the bottom piece for clamping the two piece housing together with screws.

For each set of housing pieces, two stainless steel pins were added onto the bottom piece, and holes were drilled out on the top piece at corresponding positions. These pins would guide the top piece toward the right position relative to the bottom piece during device assembly.

4.3.3.4 Construction of a bubble tip as an air bubble trap

Bubble tips were made from polypropylene gel loading tips. Two gel loading tips were cut for each bubble tip (Figure 4.1); (A) was cut at about 8 mm above the flexible capillary tip, and (B) was cut at about 5 mm above the flexible capillary tip. (B) was then inserted into the opening of (A) to achieve a tight fit. For better sealing, polydimethylsiloxane (PDMS) prepolymers were mixed at a 10 :1 w/w-mixture of monomer and hardener (Sylgard 184, Dow Corning). The mixture was degassed under vacuum for 10 min, and then was used to seal the connection. The assembled bubble tips were baked at 60°C oven overnight to cure the PDMS adhesive. This PDMS sealing process may be omitted as the binding strength between part (A) and part (B) are usually sufficient under low pressure situation with microCCA. To use the bubble tip as a bubble trap, the shorter end of bubble tip was connected to the tubing that comes out the peristaltic pump. The longer end was inserted into the inlet hole on the top housing piece of the microCCA device.

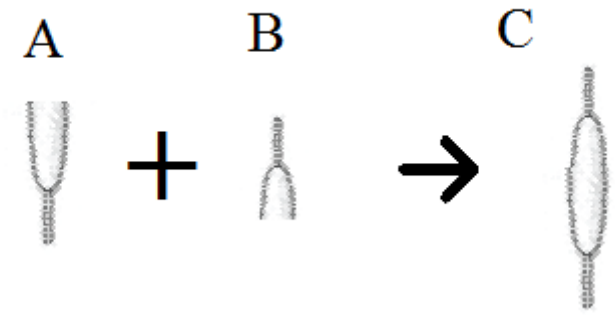

Figure 4.1 Construction of the bubble tip as a debubbler.

4.3.4 Cell culture on the microCCA device

HepG2/C3A, Ishikawa-GFP and MCF7-GFP cells were grown in T25 cell culture flasks until they reached 80% confluence. Cells were then detached and re-suspended

in cell culture medium. The microCCA chip was first coated with 8 ug/cm^2 human plasma fibronectin (Chemicon International Inc., Temecula, CA) in DPBS for 30 min at room temperature. Upon removal of the fibronectin solution, MCF7-GFP cells were seeded into the mammary chamber at a concentration of 250,000 cells per cm^2, Ishikawa-GFP cells were seeded into the uterine chamber at a concentration of 500,000 cells per cm^2, and HepG2/C3A cells were seeded into the liver chamber at a concentration of 300,000 cells per cm^2. The chips were kept in the cell culture incubator overnight to allow the cells to attach and spread. To reduce evaporation of the medium and avoid drying of the cell suspension, several drops of cell culture medium were placed on the bottom of the culture dish holding the chips. In experiments testing surface treatment different conditions, the bottom of wells in a 24-well plates were treated with collagen, 4 ug/cm^2 poly-D-lysine in DPBS, 8 ug/cm^2 fibronectin, or fibronectin alone for 30 min before cell suspension being added to the wells. After 24 h cell attachment, 0.5 ml cell culture media with 10^{-9} M E2 or no E2 were added into each well. Cell responses were recorded after 48 h.

4.3.5 MicroCCA assembly

Before assembly of the microCCA device, tubing and reservoir coverings were first sterilized with dry autoclaving for 30 min. The commercial peristaltic pump was wiped with 70% alcohol and placed into the cell culture laminar hood. Tubing connected with the bubble tip was placed into the cassette of the peristaltic pump. The longer end of the bubble tips should point upward for easy removal of the air inside the body of the bubble tips when medium was introduced. The tubing was briefly rinsed with DPBS at 50 rpm, and then rinsed with cell culture medium at 5 rpm for 30 min. Flow rate was further slowed down to 0.75 rpm before assembling chips. Housing pieces for microCCA were wiped with 70% alcohol and allowed to air dry.

The top housing pieces were then cleaned in an oxygen plasma cleaner (Harrick Plasma, Ithaca, NY) for 2 min to increase wettability. Plasma treatment also improved sterilization. Then 0.5 ml cell culture media were immediately pipetted onto the plasma treated surface of each top housing piece to help maintain the hydrophilic nature of the plastic pieces.

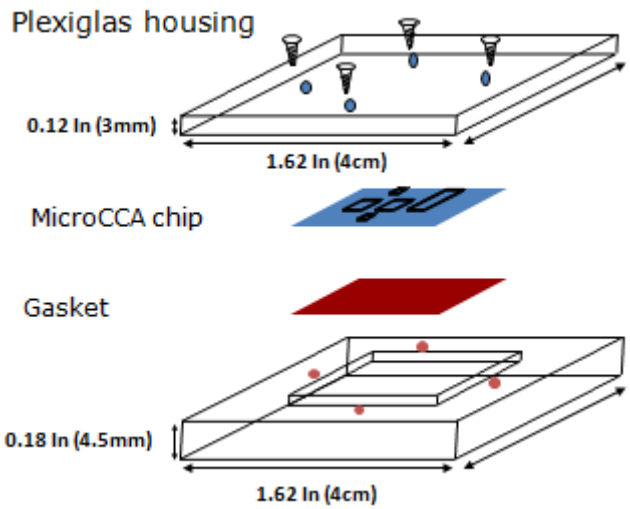

Figure 4.2 Assembly of the microCCA devices.

To sandwich a microCCA chip between the Plexiglas housing pieces, the microCCA chips were first placed into the bottom housing piece (Figure 4.2). A PDMS gasket was used under the chips as a cushioning material for better sealing. Then 300 ul cell culture medium was added onto the chip to cover all the chambers and channels. The longer end of the bubble tip was then inserted into the inlet hole in the top housing piece. The inner side of the top housing piece to be in contact with the microCCA chip was then rinsed with 1 ml media to remove any air bubbles. The top housing piece was then pushed straightly down onto the bottom housing piece with the guidance of the guiding pins and screws were tightened. The outlet tubing was then inserted into

the outlet hole in the top housing piece. Finally the medium reservoir with 200 ul cell culture medium was connected with the tubing to form a closed recirculation system.

4.3.6 Fabrication of the PDMS micro pump

The PDMS micro pump has two main components, the membrane and the pump body. To make the PDMS membrane, silicon wafers were coated with (1H, 1H, 2H, 2H-Perfluorooctyl)Trichlorosilane (FOTS) (oxygen plasma 60 s, reaction 600 s), which is an excellent antistiction coating and is usually used as a release layer, on a Molecular Vapor Deposition tool (MVD100, Applied Microstructures Inc., San Jose, CA). PDMS was mixed at ten parts of polymer precursor and one part of cross-linking agent by weight. A 50 um PDMS membrane was generated by spin coating of PDMS mixture on a piece of silicon wafer at 1400 rpm for 45 s. The membrane was then cured on a 100 °C hot plate for 4 min and in a 60 °C oven for 1.5 h. Thickness of the PDMS membranes was measured with a Tencor P10 profilometer (KLA-Tencor, San Jose, CA).

The body of the micropump was fabricated using a soft lithography method (Figure 1.2). First, SU8 2050 negative photoresist (MicroChem, Newton, MA) was spun onto a silicon wafer to form a layer with a thickness of 50 um. Then it was soft-baked at 65 ◦C for10 min and then at 95 ◦C for 20 min. A standard photolithography process was performed for pattern transfer, followed by a post-exposure-bake process at 65 ◦C for 3 min and at 95 ◦C for 10 min. Finally, the SU8 wafer was development in SU8 developer for 2 min, rinsed with isopropanol, water and then blow dried with nitrogen. PDMS is then cast against this SU8 mold, PDMS was mixed at ten parts of polymer precursor and one part of cross-linking agent by weight, and then poured onto the SU-8 microstructure master. A vacuum process was required to remove the air bubbles

formed during the mixing. The PDMS was then cured at 60°C in an oven overnight. The PDMS inverse structures were then peeled off the master. The PDMS membrane, top and bottom pieces were all sealed together after oxygen plasma treatment for 40 s, and the final device was baked on a 120°C hot plate for 1 h. Water was filled into the medium channels to help maintain the hydrophilic property of the PDMS channels from the oxygen plasma treatment.

The device assembly with the micropump was similar to the assembly process with a peristaltic pump. However, the process is easier and more straightforward as the length of the tubing is much shorter with the micropump. The medium rinsing time was also decreased to 10 min.

4.3.7 Detection of estrogenic and antiestrogenic chemicals with microCCA

HepG2/C3A, MCF7-GFP and Ishikawa-GFP cells were seeded onto the microCCA chip as described in the section 4.3.4. Cells were allowed to attach and spread overnight. Test chemicals E2, Ral or ICI were dissolved in ethanol and added into McCoy's 5A medium with 10% CDFBS to reach a final concentration of 10^{-9} M, 10^{-6} M and 10^{-6} M respectively. Only ethanol was added in a vehicle control sample. Medium with the test chemical or the vehicle only was used to rinse the individual BPT tubing to remove contaminants and to passivate the tubing surfaces with the test chemicals. Then 200 ul medium was filled into each medium reservoir and allowed to equilibrate at 37°C in a cell culture incubator. The devices were then assembled and operated at 37°C and 5% CO2 for 48 h. At the end of the experiments, the microCCA devices were carefully disconnected from the tubing and bubble tip for cell imaging.

4.3.8 Imaging method

Cells were observed and imaged under an IMT-2 phase contrast and fluorescence microscope (Olympus America Inc., Center Valley, PA) at 100 X. Fluorescence and transmission images were captured with a Retiga CCD camera (Qimaging, Burnaby, BC, Canada) in a 12 bit grayscale format, and were analyzed using ImagePro Plus software (Media Cybernetics Inc., Silver Spring, MD).

4.4 Results and discussions

4.4.1 Construction of the microCCA device

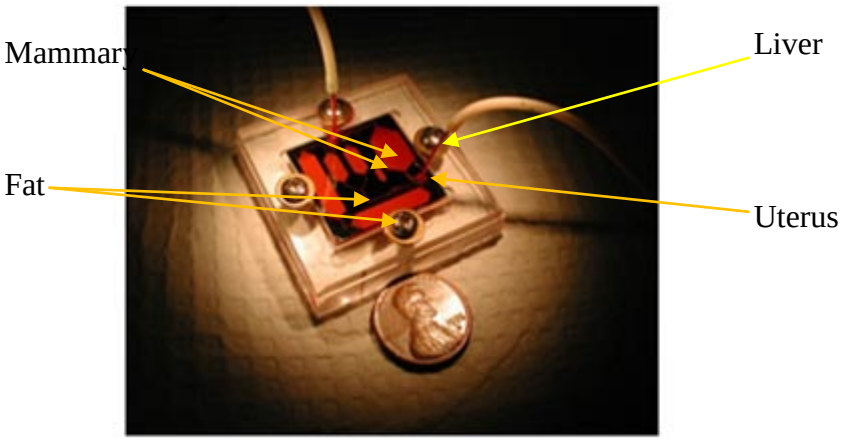

Figure 4.3 Photograph of the six chamber microCCA device.

The first version of microCCA contained six cell culture chambers for the liver, mammary, uterus and fat cells (Figure 4.3). Since environmental endocrine disruptors are mostly hydrophobic, they are mainly adsorbed into the fat tissue. In the second version with 4 chambers (Figure 4.4), the fat chamber was taken off of the chip to simplify the design and to reduce the size of the chip. The silicon chip was 2.54 cm by 2.54 cm in size, with a thickness of 525 um. Depth of the cell culture chambers were

35 um. The on-chip liquid to cell volume ratio was around 2 in this design. An ideal microfluidic cell culture device should reproduce in vivo like cellular micro environment where the physiological value of liquid to cell volume ratio is about 0.5. For monolayer culture it is difficult to obtain a ratio of 0.5 and leave sufficient space for fluid flow. For comparison, the liquid to cell volume ratio in traditional cell culture flasks and dishes is from 200 to 300. Hydrodynamic shear stress on cells was kept lower than 2 dynes/cm^2 [25] by careful design of chamber geometry and fluid flow.

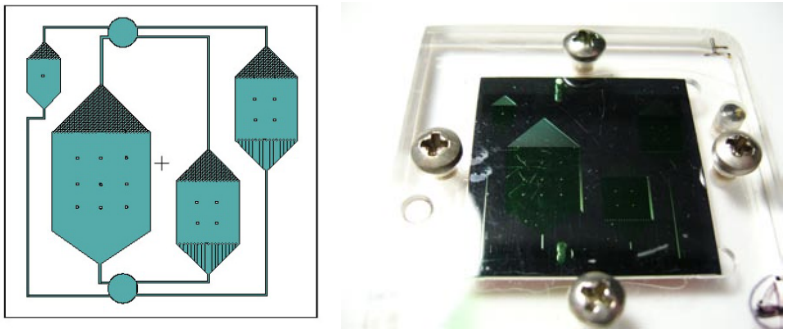

Figure 4.4 (left) Illustration and (right) photo of the four chamber microCCA.

Three cell lines were picked for on-chip cell culture. The HepG2/C3A cell line, which is a subclone of HepG2, was used as a model for the liver. This cell line has detectable CYP1A1/2, which are responsible for the metabolism of estrogens such as E2 and trans-stilbene. MCF7-GFP developed from MCF-7 cell line was used to imitate the mammary tissue. Ishikawa-GFP was developed from Ishikawa carcinoma cell line to represent the endometrial tissue. In the previous work on microCCA, cell responses were characterized mainly by cell viability and glutathione (GSH) depletion. Usually the cells were stained with live/dead molecular probes, such as Calcein AM and ethidium homodimer-1 (EthD-1) to indicate their viability and proliferation ability. Such assessment is only for end point measurement. The introduction of GFP reporter into the cell line allowed direct visualization of cell response to estrogenic and

antiestrogenic compounds without additional staining. In addition, cell responses can be monitored in real time or at multiple time points. The construction of MCF7-GFP and Ishikawa-GFP cell lines has been described in chapter two. In both cell lines, expression of GFP increases when cells are exposed to 10^{-11} M or higher concentrations of E2.

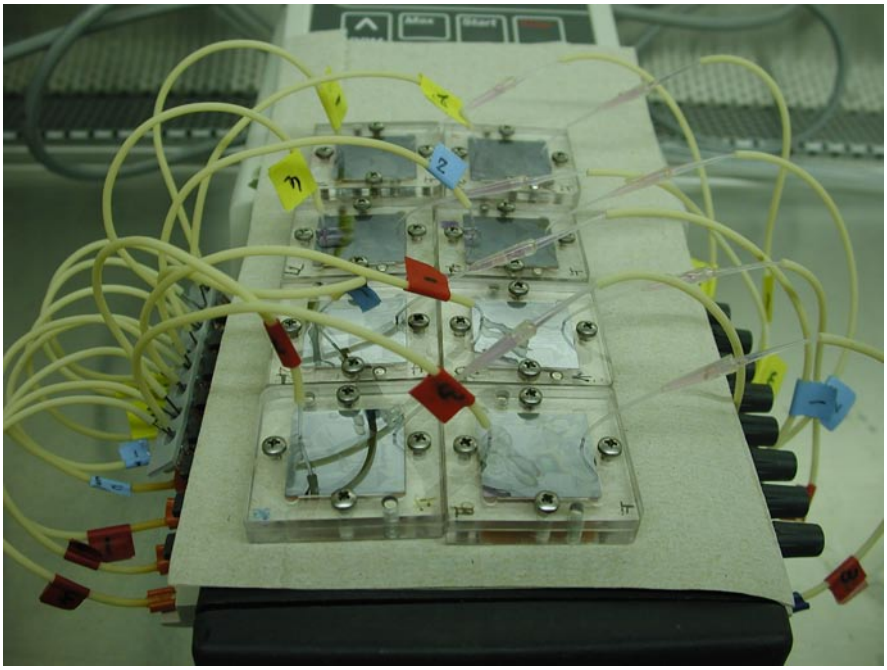

Figure 4.5 Photography of the microCCA experimental setup.

The culturing of cells on silicon devices has been described in several publications. Methods of silicon surface treatment varied with different cell lines to be cultured onto the silicon device. Poly-D-lysine and fibronectin have been used previously in our lab to attach HepG2/C3A, bone marrow, and uterine sarcoma cell lines onto microCCA [26]. However, in this study, MCF7-GFP cells were found to aggregate when cultured on surfaces treated with poly-D-lysine. Cells piled up to each other and produce false

GFP signals. For this reason, only fibronectin was used to attach MCF7 cells onto the chip.

Figure 4.5 shows a photograph of the experimental setup consisting of the microCCA chip coupled with a bulk peristaltic pump. The medium was aspired from the medium reservoir and was pumped through the bubble tip and the microCCA chip, then recirculated back into a reservoir containing 200 ul McCoy' 5A medium. The pump has 8 channels. Thus 8 microCCA devices are usually operated in each test.

4.4.2 Development of an in-line bubble trap

Air bubbles entering a microfluidic cell culture device may occlude the fluid channels and displace cell culture medium in the culture chamber. Cell death may result from disruption of the cell membrane by surface tension of the air-liquid interface or from lack of liquid medium and nutrition, causing experiments to fail. Long-term perfusion of microfluidic devices, such as the two to three days cell culture in microCCA devices, is very susceptible to bubble formation within the fluid network. Care is usually taken to fill microfluidic networks and connect tubing without introducing bubbles. For example, tubing should be rinsed with DPBS or medium prior to assembly to remove air from the tubing. However, bubbles sometimes nucleate within the tubing and it becomes difficult to remove them totally.

There are several ways to debubble. One method uses the buoyancy property of air bubble, which tends to float up in a liquid. However, most bubble traps are ineffective for microfluidic systems as these require tubing to connect the bubble trap to the microfluidic device, which introduces more opportunities for bubbles to enter the fluidic network. In addition, the inner volume of such bubble traps is usually large (>

1 ml) while the liquid volume in microfluidic devices is usually small (about 250 ul in microCCA). The presence of such a big bubble trap would disrupt the fluid dynamics of the microfluidic system. The second type of debubbler or degasser involves membrane base hydrophobic venting [27]. But the pressure tolerance of the membrane is lower than the one that drive the liquid through the microCCA chip. The open holes in the membrane also present a threat for sterility.

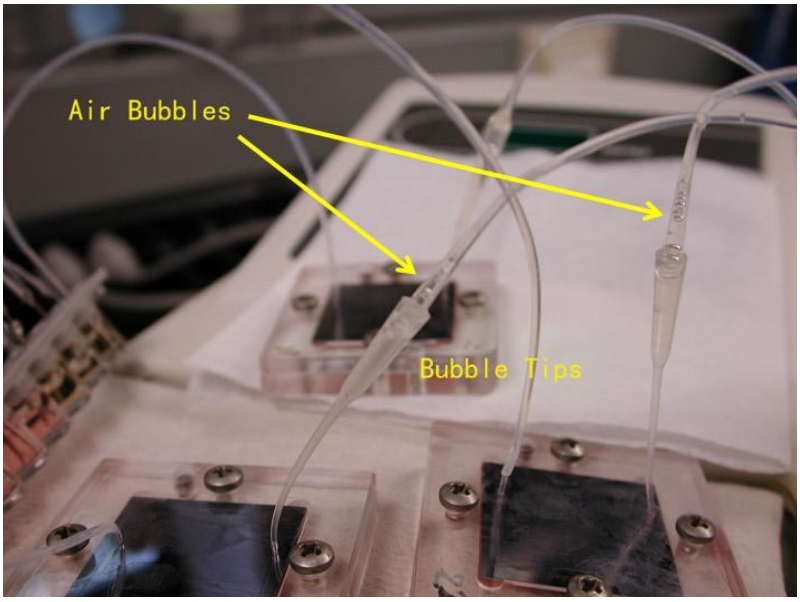

Figure 4.6 Working principle of the bubble tip. Small air bubbles were retained at the upper session of the bubble tip as indicated by the arrows.

The in-line microfluidic bubble trap described here requires no extra tubing connection. It is inserted into the flow path and connected directly to the microCCA device. It can be easily integrated into many microfluidic designs. Figure 4.5 illustrates the working principle of the bubble tip. As small air bubbles enter the bulb of the bubble tip. They tend to float up and accumulate at the upper half of the bulb

and form a small air pocket, while liquid would keep flowing down into the chip. Bubble tips should be standing upward to function well as a debubbler. This is usually easy to achieve as the bubble tip itself is stiff. Taping the tubing connected to the bubble tips onto the side wall of the peristaltic pump also helps. It should be noted that although this design worked well with our experimental design described here, it does have a limit on the volume of the air bubbles it tolerates. Too much air bubble entering the bubble tip would push down the liquid-air interface into the chip device and cause the experiment to fail.

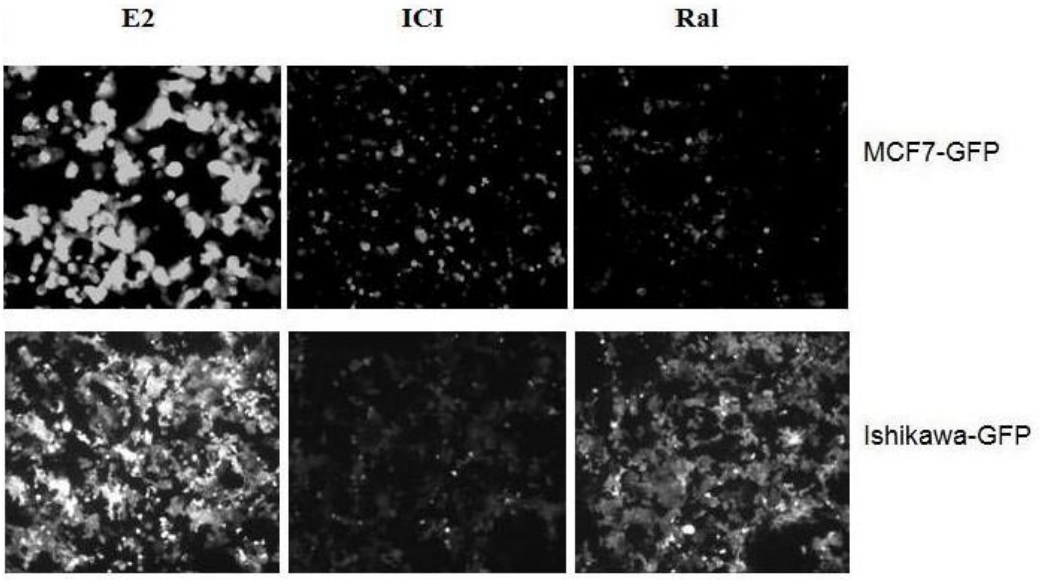

Figure 4.7 Responses of MCF7-GFP and Ishikawa-GFP cells cultured on microCCA chips to 1 nM E2, 1uM ICI 182.780 (ICI) mixed with 1 nM E2 and 1 uM raloxifene (Ral).

4.4.3 Detection of estrogenic and antiestrogenic chemicals with microCCA

E2 was used as a model chemical for estrogenic endocrine disruptors. In experiments that were carried on in a multi-well cell culture plate, 10^{-9} M E2 induced a strong GFP expression when compared to control samples after 48 h [18]. However, results were different when the experiments were carried on microCCA system with medium

recirculated by a peristaltic pump. No significant difference of the GFP intensity was observed between cells exposed to E2 and cells in the control group. Our previous study [28] suggested that the BPT tubing used with the peristaltic pump releases estrogenic contaminates. The results from the microCCA are consistent with our previous findings. In this experimental setup, the length of the microbore (ID = 0.25 mm) BPT tubing used was 55 cm. The inner volume is about 25 ul while the surface area is about 430 mm^2. The large surface area to volume ratio in the tubing, as well as in the microCCA microfluidic device itself, contributed to the accumulation of the leached contaminates.

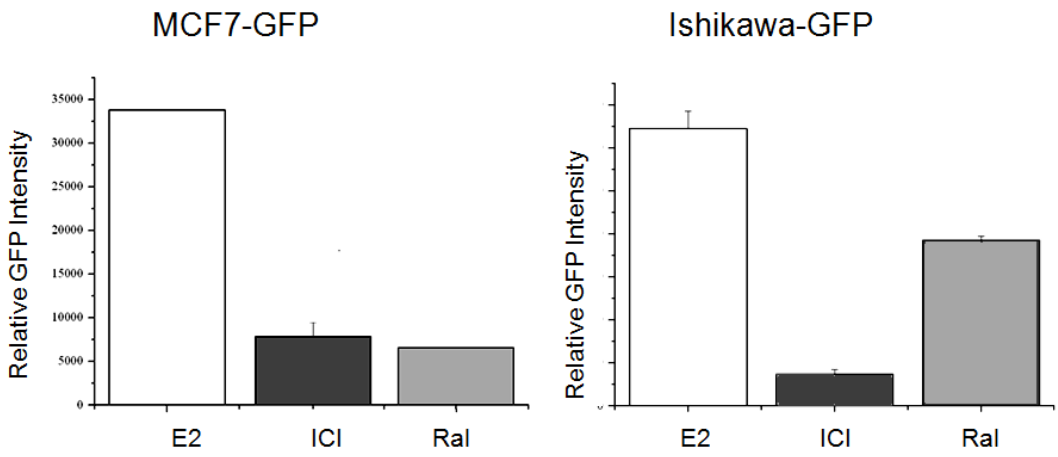

Figure 4.8 Quantification of GFP intensities in MCF7-GFP and Ishikawa-GFP cells cultured on microCCA chips with 1 nM E2, 1uM ICI 182.780 with 1 nM E2 (ICI), or 1 uM raloxifene with 1 nM E2 (Ral).

When antiestrogens ICI and raloxifene were added into the medium together with E2, they exhibited different GFP-inhibiting profile in Ishikawa-GFP and MCF7-GFP cell lines. In MCF7-GFP cells, both ICI and raloxifene inhibited the expression of GFP (Figure 4.7). In Ishikawa-GFP cell culture, ICI completely suppressed E2 induced

GFP expression. The GFP intensity also decreased with Ral treatments, but was not completely suppressed (Figure 4.7 and 4.8). These results were consistent with our previous results, which showed that raloxifene was able to induce GFP expression by binding to estrogen receptors [18]; And raloxifene has a high affinity with the estrogen receptor and compete with E2 to bind to estrogen receptors, yet it is less potent than E2.

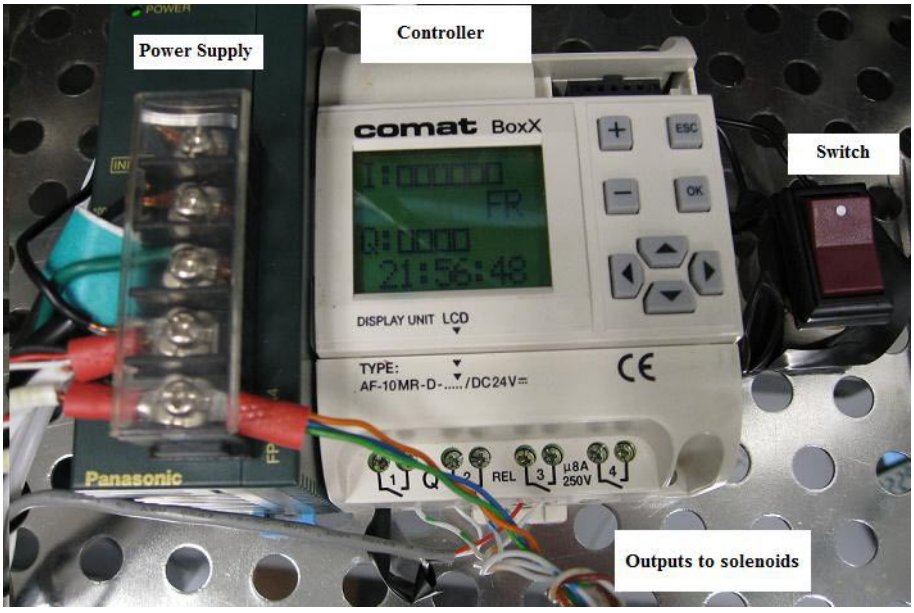

Figure 4.9 The control system of the micropump with power supply and the stand-alone program box.

4.4.4 Development and characterization of the PDMS micropump

To overcome the interference caused by contaminants leaching from BPT tubing, a micropump was developed to eliminate the use of the BPT. The micropump consisted of three layers of PDMS plates; a top layer with medium/liquid channels, a PDMS membrane layer as the diaphragm, and the bottom layer with air chambers. Depth of

the medium channel and air chambers were 50 um. The thickness of the PDMS membrane was 35 um.

The pump had three pneumatic microvalves that open and close via an applied air pressure (compressed nitrogen, 138 kPa) and vacuum (-103 kPa) regulated by a micro processor. The reason to use compressed nitrogen instead of other gases such as the carbon dioxide (CO_2) and oxygen is due to the low permeability of PDMS to N2, as well as the inert nature of N2. The microvalves were controlled by a stand alone micro processor (Comat BoxX controller with LCD AF-10MR-D-LCD/24V) and three three-port solenoids (S070M-5CG-32, SMC, Tustin CA) with a response time of less than 3 ms and a maximum operating pressure of 0.3MPa (43.5 Psi) (Figure 4.9). The pneumatic valves were operated in sequence to work as a peristaltic pump (Figure 4.10). The valves were programmed to open and close sequentially by following a pattern denoted by (100), (110), (011), and (001). The logical "1" is defined as the down motion of the PDMS thin membrane, and medium is draw into the chamber. "0" is defined as the up motion of the PDMS thin membrane, and medium is pushed out of the chamber.

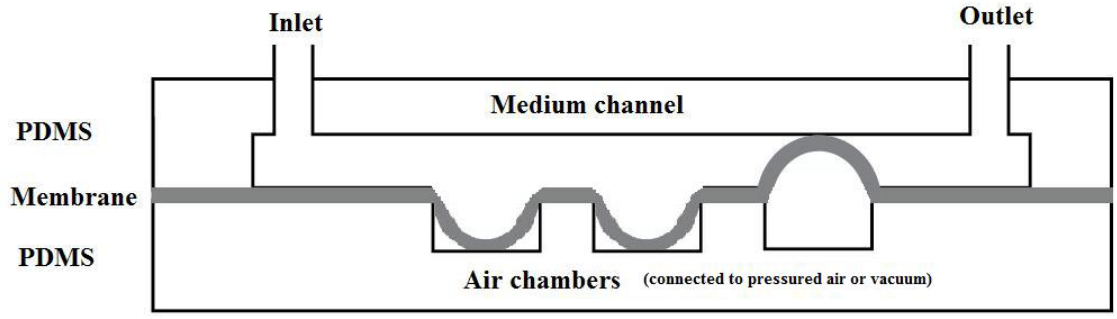

Figure 4.10 Illustration of the structure of the micropump at (001) state.

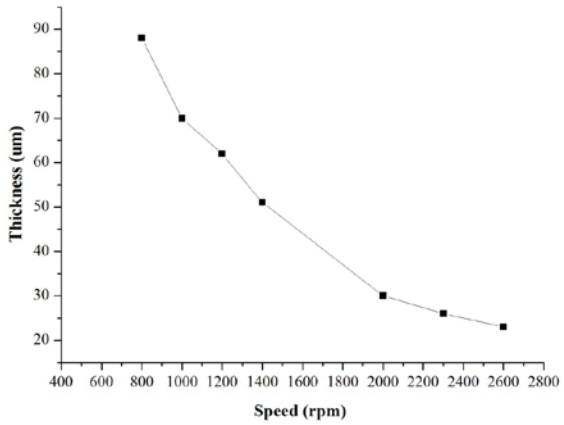

Figure 4.11 Spinning curve of PDMS. PDMS was mixed at ten parts of polymer precursor and one part of cross-linking agent by weight. Spinning time was 45 s.

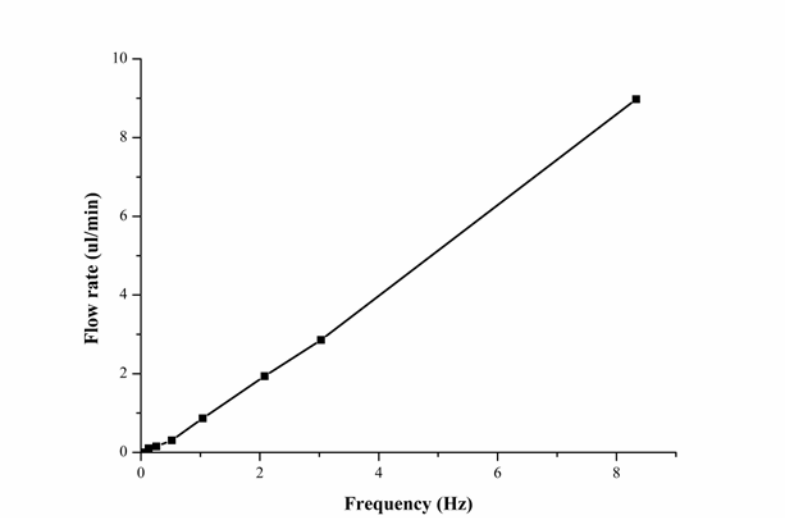

Figure 4.12 A graph plotting flow rate as a function of actuation frequency for the micropump with a flow channel depths of 50 um. Thickness of the actuation membrane was 30 um.

Figure 4.11 is the measured spinning curve of PDMS that was mixed at ten parts of polymer precursor and one part of cross-linking agent by weight. The thickness of the PDMS membrane decrease as the spinning speed increased. The optimal thickness for

this application was chosen to be 30 um. A thicker membrane is less flexible and its actuation requires a higher pressure to drive. A thinner membrane may be less durable and are prone to defects. In addition, the PDMS need to be diluted in hexane for making membranes as thin as 12 um thick .

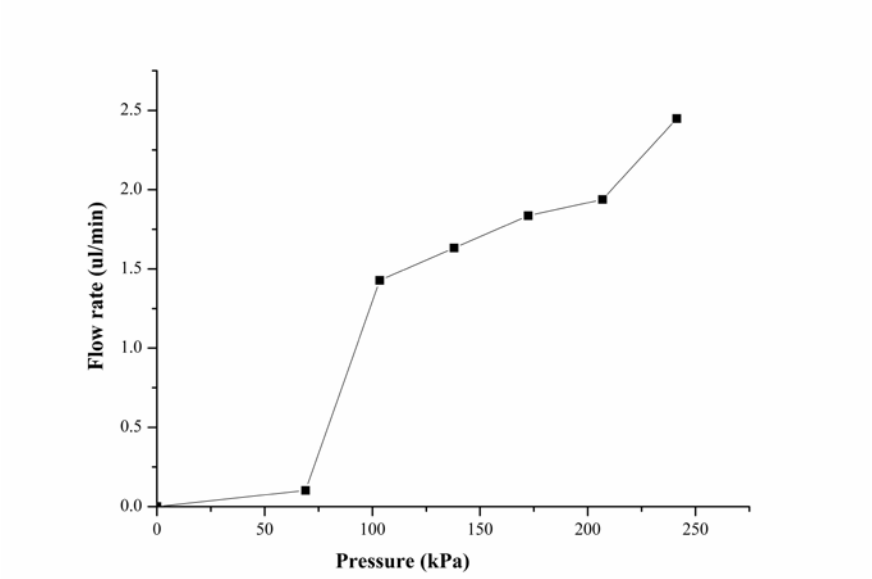

Figure 4.14 A graph plotting flow rate as a function of actuation air pressure for the micropump. Depth of the flow channel was 50 um. Thickness of the actuation membrane was 30 um. Pumping frequency was 2 Hz.

Flow output of the constructed micopump was show in Figure 4.12 and Figure 4.13. Figure 4.12 measured the pumping flow rate as a function of the actuation frequency. For a micro pump with the depth of the medium channel and air chambers being 50 um and the thickness of the PDMS membrane being 35 um, the flow rate increased linearly with the pumping frequency up to 8 Hz. A 3.2 ul/min flow rate was obtained at 3 Hz frequency. This was the flow rate designed for the microCCA device described in section4.3.3.1. The pumping performance was also affected by the air pressure that was used to actuate the membrane as shown in Figure 4.13. With a pressure of 68.9 kPa (10 psi) or lower, the deformation of the membrane was not sufficient to drive the

pump. On the other hand, an air pressure higher than 103 kPa (15 Psi) only increased the flow rate slightly as the deformation of the membrane reaches its maximal amount.

4.4.5 Operation of the microCCA device with PDMS micropumps

Figure 4.14 showed the final microCCA experimental setup with the PDMS micropump. The micropump may be placed under or by the side of the microCCA device. The total length of the PTFE tubing used with each microCCA device was about 8 cm and can be further shortened if necessary. Four pumps were fabricated on the PDMS slab in Figure 4.14.

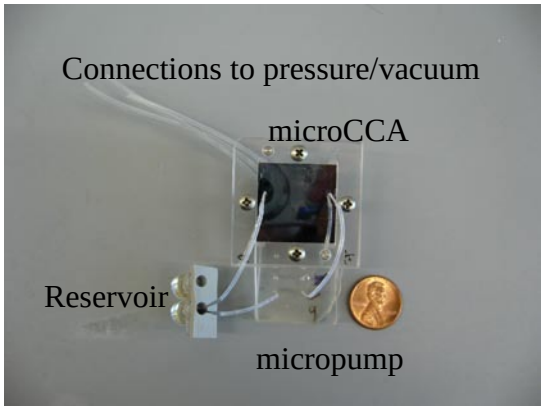

Figure 4.14 Experimental setup of the microCCA device with a PDMS micropump

In the previous microCCA experimental setup, a commercial peristaltic pump was used to recirculate the flow. Contaminations released from the BPT tubing used with the peristaltic pump caused GFP expression in both Ishikawa-GFP and MEF7-GFP cells. Length of the BPT tubing was about 55 cm. Here with the PDMS micropump, PTFE tubing replaced BPT tubing. And the length was greatly shortened as well to about 8 cm. Preliminary results from this micropump setup showed that no contamination caused GFP expression in Ishikawa-GFP cells after 48 h (Figure 4.15) in the control samples. Also estrogen induced increase of GFP expression was observed (Figure 4.15).

Challenges remained to integrate the micropump and microCCA devices together for long-term experiments (e.g. longer than 24 h). The bonding between the three PDMS layers of the micropump needs to be strengthened. Currently the three layers were bonded together with air plasma surface treatment. Damage of the sealing and resulted pump leakage was sometimes observed with 48 h experiment setups. Oxygen plasma, instead of air plasma, has been reported to lead to better adhesion between PDMS layers, and may be tested when available. A partial curing method was demonstrated to be a considerable improvement in bond strength and consistency over oxygen plasma [29]. But our results indicated that this improvement is minimal and insufficient for our applications. In our setup the pump was driven by 140 KPa air pressure to overcome the resistance introduced by the microCCA and the fluidic recirculation system. Wider channels on the microCCA devices may help drop the pressure requirements, relieve the leakage problem and improve the pump performance.

As PDMS surface is extremely hydrophobic, hydrophobic molecules, including hormones and proteins, are susceptible to irreversibly adsorption onto the surface. The responses of Ishikawa-GFP cells to 1uM E2 in Figure 4.14 was less strong than the cells responses observed in well plates, partially due to surface adsorption of E2 to PDMS surfaces. Several methods, including surfactant treatment [30], parylene coating [31], grafting of epoxy-modified hydrophilic polymers [32], have been reported in the literature to alleviate surface adsorption in PDMS based devices. However, our preliminary results from surfactant Pluronic® F-68 surface treatment showed no significant improvement. Further investigations on this issue are needed to increase the sensitivity of assays based on PDMS devices.

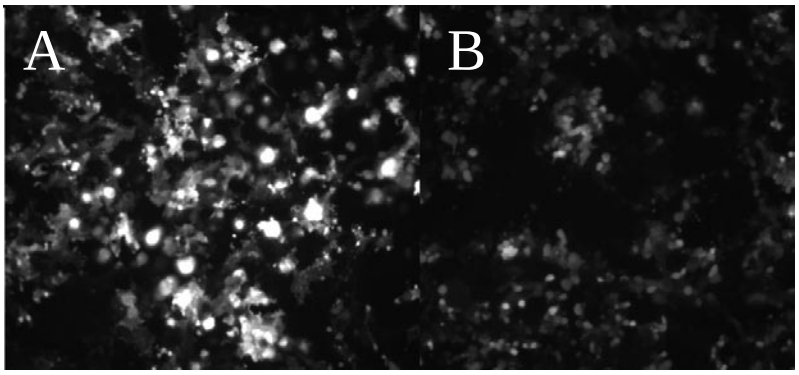

Figure 4.15 Responses of Ishikawa-GFP cells on microCCA after exposure to (A) 1 uM E2 and (B) control situation without estrogen for 48 h.

4.5 Conclusions

In conclusion, a prototype microCCA with a pneumatic micropump has been developed to demonstrate the detection of estrogens and antiestrogens with E2, ICI and raloxifene as model reagents. The in-line bubble tip allowed easy removal of fine air bubbles trapped in the fluidic pathways. The micropump improved the contamination leakage problem associated with a bulky traditional peristaltic pump. Multiple cell types and recirculation medium allow researchers to address tissue specific responses and potentially to study effects of drug metabolites in a dynamic system that mimics the time dependent changes in drug concentrations, and the microfluidic shear situation inside a human body. This system is compact in size and relatively inexpensive to produce. The development of the microCCA and incorporation of the micropump may offer an advanced tool for fast and precise detection of estrogenic environmental endocrine disruptors, for screening of antiestrogen drug candidates, and for better prediction of the toxicity of such compounds.

REFERENCES

1. Bitman, J., et al., *Estrogenic activity of o,p'-DDT in the mammalian uterus and avian oviduct.* Science, 1968. **162**(851): p. 371-2.
2. Price, T.M., S.K. Murphy, and E.V. Younglai, *Perspectives: the possible influence of assisted reproductive technologies on transgenerational reproductive effects of environmental endocrine disruptors.* Toxicol Sci, 2007. **96**(2): p. 218-26.
3. Swan, S.H., et al., *Decrease in anogenital distance among male infants with prenatal phthalate exposure.* Environ Health Perspect, 2005. **113**(8): p. 1056-61.
4. Buck Louis, G.M., C.D. Lynch, and M.A. Cooney, *Environmental influences on female fecundity and fertility.* Semin Reprod Med, 2006. **24**(3): p. 147-55.
5. Hileman, B., *Bisphenol A may trigger human breast cancer.* Chemical and Engineering News (CEN), 2006. **84**(50): p. 10.
6. Arnold, S.F., et al., *Synergistic activation of estrogen receptor with combinations of environmental chemicals.* Science, 1996. **272**(5267): p. 1489-92.
7. O'Connor, J.C., et al., *Evaluation of Tier I screening approaches for detecting endocrine-active compounds (EACs).* Crit Rev Toxicol, 2002. **32**(6): p. 521-49.
8. Owens, W. and H.B. Koeter, *The OECD program to validate the rat uterotrophic bioassay: an overview.* Environ Health Perspect, 2003. **111**(12): p. 1527-9.
9. Hoshino, N., M. Iwai, and Y. Okazaki, *A two-generation reproductive toxicity study of dicyclohexyl phthalate in rats.* J Toxicol Sci, 2005. **30 Spec No.**: p. 79-96.

10. Jacobs, M.N., *In silico tools to aid risk assessment of endocrine disrupting chemicals.* Toxicology, 2004. **205**(1-2): p. 43-53.
11. Pike, A.C., et al., *Structural aspects of agonism and antagonism in the oestrogen receptor.* Biochem Soc Trans, 2000. **28**(4): p. 396-400.
12. Brzozowski, A.M., et al., *Molecular basis of agonism and antagonism in the oestrogen receptor.* Nature, 1997. **389**(6652): p. 753-8.
13. Francois, E., et al., *DNA microarrays for detecting endocrine-disrupting compounds.* Biotechnol Adv, 2003. **22**(1-2): p. 17-26.
14. Fujimoto, N., et al., *Identification of estrogen-responsive genes in the GH3 cell line by cDNA microarray analysis.* J Steroid Biochem Mol Biol, 2004. **91**(3): p. 121-9.
15. Wang, D.Y., et al., *Identification of estrogen-responsive genes by complementary deoxyribonucleic acid microarray and characterization of a novel early estrogen-induced gene: EEIG1.* Mol Endocrinol, 2004. **18**(2): p. 402-11.
16. Dickson, R.B. and M.E. Lippman, *Growth factors in breast cancer.* Endocr Rev, 1995. **16**(5): p. 559-89.
17. Legler, J., et al., *Development of a stably transfected estrogen receptor-mediated luciferase reporter gene assay in the human T47D breast cancer cell line.* Toxicol Sci, 1999. **48**(1): p. 55-66.
18. Xu, H., W.L. Kraus, and M.L. Shuler, *Development of a stable dual cell-line GFP expression system to study estrogenic endocrine disruptors.* Biotechnol Bioeng, 2008. **101**(6): p. 1276-1287.
19. Gerlowski, L.E. and R.K. Jain, *Physiologically based pharmacokinetic modeling: principles and applications.* J Pharm Sci, 1983. **72**(10): p. 1103-27.

20. Gentry, P.R., et al., *Application of a physiologically based pharmacokinetic model for isopropanol in the derivation of a reference dose and reference concentration.* Regul Toxicol Pharmacol, 2002. **36**(1): p. 51-68.

21. Andersen, M.E., et al., *Physiologically based pharmacokinetics and the risk assessment process for methylene chloride.* Toxicol Appl Pharmacol, 1987. **87**(2): p. 185-205.

22. Byczkowski, J.Z. and J.W. Fisher, *A computer program linking physiologically based pharmacokinetic model with cancer risk assessment for breast-fed infants.* Comput Methods Programs Biomed, 1995. **46**(2): p. 155-63.

23. Luu, H.M. and J.C. Hutter, *Bioavailability of octamethylcyclotetrasiloxane (D(4)) after exposure to silicones by inhalation and implantation.* Environ Health Perspect, 2001. **109**(11): p. 1095-101.

24. Sin, A., et al., *The design and fabrication of three-chamber microscale cell culture analog devices with integrated dissolved oxygen sensors.* Biotechnol Prog, 2004. **20**(1): p. 338-45.

25. Powers, M.J., et al., *A microfabricated array bioreactor for perfused 3D liver culture.* Biotechnol Bioeng, 2002. **78**(3): p. 257-69.

26. Tatosian, D.A., *Developemnt of a microscale cell culture analog device to study multidrug resistance modulators*, in *Chemical Engineering*. 2007, Cornell university: Ithaca. p. 186.

27. Meng, D.D. and C.J. Kim, *Micropumping of liquid by directional growth and selective venting of gas bubbles.* Lab Chip, 2008. **8**(6): p. 958-68.

28. Xu, H. and M.L. Shuler, *Quantification of chemical-polymer surface interactions in microfluidic cell culture devices.* Biotechnol Prog, 2009. **25**(2): p. 543-51.

29. Eddings, M.A., M.A. Johnson, and B.K. Gale, *Determining the optimal PDMS-PDMS bonding technique for microfluidic devices.* J. Micromech. Microeng, 2008. **18**(067001).

30. Wu, M.H., et al., *Development of perfusion-based micro 3-D cell culture platform and its application for high throughput drug testing.* Sensors and Actuators B-Chemical, 2008. **129**(1): p. 231-240.

31. Ryu, K.S., et al., *Micro magnetic stir-bar mixer integrated with parylene microfluidic channels.* Lab Chip, 2004. **4**(6): p. 608-13.

32. Wu, D., et al., *Grafting epoxy-modified hydrophilic polymers onto poly(dimethylsiloxane) microfluidic chip to resist nonspecific protein adsorption.* Lab Chip, 2006. **6**(7): p. 942-7.

CHAPTER 5

DEVELOPMENT OF DISPOSABLE PDMS MICRO CELL CULTURE ANALOG DEVICES WITH PHOTOPOLYMERIZABLE HYDROGEL ENCAPSULATING LIVING CELLS

5.1 Abstract

In previous studies we have developed silicon based micro cell culture analog (microCCA) devices to address tissue-tissue interaction and for simultaneous toxicity assessment of multiple types of cells. However, the development of PDMS micro devices have been delayed due to the difficulty of seeding multi cell types into a closed PDMS device. Approaches with microvalves to control the flow are complex, expensive and inconvenient to use. Here we described a simple alternative way for patterning multi types of cells into individual cell culture chambers within a closed PDMS microCCA device. Photopolymerizable hydrogels, with polyethylene glycol diacrylate (PEG DA) as a model prepolymer, were used for three dimensional (3D) cell encapsulations. A fluorescence microscope based direct pattern writing method was used for one-step cell encapsulation and hydrogel patterning. More than 90% of the cells remained viable after polymerization. The capability of such a PDMS microCCA device with hydrogel containing living cells as a biosensor was demonstrated with Triton X-100 as a model toxicant. All cells on the microCCA device lost their viability after exposure to 0.02% Triton X-100. The combination of photopolymerizable hydrogels and the microfluidic cell culture device will make it possible to fabricate simple and low cost biosensors for drug development, environmental toxicity study and clinical diagnoses.

5.2 Introduction

Poly (dimethylsiloxane) (PDMS) based soft lithography has become popular for the microfabrication of cell culture devices [1, 2]. Structures on a micrometer scale can be easily made with soft lithography requiring less complicated facilities than photolithography [3]. PDMS is inexpensive, bio-compatible, gas permeable, and the surface can be easily modified for cell attachment [4]. In addition, PDMS microfluidic structures can be easily sealed to a glass surface by introducing both the PDMS and glass into oxygen plasma to form a permanent bond. Both the glass and the PDMS are good supporting materials for cell adhesion and optical analysis. The overall cost of such devices is low enough for making disposable biological and medical devices to avoid cross contamination.

Loading of cells into the PDMS micro devices usually involves three procedures: surface coating, cell seeding and medium rinsing. Poly-D-lysine, fibronectin, collagen and other components of extra cellular matrix or synthetic polymers are used to alter the surface charge and hydrophobicity or introduce binding sites for cells. Cell suspension is then introduced into the channel or microfluidic pathway, and cells are allowed to attach to the inner surface of the device to form a monolayer for a typical time of four to eight hours. Cell culture medium is then introduced to rinse loosely attached cells, provide nutrition, and in many applications, to provide hydrodynamic forces necessary for specific cellular functions. Cell loading, however, is usually performed after the PDMS-glass seal, as the cells would be damaged by the oxygen plasma. Such an approach works well for attaching one type of cell, but it is difficult to obtain controlled spatial distribution of multi types of cells in a microfluidic device or accurate modeling of the cellular microenvironment. With a microfluidic system,

micro valves can be fabricated or incorporated into the device to manipulate the flow. By controlling the open/close state of each valve, cell suspension may be dispensed into only the destination chamber or area, but not the other area of the device [2, 5]. However, this method requires a complicated control system with a lab view interface. And the introduction of micro valves not only increases the cost and difficulty of operation, but also interferes with the microfluidic system, for example, by increasing the dead volume in the culture device.

Another approach skips the PDMS-glass bonding process. Instead, cells are seeded onto a PDMS slab by direct cell seeding onto a specific area or facilitated by micro contact printing. However, extra peripheral components such as bulky housing pieces are necessary to enclose the PDMS slab to form a close system. Cell co-culture is necessary to study cell interactions. Coculture of cells also has been found to enhance differentiation and improve expression of in vivo functions of cells cultured in vitro [6-8]. In addition, coculture of multi type of cells within different compartments of a device is the concept behind a microCCA device, which is a physical replica of the human body with different cell lines cultured in different organ or tissue compartments to represent each organ. A liver compartment is usually included to study drug metabolism, including the effect of metabolites on target tissues. The current microCCA devices are made from silicon and a Plexiglas housing is used to form a close fluidic structure. A novel method is needed to enable devices, like the microCCA, to be made with PDMS/glass and become disposable. A challenge is to load multi types of cells into different compartments of a closed PDMS device.

3D cell cultures provides more physiological relevant cellular environment than traditional 2D cell culture, and also protect cells from hydrodynamic forces. Cells are

usually encapsulated in porous materials or in hydrogels. Porous materials are most often used as temporary supporting structure to from artificial tissue, and degrade with time under physiological conditions. Porous polymers such as polylactic acid (PLA), polyglycolic acid (PGA), poly (lactic-co-glycolic acid) (PLGA) are constructed with various pore sizes to house cell cultures. Hydrogels are three-dimensionally cross-linked macromolecules of hydrophilic polymers. Hydrogels are high in water content, and possess a degree of flexibility very similar to natural tissue. "Naturally based" hydrogels such as Matrigel (made of native extracellular matrix proteins, ECMs), collagen (the major extracellular matrix protein), gelatin and hyaluronic acid provide endogenous signals that promote the cellular interactions that underlie tissue formation. ECMs contain essential proteins that help cells attach, grow and differentiate. Some other examples of natural hydrogels include dextran and alginate. Hydrogels to mimic the extracellular matrix can be created from synthetic molecules such as poly (ethylene glycol), polyglycolide, polylactide, acrylamide derivatives, calcium alginate and agarose [9, 10]. These polymers are cross-linked using ultraviolet light, radioactive rays, chemical cross-linking agents, ion solutions, or via temperature control for thermo-responsive hydrogels to reach a three-dimensional form. The advantages of synthetic gels include their consistent composition and predictable manipulation of mechanical, chemical and physical properties such as hydrophobicity, as well as degradability that can be tailored for different applications. However these gels often lack functional sites to interact with soluble or cell-surface proteins [11]. Proteins and positive charged components are often added into the composition to support cell-gel interactions. Cells are usually incubated within the polymer during this process and remain encapsulated after the gel is formed.

Although hydrogels are soft in texture and easy to handle at microliter scale, generation of micro structures of hydrogels containing living cells with controlled spatial distribution can be challenging, mainly because of the limitation of crosslinking methods. It is preferred that gel formation occurs at physiological temperature and pH to enhance maintenance of cell function. The crosslinking process is required to occur in the micro device rather than being transferred into the micro devices due to the difficulty of handling soft microscale gels.

Recent advances in hydrogel technology can support this objective. The gel may be a bulky slab or have microstructures in an array within a microfluidic network. To form a hydrogel slab in a microchannel, Frisk et.al injected Matrigel into a channel. The gelling process at 37°C caused Matrigel to shrink and generate a gap between the ceiling of the channel and the bulk hydrogel for medium perfusion [12]. Laminar flow has been used to partition microchannels with multiple microslabs of matrigels [13]. For micropatterning of hydrogels, gels may be deposited onto a surface by spinning, molding [14], or with a jet printer [15]. In addition, PDMS stamps have been used for micro contact printing of thermally curable gels and synthetic sol-gel transition peptide hydrogels such as Puramatrix [16].

A most interesting method, however, is to use ultraviolet (UV) light to pattern photopolymerizable hydrogels. The most obvious advantage of photo crosslinking is that no contact between the crosslinking tool, here the light source, and the precursor solution is required, which allows the manipulation of the crosslinking process in a closed PDMS device through the PDMS or glass layers. Examples of polymers that can be UV crosslinked include polyethylene glycol diacrylate (PEG DA), dextran acrylate, and Pluronic™-DA. PEG [17], Pluronics [18] and certain dextrans [19] are

FDA-approved for use in medical applications. PEG hydrogel microstructures were reported in 2000 to form active hydrogel components for self-regulated flow control [20]. A minimum feature size of 25 um, which was coincided with the minimum resolution of the photomask, was stated.

Using PEG, Revzin et.al reported the formation of micro structures as small as 7-10 um diameter [21]. PEG hydrogels encapsulating living 3T3 fibroblast were also generated by spin coating of cell-polymer precursor solution onto a glass substrate and then exposing the layer to 365 nm UV light through a photo mask [22]. Koh et.al also reported the fabrication of microstructures with 100 um diameter in a microfluidic channel or a single chamber with macrophage or fibroblast [23]. An cell microarray was also formed by PDMS molding [14]. Liu and coworkers was able to photopattern hydrogels of multiple cellular domains into a single "hybrid" hydrogel layer, and patterns of multiple cell types in multiple layers simulating use in a tissue engineering application [24]. PEG hydrogels was also constructed in microfluidic systems as functional components for pH sensing [25], and this technique may be possibly used for controlled release or delivery of small hydrophobic drugs [26]. A closed microfluidic network also promotes photopolymerization by limiting oxygen availability since oxygen was found to inhibit photopolymerizations [27]. With a photomask was inserted into the field–stop of the microscope to be used for projection, features down to 400 nm can be achieved with PEG polymeric particles [28], while photopatterned hydrogels microstructures containing living cell can be as small as 100 um feature size [29]. By combing photo- and electro patterning methods, Albrecht et.al was able to fabricate living cell arrays and position cells within a prepolymer solution prior to crosslinking and forming cell patters with micro resolution [29].

In this work, we present an approach using photopolymerizable hydrogels for patterning cell cocultures in a three compartment PDMS micro cell culture analog device. We are the first to pattern different cell types into multi compartments of a microfluidic network. The use of UV crosslinking technique eliminates the necessity to incorporate complex microfluidic control components, such as valves and multi inlets/outlets to control spatial specific cell seeding. PEG-DA was used as a model polymer as it is a well known hydrophilic, biocompatible material. It is usually used for surface modification of biomedical devices. In addition to micropatterning with a photomask and a UV spot light source, a direct writing method with UV light from a standard fluorescence microscope is described. As a demonstration, cells encapsulated in the microgels in a microCCA device were challenged with Triton X-100, and the change of cell viabilities was observed. The methods described here may contribute to the development of low cost and disposable multi-cell-based biosensors for both clinic and research purposes.

5.3 Materials and methods

5.3.1 Chemicals and reagents

Unless mentioned otherwise, chemical reagents were purchased Sigma-Aldrich Corp. (St. Louis, MO). Fetal bovine serum (FBS) was from Hyclone (Logan, UT). PDMS prepolymers were from Corning Inc. (Corning, NY). CellTracker™ Green CMFDA (5-chloromethylfluorescein diacetate, CellTrace™ calcein blue AM, SYTO® 59 red fluorescent nucleic acid stain and the live/dead cell viability kit were from Invitrogen (Carlsbad, CA).PEG-DA was dissolved in phosphate-buffered saline (pH 7.4, Invitrogen; Carlsbad, CA). The photoinitiator, 2-hydroxy-1-[4-(hydroxyethoxy)

phenyl]-2-methyl 1-propanone (Irgacure 2959; Ciba, Tarrytown, NY) was dissolved in DMSO.

To synthesize PEG-DA (MW 4000), 4.0 g (1 mmol) were dissolved in 100 ml of benzene and heated to 45C with stirring until a complete dissolution. After the solution was cooled to room temperature, 10.5 mmol of triethylamine, at a concentration five times molar excess of each –OH group on PEG4000, was added to the PEG solution. Then 10 mmol of acryloyl chloride, also at a concentration five times molar excess of each –OH group on PEG4000, was added dropwise to the PEG4000 solution to form acrylate diesters of PEG4000. The mixture was stirred at 0 ^{o}C (ice bath) for 24 h under nitrogen atmosphere. The insoluble triethylamine salts formed during the reaction were removed by filtration and the PEG-DA 4000 product was precipitated in 500 ml chilled hexane and collected by filtration. Further purification was performed by redissolving in 20 ml of benzene and reprecipitated in 500 ml of chilled hexane twice. The PEG-DA 4000 polymer was finally dried for 24 h in vacuo oven at room temperature and stored at 4C for future use.

5.3.2 Cell culture

MCF7cells were maintained in Dulbecco's Modified Eagle's Medium (DMEM) (MP Biomedicals, Solon, OH) supplemented with 5% heat inactivated FBS. Ishikawa Cells have been maintained in Minimum Essential Medium (MEM) (Invitrogen, Carlsbad, CA) with 10% FBS. HepG2/C3A cells were obtained from the American Type Culture Collection (Manassas, VA), and were maintained in MEM with 1.0 mM sodium pyruvate and 10% FBS. All the cells were cultured at 37°C in a humidified, 5% CO2, 95% atmosphere incubator.

5.3.3 Design and fabrication of PDMS microCCA device

PDMS microCCA devices were designed based on a simplified PBPK model of the human body. The body is divided into liver, mammary gland, uterus, and the other tissues which include tissues non-reactive and non adsorbing tissues.. Parameters, such as blood flow rate, residence time, etc are obtained from the literature. Physical parameters of each chambers and channels are carefully adjusted and calculated to balance the pressure drop between medium inlet/outlet, to maintain the residence time consistent with in vivo situations. The widths of the channels were designed to be wider than that in the silicon based microCCA devices described in chapter 4 for easy introduction and clearance of the polymer precursor solution.

PDMS microCCA devices were fabricated by PDMS molding from SU-8 masters. An SU8 mold master is fabricated by spinning SU8 2075 (MicroChem Corp., Newton, MA) onto silicon wafer at 500 rpm for 5 s then 1250 rpm for 30 s to reach a 200 um thickness of the SU8 layer. The resist layer was baked at 65°C for 10 min, 95°C for 40 min, and then was exposed to UV light (405 nm) with a Hybrid Technology Group's system III-HR contact/proximity mask aligner (HTG) (San Jose, CA). for 50 s and baked at 65°C for 5 min, 95°C for 20 min and 65°C for another 1 min. Development was done by immersing in SU8 developer (MicroChem Corp., Newton, MA) for several min to remove non-irradiated SU8 on the wafer. The mold was then treated with FOTS, also known as (1H, 1H, 2H, 2H-Perfluorooctyl) Trichlorosilane, as a release layer.

To make PDMS devices, a 10 :1 w/w-mixture of monomer and hardener (Sylgard 184, Dow Corning) was degassed under vacuum for 10 min to remove air bubbles in the PDMS mixture. The PDMS layer was cured by baking at 65°C for 2 h. The device was peeled off the master and holes were punched as the inlet and outlet with a needle. For permanent boding of PDMS and glass, both PDMS and borofloat glass wafer (d=100mm) (Mark Optics, Santa Ana, CA) were treated with a oxygen plasma machine (Harrick Plasma, Ithaca, NY) for 40 s before contact. Tubing was inserted and PBS was introduced into the device immediately after the oxygen plasma treatment to help maintain the hydrophilic property of the channel inner surface.

5.3.4 Surfaced treatment of PDMS devices

For patterning hydrogels on glass slides (Mark Optics, Santa Ana, CA), the glass substrates were first treated with 3-Methacryloxypropyltrichlorosilane (MAOPTS) (RF 60 s, reaction 600 s) on a Molecular Vapor Deposition tool (MVD100, Applied Microstructures Inc., San Jose, CA). MAOPTS is a useful monolayer for creating surface functionalization to promote the polymer adhesion to the glass slide.

For the microCCA device, surface treatment was performed after the bonding between PDMS and the glass substrate as described in the literature [21, 23]. In brief, the inner surfaces of microchannels were treated for 5 min with a 1 mM solution of MAOPTS in a 4:1 ratio of heptane-carbon tetrachloride, followed by washing with hexane and water.

5.3.5 Photopatterning of hydrogels

5.3.5.1 Photopatterning of hydrogels with a photomask

Photomasks were made by direct printing on a transparency film at 5080 dpi with a high resolution printer (Pageworks, Cambridge MA). The prepolymer solution was prepared to contain 15 % or 20% w/v PEGDA 700 or PEGDA 4000 and 20×10^6 cells mL^{-1} in PBS. Then Irgacure 2959 photoinitiator was added into the prepolymer solution at 0.1% w/v before UV exposure. To generate patterns on a glass slide, 8 ul of the pre-polymer solution was pipette onto a flat polypropylene surface. Then 180 um thick glass pieces were used as spacers, which determined the thickness of the precursor solution. The precursor droplets were then covered with a glass cover, with the MAOPTS treated side facing down. A photomask was aligned over the precursor solutions and then exposed to 365 nm UV light (UVP Black-Ray, long wave UV spot lamp, Upland, CA) for 120 s. Polymerization time varied depending on polymer composition. PEG prepolymer solution crosslinked covalently via radical chemistry upon UV exposure. After UV polymerization, uncrosslinked precursor solution was rinsed off with PBS.

For microCCA, the prepolymer solution was injected into the cell culture chambers via the inlet hole using a syringe. A photomask was secured on top of the chamber with emulsion side facing the glass. Foil was used to cover or reveal individual cell culture chambers for UV exposure. The remaining uncrosslinked prepolymer solution and cells were then flushed from the chamber with PBS. To add additional cell types in the mammary chamber, the next cell/prepolymer solution was injected into the chamber and pumped around already crosslinked hydrogel microstructures followed by UV exposure.

5.3.5.2 Patterning with direct writing on a fluorescence microscope

For direct pattern writing into the microCCA device, the prepolymer solution was prepared and injected into the cell culture chambers in the same way as patterning with a photomask. Instead of using a UV spot lamp for exposure, an inverted microscope was used to directly write the pattern onto the substrate. The microCCA device was positioned onto the sample stage of a fluorescence microscope (Olympus America Inc., Center Valley, PA) and exposed to UV with a 40 X objective (Olympus SPlan 40 PL, NA 0.40). A DAPI filter set (Chroma Technology Corporation, Rockingham, VT) was used to select the desired wavelength. Typical exposure times used were 1 to 3 s. Patterns within a chamber were written by moving the sample stage. The remaining uncrosslinked prepolymer solution and cells were then flushed out of the chamber with PBS. To pattern hydrogel microstructures encapsulating HepG2/C3A cells into the liver chamber, prepolymer solution mixed with cells was then injected into the chamber followed by UV exposure. The direct writing procedure was repeated in the mammary and uterus chambers with respective cells.

5.3.6 Live/dead cell viability assay

Cell death was monitored using a Live/Dead Cell viability/cytotoxicity kit (Invitrogen, Carlsbad, CA) to analyze cell viability after encapsulation. In this assay, the intracellular esterases of the live cells convert the non-fluorescent calcein acetoxymethyl (calcein AM) to a fluorescent calcein. EthD-1 enters the dead cells through the damaged membranes and becomes fluorescent when bound to nucleic acids. Calcein AM dye produces a bright green fluorescence in live cells, whereas EthD-1 produces a bright red fluorescence in dead cells.

5.3.7 Optical imaging

Cells were observed and imaged under an IMT-2 phase contrast and fluorescence microscope. Fluorescence and transmission images were captured with a Retiga CCD camera (Qimaging, Burnaby, BC, Canada) in a 12 bit grayscale format, and were analyzed using ImagePro Plus software (Media Cybernetics Inc., Silver Spring, MD). The fluorescence intensity in cells was calculated as the average optical density per pixel of cells. The optical cubes used for CellTracker™ Green CMFDA, CellTrace™ calcein blue AM and SYTO® 59 were fluorescein isothiocyanate (FITC), 4'-6-Diamidino-2-phenylindole (DAPI) and tetramethylrhodamine isothiocyanate (TRITC) cubes.

5.4 Results and discussions

5.4.1 UV polymerized hydrogels for cell culture

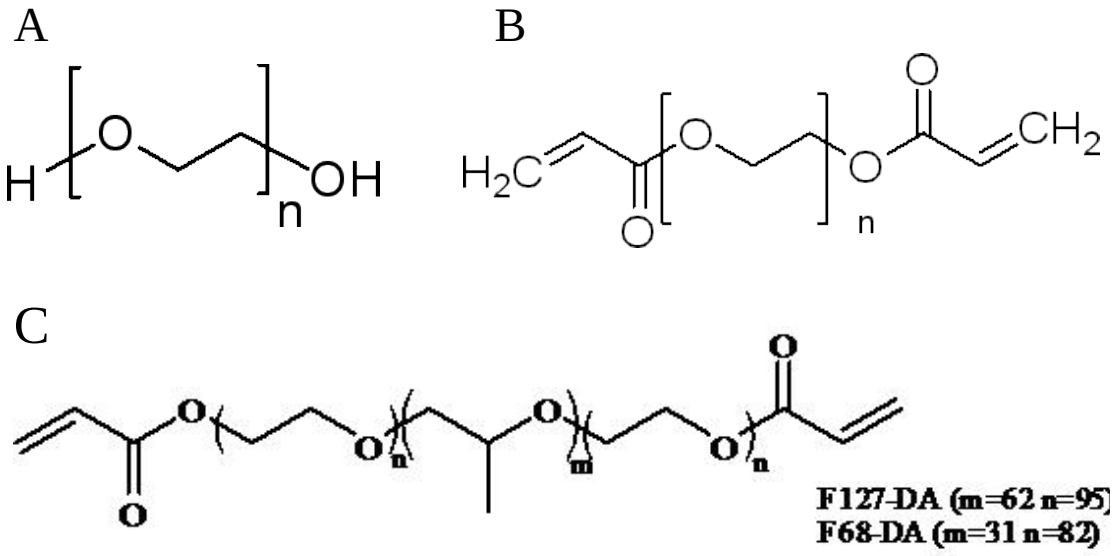

Figure 5.1 Structure of (A) poly(ethylene glycol), (B) poly(ethylene glycol) diacrylate (PEG-DA) and (C) Pluronic F127-DA and F68-DA

In this work, PEG-DA was used as a model polymer tested for its capability for encapsulating cells in a microCCA device. The method described here, however, is useful for all other photopolymerizable polymers, such as Pluronic ® DA[30] and dextran-acrylate [31] (Figure 5.1). The polymerization process involves the induction of free radicals through photo initiators. The formation of hydrogel microstructures from polymer acrylates was based upon the UV initiated free-radical polymerization of acrylate end groups. The photoinitiator dissociates upon exposure to UV radiation, creating highly reactive methyl and benzaldehyde radicals, which then attack unsaturated carbon-carbon double bonds of acrylate functionalities on the macromer, thus initiating free radical polymerization results in the formation of a highly cross-linked network. This network represents a three-dimensional, insoluble structure, capable of entrapping proteins [21] as well as live cells inside the gel matrix.

Only recently have photopolymerizable hydrogels been used for live cell encapsulation and culture [22]. The advantage of using photopolymerizable hydrogels is that the patterning requires no direct contact of the light source and the patterning surface. Cells can be encapsulated into hydrogels via UV light through a glass slide, plastic cover, PDMS pieces, or other materials that are UV transparent. The mechanical properties of the hydrogels formed after UV exposure is affected by the structure of the precursor, concentration of the prepolymers, exposure time as well as the dimensions of the final gel. Viability of the cells inside the hydrogel after polymerization can be affected by parameters of the UV exposure, which also determines the resolution of the final features in the patterned hydrogel. A powerful UV source is favorable for faster gelling, yet the high power may also lead to cell damage, while a low energy source may cause a loss of resolution due to radical diffusion. A long time UV exposure (> 5 min) may also cause thermal damage.

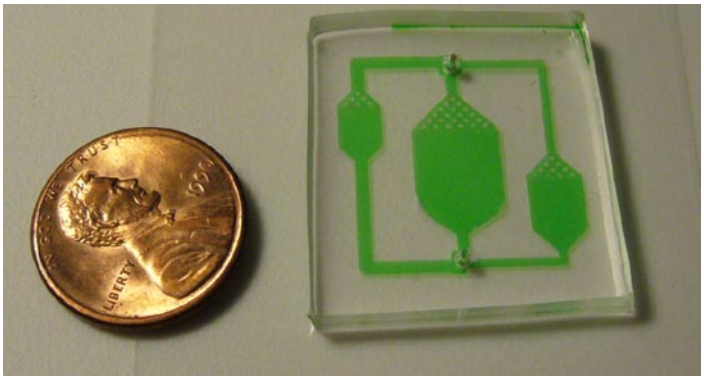

Figure 5.2 PDMS based three chamber microCCA device. Fluidic pathways were visualized with green food dye. The three chambers represent the uterus tissue, liver and mammary tissue respectively (from left to right).

5.4.2 Construction of the microCCA device

Silicon based multi-chamber cell culture analog devices have been constructed previously in our group [32-34], and a microCCA device with four culture chambers has been described in Chapter 4. However, silicon based micoCCA devices have several disadvantages. It is costly for making prototypes due to the high cost of silicon wafer and the photolithography fabrication process in a clean room. Furthermore, in order to enclose the microCCA device into a microfluidic system, a housing made from hard plastic is machined to contain the device and to connect the device to an external pump or a fluid handling system. Excellent sealing between the housing, the silicon chip and the tubing connections is required, which makes the assembly process difficult and variable due to personal practices. And chemical cross contamination is a problem when housing pieces are reused, as plastic is prone to chemical adsorption. A PDMS microCCA device, instead, is lower in cost, less expensive to fabricate, and easy to seal by plasma treatment and require no extra housing. In addition, silicon is opaque while PDMS is optically transparent.

In this work we designed and fabricated a new version of a PDMS based microCCA device (Figure 5.2). The devices are meant to be disposable. The new design is a three chamber cell culture device with relatively wider channels to facilitate precursor solution removal after photo crosslinking. Pillars were used at inlets to improve mixing and for even chemical distribution across the chamber. The depth of the chambers were 50 um or 175 um. The device was 2.5 cm x 2.5 cm in size. Thickness of the device is about 2.5 mm to 5 mm as determined by the thickness of the PDMS slab. A short PDMS cure time of 1.5 to 3 h worked well while a baking time longer than 24 h may cause PDMS to stick to the SU8 master, and break at elbows and at other small features.

The three chambers represent the uterus tissue, liver and mammary tissue respectively. Three cell lines were picked for on-chip cell culture. The HepG2/C3A cell line was used as a model for the liver. This cell line has detectable CYP1A1/2 activity, which is responsible for the metabolism of estrogens such as E2 and trans-stilbene. MCF7-GFP developed from MCF-7 cell line was used to imitate the mammary tissue. Ishikawa-GFP was developed from Ishikawa carcinoma cell line to represent the endometrial tissue. GFP intensity in MCF7-GFP and Ishikawa-GFP cells increase when the cells were exposed to estrogens [35].

5.4.3 Photopatterning with a UV lamp

UV spot lamps are commonly used to photopolymerize hydrogels [14, 21, 23, 25]. A photomask was aligned on top of the precursor solution for selective UV exposure. Figure 5.3 shows arrays of cylindrical microstructures with a diameter of 300 um created from PEG-DA700. The thickness of the gels was about 175 um, which is

adjustable by controlling the thickness of the spacer between the two pieces of cover glass.

Uncrosslinked precursor solutions were rinsed off with PBS. However, the PEG microstructures were easily disturbed and displaced during this rinsing process. Surface treatment with MAOPTS was able to form a mono layer of MAOPTS and leaves free methacrylate groups on the surface of the glass slide, which react with PEG-DA during UV crosslinking and promote the adhesion of PEG microstructures to the glass slide [21].

A UV lamp doses a large working area and allows the generation of many microstructures all at once. However, in our setup the exposure time required for gelling was relatively long, with 2 min exposure required for PEG 700 and 3 min for PEG 700/DA / PEG 4000/DA mixtures. The cell viability was greatly affected by polymerization with less than 50% of the population being viable (data not shown). In addition, since the light from the spot lamp was divergent, the polymerization speed was affected greatly by the position of the precursor solution in relative to the light source. It was challenging to use this system to generate consistent data.

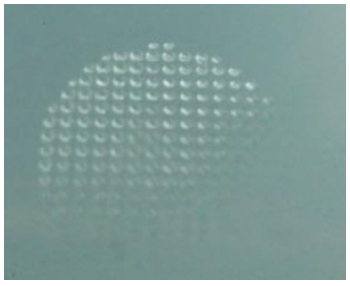

Figure 5.3 PEG/DA 700 microstructures generated with photopatterning with a UV lamp. Diameter of each cylindrical microstructure was 300 um.

5.4.4 Photopatterning with a fluorescence microscope

A fluorescence microscope is readily available in most biology labs and provides an alternative source for UV polymerization. A DAPI filter cube allows the light with wavelengths of 340 ± 40 nm to pass through, which is the range for UV light induces the PEG polymerization process. The lens narrow the light beam and providers a high light intensity near the focus point, which results in a fast photocrosslinking speed. The typical exposure time that was required for PEG crosslinking with a UV spot lamp was 2 min to 5 min while 0.5 s to 3 s was necessary on a fluorescent microscope. The diameters of the PEG dots generated near the focus with a 40 X objective were measured to be 400 um to 600 um.

A second advantage of using the fluorescence microscope for UV crosslinking is that it allows real-time monitoring of the polymerization progress. As the precursor solution is exposed to the UV light through a DAPI filter cube, the cell status and formation of the hydrogel may be observed simultaneously through transmission light microscopy or through fluorescence dyes if the dye spectrum fits that of the DAPI cube. Figure 5.4 shows the UV crosslinking process with PEG to encapsulate Ishikawa cells. The PEG700 hydrogel was observed to have clear borders visible in both transmission and fluorescence images, which stood out and separated it from the surrounding uncrosslinked precursor solution, even before the PBS rinsing. The red fluorescence of the cells is from SYTO 59 probe and was observed by changing the optical filter cube. However, it is possible to observe the fluoresce at the same time the hydrogel is being formed when blue fluorescent dyes, such as DAPI, Calcein blue AM and CellTracker™ blue that fit the DAPI filter cube, is used to visualize live cells or other cell functions.

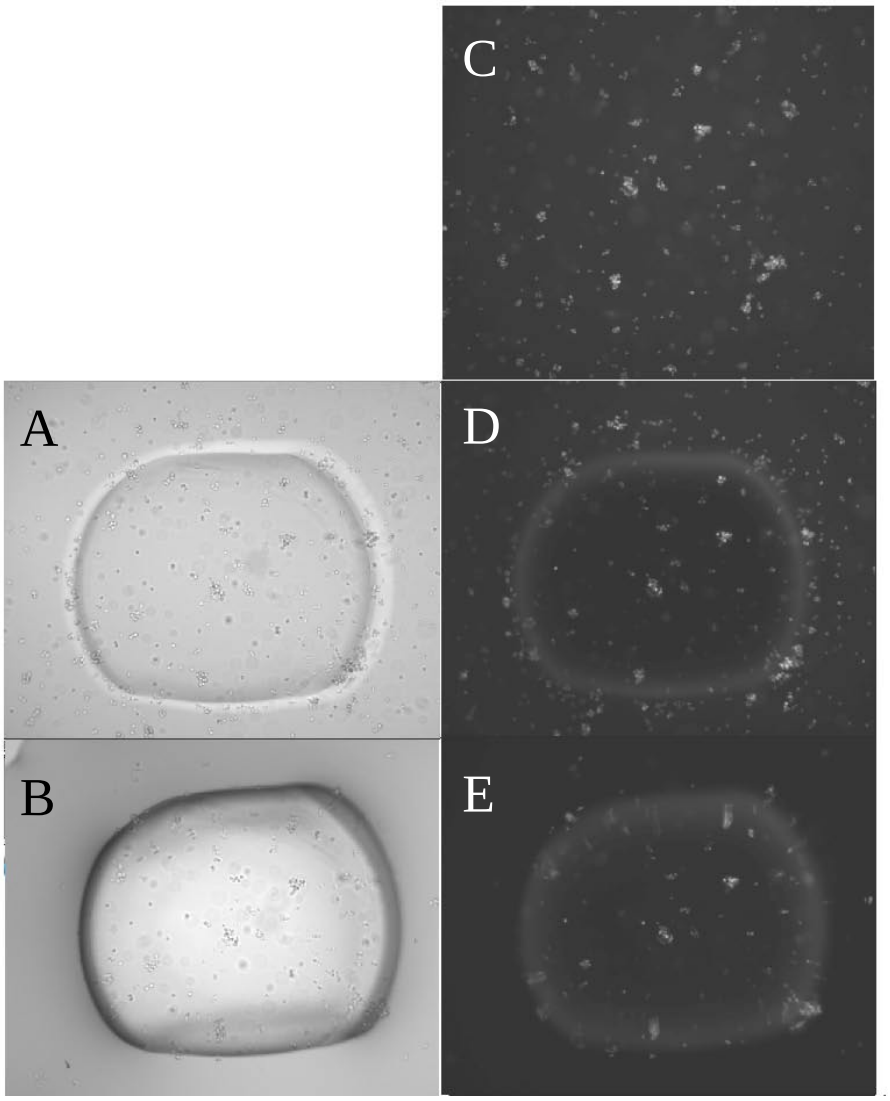

Figure 5.4 Encapsulation of Ishikawa cells in PEG DA 700. (A) and (B) are transmission images and (C) to (E) are fluorescent images. Cells were stained with SYTO 59 for visualization purpose. (C) Precursor solution was injected into the cell chamber. (A) and (D) Gel was formed upon UV exposure. (B) and (E) Rinsing with PBS removed uncrosslinked prepolymer solutions as well as loose cells around the hydrogel structure. These images show that with PEG DA 700, the polymerization progress can be monitored in real-time.

The diameter and the thickness of the hydrogel dots were affected by the time of exposure. Figure 5.5 showed the PEG/DA 700 hydrogel microstructures formed with a

fluorescence microscope. The diameters of the dots for 1 s, 2 s, 3 s and 4 s exposure were measured to be about 400 um, 500 um, 550 um and 600 um, Increase of exposure time also increased the thickness of the hydrogel microstructures.

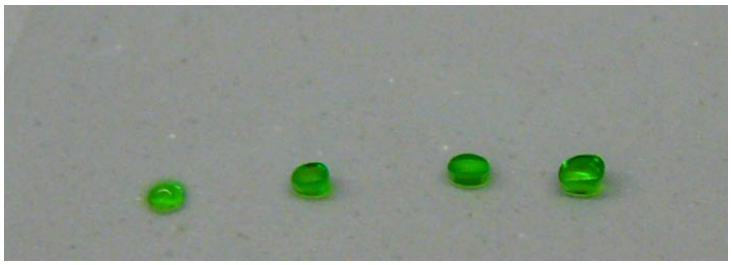

Figure 5.5 Effect of UV exposure time on the size and thickness of the formed hydrogel. The UV exposure time for the polymerization was 1 s, 2 s, 3 s and 4 s respectively from left to right.

To demonstrate the capability direct pattern writing with a fluorescence microscope, letters were written onto a glass substrate. Figure 5.6 are images of the written pattern, the letter C and letter U, generated with PEG700/4000 DA with live cells encapsulated in the gel. The letters were written by moving the sample stage of the fluorescence microscope manually. In Figure 5.6 A, the hydrogel was stained with green food dye to visualize the letters. Figure 5.6 B is the fluorescence photo of same hydrogel structure, where cells were stained with SYTO 59 that bind to nucleic acid and generate a red fluorescence.

Although several groups have used a fluorescence microscope as a UV source to crosslink hydrogels, the patterns were generated with a photo mask rather than with direct writing [20]. Direct writing with a microscope allows easy control over a single hydrogel microstructure. As shown in Figure 5.6, the individual hydrogel microstructures can be placed separated, adjacent or overlapping to each other. This

method may be combined with an automatically controlled microscope sample stage for precise cell placement to study migrations, cell-cell and cell-biomaterial interactions. The size of the hydrogel dots generated with our current optical setup were relatively large (~ 400 um), but may be reduced with different objectives and optimized optical setups.

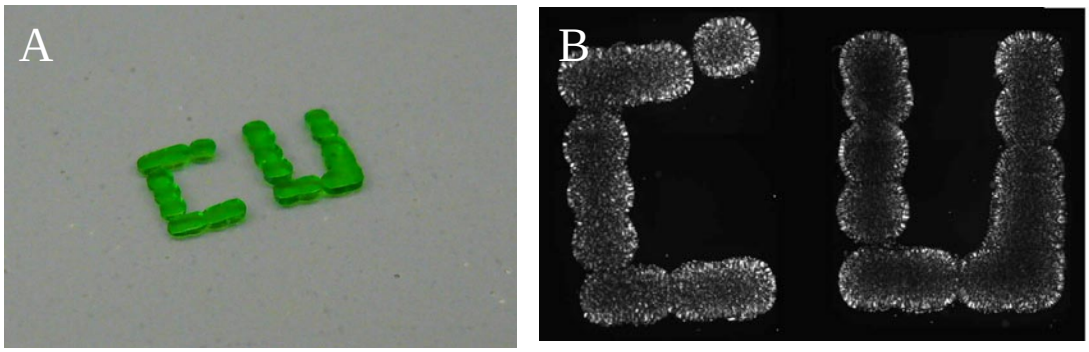

Figure 5.6 PEG/DA 700/4000 microstructures generated with direct pattern writing on a fluorescence microscope.

5.4.5 Patterning multi types of cells inside a microCCA device

Photocrosslinking enables polymerization without direct contact between an "inducer" and the prepolymer solution. Hydrogels with different compositions can be formed at specified sites very close to each other. Such a property allows patterning of multi types of cells in one chamber or in different chambers that are connected together in a microCCA device.

Figure 5.7 is an image demonstrating the patterning of three different hydrogel microstructures adjacent to each other in a chamber of 8 mm by 8 mm. Ishikawa cells were mixed with PEG 700/4000 DA (v/v 1:4) precursor solution, and then stained with either CellTracker Green, Calcein blue AM or SYTO 59 red. Precursor solutions

with cells stained green were first injected into the liver chamber and a hydrogel dot was formed by direct UV writing through an objective with a DAPI filter cube. Then the PBS was injected into the chamber to rinse off loose precursor solutions. Then the sample stage was moved and same procedures were repeated with precursor solution mixed with Ishikawa cells stained blue and that with cells stained red to form hydrogel dots at different spots.

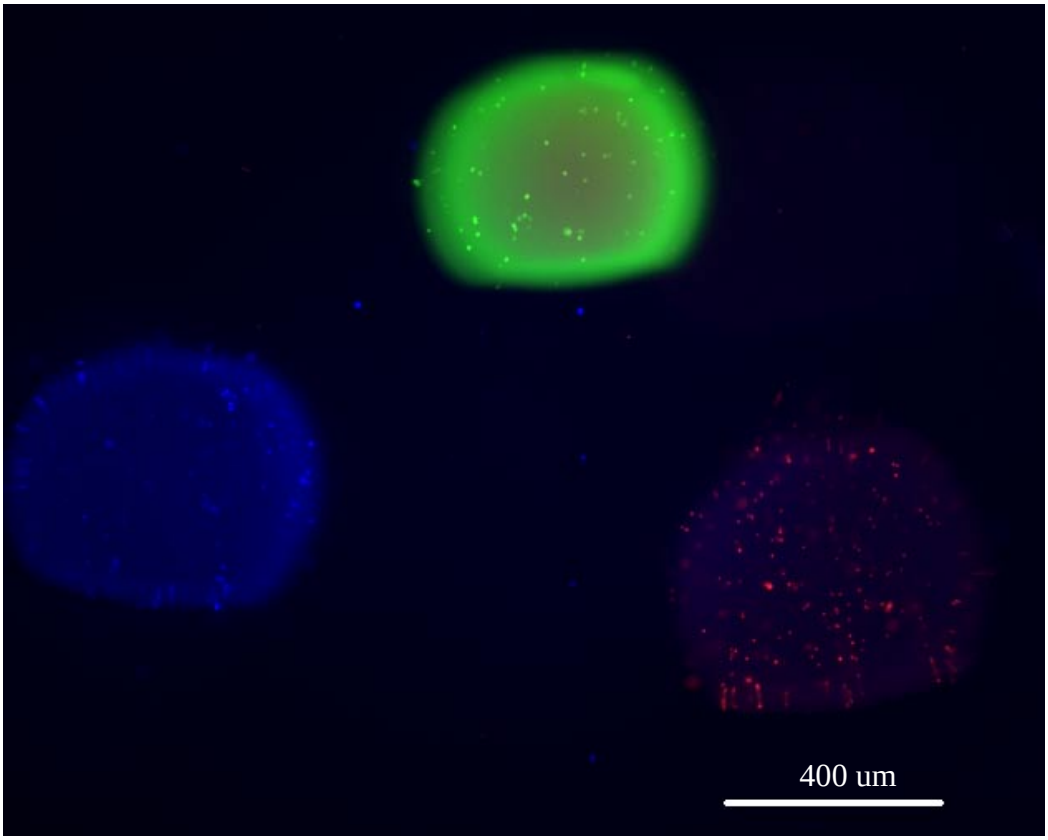

Figure 5.7 Copatterning of multi-types of cells in a microfluidic cell culture chamber. Ishikawa cells were stained with CellTracker™ Green, CellTrace™ calcein blue AM and SYTO® 59 red fluorescent nucleic acid stain respectively. The gel dots were formed with a DAPI filter on a fluorescence microscope.

With the same method, three types of cells were patterned into individual cell culture chambers of the microCCA device described in section 5.4.2. HepG2/C3A cells encapsulated in PEG 700/4000 were patterned into the liver cell culture chamber, and Ishikawa cells and MCF7 cells were patterned into the uterus and mammary cell culture chambers respectively (Figure 5.8).

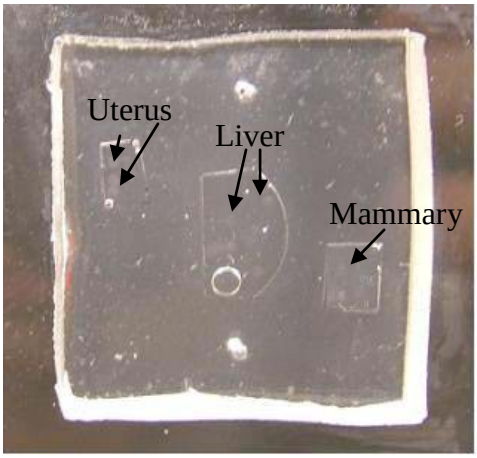

Figure 5.8 Patterning of three different type of cells in a microCCA device. Ishikawa, HepG2/C3A and MCF-7 cells were encapsulated into the hydrogel dots inside the uterus, liver and mammary cell culture chamber respectively. The hydrogels were not visualized very clearly due to their small size and transparent nature.

MAOPTS treatment of the glass slide was used for promote adhesion of the PEG hydrogel to the glass surface after UV exposure. Without surface modification, the formed hydrogel microstructures do not bind effectively to the glass surface and easily detach from the glass surface with PBS rinsing. However, in a PDMS based microCCA device, we found that MAOPTS treatment was not necessary, likely due to the fact that the formed microhydrogel was sandwiched between the PDMS and the cover glass. Results from our experiment showed no displacements of the formed PEG

700 or PEG 700/4000 hydrogel dots when PBS rinsing was performing manually or with a pump with flow rates less than 2 ml per min.

5.4.6 Cell viability measurements

The viability of Ishikawa cells were assessed before and 30 min after the polymerization process. We observed a more than 50% of cell death after UV crosslinking with a UV spot lamp (UV exposure time 2.5 min) (data not shown). With direct writing using a 40 X, no obvious decrease of cell viability after UV crosslinking (UV exposure time 2 s) was observed (Figure 5.9). The improved cell viability may result from the significant decrease of the UV exposure time with the direct writing method.

Others have reported better cell viabilities (> 80% viable cells) after polymerization with a UV spot lamp [22, 23, 29]. Part of the reason may be the difference of cells types used in each study, as fibroblasts [22, 23, 29] and endothelial cells used in this study may have various sensitivity to UV and free radical induced damages. It has been discovered previously that endothelial cells display lower antioxidant enzyme activities, are inherently more sensitive to the harmful effects of reactive oxygen metabolites [36] and oxygen toxicity [37] than fibroblasts.

5.4.7 Responses of PEG encapsulated cells in microCCA devices

The microCCA with cells encapsulated in PEG may be used as biosensors to detect toxins. Here we used Triton X-100 as a model reagent. Triton X-100 is a non-ionic surfactant, which is widely common for the solubilisation of membranes under non-denaturing conditions [38]. Exposure to Triton X-100 may induce a rapid cell death by necrosis caused by the permeabilisation of the cell membranes [39].

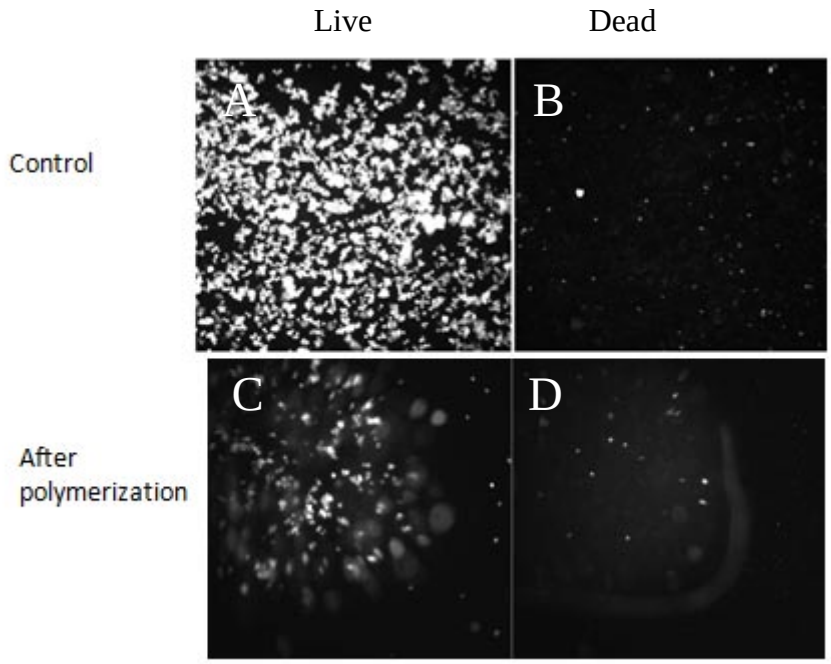

Figure 5.9 Viability of Ishikawa cells (A), (B) in the control samples and (C), (D) in a three dimensional hydrogel microstructure 30 min after photopolymerization. (A) and (C) showed live cells stained bright; (B) and (D) showed dead cells. Control samples were uncrosslinked precursor solution mixed with cells.

Ishikawa and HepG2/C3A cells were first patterned into the uterus chamber and the liver chamber via direct pattern writing in microCCA devices. Viability of these PEG encapsulated cells patterned were measured after 20 min exposure to 0.02% Triton X-100. Results showed that both HepG2/C3A cells and Ishikawa cells were 100% dead while more than 90% of the cells remained live in the control samples (Figure 5.10). This result indicating that (1) Triton X-100 may readily diffuse into the micro hydrogel structure; (2) Cells encapsulated within the microhydrogel structures retained their viability and metabolic active; (3) The microCCA with PEG encapsulated cells

was capable of simultaneous assessment of chemical toxicity with multiple types of cells.

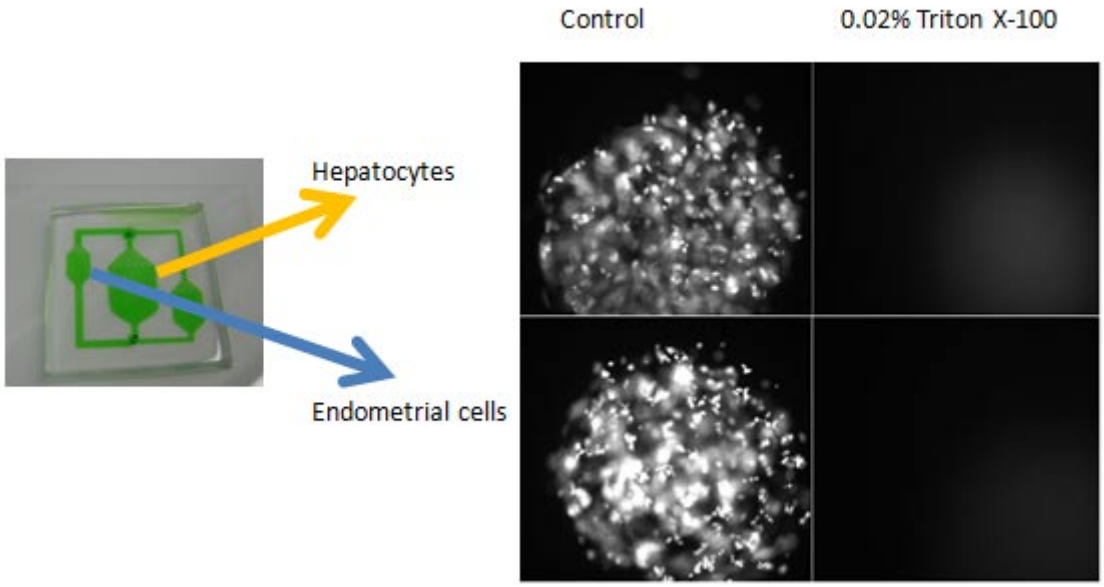

Figure 5.10 Viability of hepatocytes HepG2/C3A cells and endometrial Ishikawa cells in the control samples or in samples with 0.02% Triton X-100. Cells were encapsulated inside PEG 700/4000 and patterned into microCCA chambers.

Crosslinking of photopolymerizable prepolymers form a 3D network within the hydrogel. Heavily crosslinked hydrogels have smaller values of mesh size and number average molecular weight between crosslinks, which lead to a decreased mass transfer of molecules. For example, Ricin (MW 60000) failed to penetrate into the PEG DA (MW 575) hydrogel in a study [23]. PEG DA with a larger molecular weight, such as PEG DA (MW 4000), is preferred when working with large molecular compounds. Solute diffusion within a hydrogel should be carefully investigated when designing photopolymerizable hydrogels for a specific application, especially when large macromolecules are involved.

5.5 Conclusion

In this work we developed a new method for direct patterning of different types of cells into different chambers in a closed PDMS microfluidic cell culture device. Ishikawa, MCF-7 and HepG2/C3A cells were patterned into their individual cell culture chambers, and the cells maintained good cell viability after UV polymerization. The encapsulated cells in microCCA responded well when exposed to a model reagent, Triton X-100. Although PEG was used as a model polymer in this study, the method is versatile and is suitable for other photocurable polymers such as dextran-DA. The method described here allows us to design and fabricate low-cost and disposable multi type-cell based biosensors, including the PDMS microCCA device described here, for drug screening and environmental toxin detections. A more useful system may be constructed in combine with other hydrogel based techniques, such as functional hydrogel structures for autonomous flow control [20] and intra channel pH sensing with PEG patch [25].

REFERENCES

1. Leclerc, E., Y. Sakai, and T. Fujii, *Microfluidic PDMS (polydimethylsiloxane) bioreactor for large-scale culture of hepatocytes.* Biotechnol Prog, 2004. **20**(3): p. 750-5.
2. Gu, W., et al., *Computerized microfluidic cell culture using elastomeric channels and Braille displays.* Proc Natl Acad Sci U S A, 2004. **101**(45): p. 15861-6.
3. Whitesides, G.M., et al., *Soft lithography in biology and biochemistry.* Annu Rev Biomed Eng, 2001. **3**: p. 335-73.
4. Lee, J.N., et al., *Compatibility of mammalian cells on surfaces of poly(dimethylsiloxane).* Langmuir, 2004. **20**(26): p. 11684-91.
5. Huang, C.W. and G.B. Lee, *A microfluidic system for automatic cell culture.* Journal of Micromechanics and Microengineering, 2007. **17**(7): p. 1266-1274.
6. Thomas, R.J., et al., *The effect of three-dimensional co-culture of hepatocytes and hepatic stellate cells on key hepatocyte functions in vitro.* Cells Tissues Organs, 2005. **181**(2): p. 67-79.
7. Bhatia, S.N., et al., *Effect of cell-cell interactions in preservation of cellular phenotype: cocultivation of hepatocytes and nonparenchymal cells.* Faseb J, 1999. **13**(14): p. 1883-900.
8. Bhatia, S.N., et al., *Microfabrication of hepatocyte/fibroblast co-cultures: role of homotypic cell interactions.* Biotechnol Prog, 1998. **14**(3): p. 378-87.
9. Woerly, S., G.W. Plant, and A.R. Harvey, *Cultured rat neuronal and glial cells entrapped within hydrogel polymer matrices: a potential tool for neural tissue replacement.* Neurosci Lett, 1996. **205**(3): p. 197-201.

10. Dillon, G.P., et al., *The influence of physical structure and charge on neurite extension in a 3D hydrogel scaffold.* J Biomater Sci Polym Ed, 1998. **9**(10): p. 1049-69.
11. Cushing, M.C. and K.S. Anseth, *Materials science. Hydrogel cell cultures.* Science, 2007. **316**(5828): p. 1133-4.
12. Frisk, T., et al., *A concept for miniaturized 3-D cell culture using an extracellular matrix gel.* Electrophoresis, 2005. **26**(24): p. 4751-8.
13. Wong, A.P., et al., *Partitioning microfluidic channels with hydrogel to construct tunable 3-D cellular microenvironments.* Biomaterials, 2008. **29**(12): p. 1853-61.
14. Koh, W.G., L.J. Itle, and M.V. Pishko, *Molding of hydrogel multiphenotype cell microstructures to create microarrays.* Analytical Chemistry, 2003. **75**(21): p. 5783-5789.
15. Hahn, M.S., et al., *Photolithographic patterning of polyethylene glycol hydrogels.* Biomaterials, 2006. **27**(12): p. 2519-24.
16. Kim, M.S., J.H. Yeon, and J.K. Park, *A microfluidic platform for 3-dimensional cell culture and cell-based assays.* Biomed Microdevices, 2007. **9**(1): p. 25-34.
17. Hamidi, M., A. Azadi, and P. Rafiei, *Pharmacokinetic consequences of pegylation.* Drug Deliv, 2006. **13**(6): p. 399-409.
18. Matthew, J.E., et al., *Effect of mammalian cell culture medium on the gelation properties of Pluronic F127.* Biomaterials, 2002. **23**(23): p. 4615-9.
19. Fishbane, S. and E.A. Kowalski, *The comparative safety of intravenous iron dextran, iron saccharate, and sodium ferric gluconate.* Semin Dial, 2000. **13**(6): p. 381-4.

20. Beebe, D.J., et al., *Functional hydrogel structures for autonomous flow control inside microfluidic channels.* Nature, 2000. **404**(6778): p. 588-90.

21. Revzin, A., et al., *Fabrication of poly(ethylene glycol) hydrogel microstructures using photolithography.* Langmuir, 2001. **17**(18): p. 5440-5447.

22. Koh, W.G., A. Revzin, and M.V. Pishko, *Poly(ethylene glycol) hydrogel microstructures encapsulating living cells.* Langmuir, 2002. **18**(7): p. 2459-2462.

23. Koh, W.G. and M.V. Pishko, *Fabrication of cell-containing hydrogel microstructures inside microfluidic devices that can be used as cell-based biosensors.* Anal Bioanal Chem, 2006.

24. Liu, V.A. and S.N. Bhatia, *Three-dimensional photopatterning of hydrogels containing living cells.* Biomedical Microdevices, 2002. **4**(4): p. 257-266.

25. Zhan, W., G.H. Seong, and R.M. Crooks, *Hydrogel-based microreactors as a functional component of microfluidic systems.* Analytical Chemistry, 2002. **74**(18): p. 4647-4652.

26. Missirlis, D., et al., *Doxorubicin encapsulation and diffusional release from stable, polymeric, hydrogel nanoparticles.* Eur J Pharm Sci, 2006. **29**(2): p. 120-9.

27. Decker, C. and A.D. Jenkins, *Kinetic Approach of O-2 Inhibition in Ultraviolet-Induced and Laser-Induced Polymerizations.* Macromolecules, 1985. **18**(6): p. 1241-1244.

28. Dendukuri, D., et al., *Stop-flow lithography in a microfluidic device.* Lab Chip, 2007. **7**(7): p. 818-28.

29. Albrecht, D.R., et al., *Photo- and electropatterning of hydrogel-encapsulated living cell arrays.* Lab Chip, 2005. **5**(1): p. 111-8.

30. Cellesi, F., N. Tirelli, and J. Hubbell, *Materials for cell encapsulation via a new tandem approach combining reverse thermal gelation and covalent crosslinking.* Macromolecular Chemistry and Physics, 2001. **203**(10-11): p. 1466-1472.

31. Ferreira, L., et al., *Biocompatibility of chemoenzymatically derived dextran-acrylate hydrogels.* J Biomed Mater Res A, 2004. **68**(3): p. 584-96.

32. Sin, A., et al., *The design and fabrication of three-chamber microscale cell culture analog devices with integrated dissolved oxygen sensors.* Biotechnol Prog, 2004. **20**(1): p. 338-45.

33. Viravaidya, K., A. Sin, and M.L. Shuler, *Development of a microscale cell culture analog to probe naphthalene toxicity.* Biotechnol Prog, 2004. **20**(1): p. 316-23.

34. Tatosian, D.A. and M.L. Shuler, *A novel system for evaluation of drug mixtures for potential efficacy in treating multidrug resistant cancers.* Biotechnol Bioeng, 2008.

35. Xu, H., W.L. Kraus, and M.L. Shuler, *Development of a stable dual cell-line GFP expression system to study estrogenic endocrine disruptors.* Biotechnol Bioeng, 2008. **101**(6): p. 1276-1287.

36. Aalto, T.K. and K.O. Raivio, *Differential sensitivity of human fibroblasts and endothelial cells to reactive oxygen metabolites.* Pediatr Res, 1992. **32**(6): p. 654-7.

37. Michiels, C., O. Toussaint, and J. Remacle, *Comparative study of oxygen toxicity in human fibroblasts and endothelial cells.* J Cell Physiol, 1990. **144**(2): p. 295-302.

38. Weyermann, J., D. Lochmann, and A. Zimmer, *A practical note on the use of cytotoxicity assays.* Int J Pharm, 2005. **288**(2): p. 369-76.

39. Borenfreund, E. and J.A. Puerner, *Toxicity determined in vitro by morphological alterations and neutral red absorption.* Toxicol Lett, 1985. **24**(2-3): p. 119-24.

CHAPTER 6

CONCLUSIONS AND FINAL RECOMMENDATIONS

6.1 Conclusions

A dual cell-line GFP expression system was constructed to study endocrine disrupting compounds with activities of estrogen receptor agonists or antagonists. The two stable cell lines, Ishikawa-GFP (uterine origin) and MCF7-GFP (breast origin), displayed increased intracellular GFP intensity with estrogens. This system also responded in a tissue specific manner to selective estrogen receptor modulators. Raloxifene and tamoxifen were effective antiestrogens in MCF7-GFP cells, but acted as partial estrogen receptor agonists in Ishikawa-GFP cells at concentrations of 0.1 nM and above. Our results also showed no low dose synergistic effects between the tested estrogenic compounds.

Physiologically realistic microCCA cell culture devices were designed and fabricated to help predict in vivo responses to EDs. The silicon microCCA device contained three cell lines for co-culture: HepG2/C3A (a hepatoma), MCF7-GFP and Ishikawa-GFP to detect estrogens and address tissue specific effects of antiestrogens. Introduction and recirculation of medium mimic the time dependent changes in drug concentrations and the microfluidic shear situation inside a body. In addition, an in-line bubble trap was incorporated into the system to overcome air bubble related cell death and device failure in previous designs.

Interactions between hydrophobic surfaces and the fluid are important in microCCA devices due to decreased fluid volume and increased surface area to volume ratio.

Significant surface adsorption of estrogen and several other hydrophobic chemicals to BPT tubing was observed with the peristaltic pumps for microCCA. Contaminants leaching out of the BPT tubing were also found to be estrogen receptor agonist, caused increased GFP expression in MCF7-GFP and Ishikawa-GFP, and interfered with the detection of estrogens. PTFE and stainless steel caused little interference. To overcome this problem, a PDMS based micropump was build to replace the previously used peristaltic pump. The benefits of the micropump are the replacement of BPT tubing with PTFE tubing, compact in size, small inner volume and the capability to allow parallel tests. Preliminary results indicated that the use of the micropump would overcome the GFP background problem associated with BPT tubing. Incorporation of the micropump with microCCA enabled the detection of cell response to estrogens.

A major limitation of silicon microCCA devices is their fragility, need for extra housing to form close cell culture compartments, and possible cross contamination problems associated with reuse. In this work disposable PDMS microCCA devices were developed, and the main challenge of seeding multiple types of cells without using complex fluidic control and expensive controlling system was solved. We developed a photopolymerizable hydrogel based method for direct patterning of Ishikawa, MCF-7 and HepG2/C3A cells into their individual cell culture chambers. Cells maintained excellent cell viability after UV polymerization. The use of this device as a biosensor was demonstrated by monitoring viability of PEG encapsulated cells in microCCA exposed to a model reagent, Triton X-100. A 20 min exposure led to 100% cell death while 90% cells in control samples were alive. These results indicate the potential of photopolymerizable hydrogels to be used with PDMS microCCA devices to detect toxins, including environmental endocrine disruptors. The overall cost of PDMS microCCA device is also much lower than silicon microCCA.

6.2 Recommendations

The mechanism or estrogen action involves multiple molecular pathways. The main molecular pathway is the ER-ERE pathway, which has been addressed in this study. In addition, the "ERα/AP-1 pathway" involves indirect recruitment of liganded ERαs to activating protein-1 (AP-1)-responsive DNA elements via heterodimers of Fos and Jun [1-3]. A retrovirus plasmid pQCXIP-AP1-GFP plasmid has been constructed, and cell infection has been finished. Further cell selection and characterization are necessary to build a responsive cell line. It would be important to test potential EDs with this cell line representing the ER-AP1 pathway as well. Other pathways may include cross talk between ER and other nuclear receptors, such as the aryl hydrocarbon receptor [4], or through disruption of cellular signaling cascades that interface with the hormone signaling systems. Further steps to address these and all other potential pathways are necessary for complete screening of EDs for their potential estrogenicity. It would be of great importance to study the mixture of EDs that act through different pathways to explore possible cocktail effects to human beings. Further, it would be interesting to develop assays to study androgenic EDs as well.

In chapter 4 we described a microCCA experimental setup with a PDMS micropump. The fluidic pathways between microCCA and the pump were connected via tubing. One area for further development is to integrate the micropump with the microCCA device for an all-in-one device with a smaller size and for more reproducible and efficient pumping with less fluidic resistance and to avoid the use of tubing. The hydrogel based PDMS microCCA platform described in chapter 5 is a key element that may enables this integration step as both are made from PDMS. Though the micropump can deliver fluid continuously and precisely, their durability remains to be

improved. Surface adsorption of hydrophobic compounds is another concern in the study of with low chemical concentrations (1uM or less), which are usually true for hormones.

In chapter 5, PEG was used at a model photopolymerizable hydrogel for cell encapsulation within microCCA. The extreme hydrophilicity of PEG limited the long -term cell viability encapsulated within PEG due to limited cell-matrix interaction, which is important for endothelial cells to survive. To solve this problem, PEG may be modified or mixed with adhesive peptides, ECMs or positively charged polymers to promote cell attachment to the PEG hydrogel structure, RGD modified PEG was reported to maintain cell viability for over a week[5]. It would be interesting to test alternative hydrogel materials, such as dextran AC, with different hydrophobicity.

One more area worth further development is the construction of cell-seeded microCCA biosensors with long-term storage capabilities that are ready to use as needed. Current experimental setups require device preparation such as cell seeding and device assembly performed right before drug dosing, which is then followed by imaging and data analysis. However, an ideal way is to have devices readily available for dosing, as cell seeding and device assembly take hours of experimental setup time , and require professional skills, PEG encapsulation provide extra protection during cryopreservation and it has been reported that cells entrapped in PEG hydrogel microstructures remained viable throughout the freezing process [6]. The concept of air-dry stabilization of mammalian cells with subsequent recovery following rehydration has also been demonstrated with Human 293H cells transfected with a cyanobacterial gene encoding sucrose phosphate synthase [7] . These techniques may potentially be used to provide stabilized mammalian cells for mammalian cell-based

biosensors with extended shelf lives. The PDMS microCCA devices and the PDMS micropump, which have been described in chapter 4 and chapter 5 respectively, provide a feasible platform for fabrication of ready-to-use biosensors for applications in drug screening, pathogen detection and in the study of endocrine disruptor as well.

REFERENCE

1. Martin, V., et al., *The estrogen responsive element of the pS2 gene is recognized by a methylation sensitive DNA binding protein.* Biol Chem, 1998. **379**(4-5): p. 409-16.
2. Cheung, E., et al., *Altered pharmacology and distinct coactivator usage for estrogen receptor-dependent transcription through activating protein-1*. Proc Natl Acad Sci U S A, 2005. **102**(3): p. 559-64.
3. Fujimoto, N., H. Honda, and S. Kitamura, *Effects of environmental estrogenic chemicals on AP1 mediated transcription with estrogen receptors alpha and beta.* J Steroid Biochem Mol Biol, 2004. **88**(1): p. 53-9.
4. Safe, S. and M. Wormke, *Inhibitory aryl hydrocarbon receptor-estrogen receptor alpha cross-talk and mechanisms of action.* Chem Res Toxicol, 2003. **16**(7): p. 807-16.
5. Koh, W.G., L.J. Itle, and M.V. Pishko, *Molding of hydrogel multiphenotype cell microstructures to create microarrays.* Analytical Chemistry, 2003. **75**(21): p. 5783-5789.
6. Itle, L.J. and M.V. Pishko, *Cryopreservation of cell-containing poly(ethylene) glycol hydrogel microarrays.* Biotechnol Prog, 2005. **21**(3): p. 1004-7.
7. Bloom, F.R., et al., *Engineering mammalian cells for solid-state sensor applications.* Biosens Bioelectron, 2001. **16**(7-8): p. 603-8.